Design, Optimization and Pharmacokinetic Evaluation of Rufinamide Nanoparticles Loaded Thermoresponsive *In-situ* Gelling Systems for Direct Nose-to-Brain Delivery

THESIS

Submitted in partial fulfilment

of the requirements for the degree of

DOCTOR OF PHILOSOPHY

by

DALVI AVANTIKA VIJAY

ID. No. 2014PH460054H

Under the Supervision of

Prof. Punna Rao Ravi

BITS Pilani

Pilani | Dubai | Goa | Hyderabad

BIRLA INSTITUTE OF TECHNOLOGY AND SCIENCE, PILANI

2021

BIRLA INSTITUTE OF TECHNOLOGY AND SCIENCE, PILANI

CERTIFICATE

This is to certify that the thesis titled **Design, Optimization and Pharmacokinetic Evaluation of Rufinamide Nanoparticles Loaded Thermoresponsive *In-situ* Gelling Systems for Direct Nose-to-Brain Delivery** submitted by **DALVI AVANTIKA VIJAY** ID No **2014PH460054H** for award of Ph.D. of the Institute embodies original work done by him/her under my supervision.

Signature of the Supervisor:

Name in capital letters: PUNNA RAO RAVI

Designation: **Associate Professor**

Date: **05-03-2021**

Abstract

Rufinamide (Rufi) is a broad spectrum anti-epileptic drug. Rufi was approved for marketing in Europe in 2007 under the trade name Inovelon®. In 2008 the US FDA approved it for treatment of Lennox Gastaut Syndrome (LGS) under the trade name Banzel®. Rufi has also been indicated for the treatment of partial seizures. Several clinical studies have shown the broad-spectrum activity of Rufi. Rufi shows low oral bioavailability. Also, its oral bioavailability increases in a non-proportional manner with increase in dose. Moreover, increase in the dose administered results in intensification of peripheral side effects. Once absorbed into the systemic circulation, in order to reach the brain, drugs have to cross the tightly regulated blood-brain barrier (BBB). This further reduces the amount of drug reaching the brain.

Despite all the shortcomings of orally administered Rufi, there have been no reports in the literature which attempt to improve the bioavailability of Rufi. Given the drawbacks of orally administered Rufi, it is imperative to look for a different formulation or a different route for administration of Rufi.

Intranasal, or more specifically, nose to brain drug delivery route is an attractive route of administration especially in case of drugs which show problems with oral administration. Direct nose to brain transport of molecules may help increase the drug's bioavailability in the brain. It is a viable option especially in case of patients suffering from epilepsy, where sometimes, swallowing of dosage form might be an issue. Nevertheless, intranasal route poses a few challenges *per se.* Immediate clearance of formulation administered through the nose by mucociliary clearance (MCC) process, specific deposition of formulation to achieve brain targeted absorption, high inter subject variability etc. However, such drawbacks associated with intranasal delivery can be addressed using several formulation strategies.

In this work, we have explored different formulation strategies to improve the direct nose to brain uptake of Rufi, while also minimizing its plasma exposure.

As a first step to evaluate the efficacy of different formulations strategies to deliver Rufi to the brain, a reliable analytical method is needed for accurate and precise quantification of Rufi. Sensitive, robust analytical and bioanalytical methods were developed to quantify Rufi from various *in vitro* and *in vivo* samples. The developed methods were validated according to the guidelines given by ICH. The developed and validated aqueous HPLC method and bioanalytical HPLC method were found to be simple, rapid, specific, precise, cost-effective and reproducible for quantification of Rufi.

A major drawback with nasal delivery is the clearance of formulations out of the nostrils either due to gravity, or by clearance through the nasopharyngeal duct by the process of MCC. To overcome this, a thermoresponsive *in situ* gel for Rufi was formulated. Tamarind seed xyloglucan (TSX), a natural, biodegradable polymer was used as a thermoresponsive polymer. The formulation was optimized using rheometric analysis, texture analysis, *in vitro*, and *in vivo* studies. Pharmacokinetic studies in rats were carried out to assess direct *nose to brain* uptake for the optimized *in-situ* gelling formulation of Rufi (Rufi-RXG) and compared with intravenous bolus, and a plain aqueous nasal suspension of Rufi (Rufi-Susp). Finally, brain targeting index %DTP was calculated. All the formulations showed gelation below 35 °C. The optimized formulation comprised 2.0% w/v RXG, 0.01% v/v thiomersal (preservative), and Rufi in suspended form. The %DTP values were 79.9 and 31.91, respectively. This indicates that with Rufi-RXG almost 80% of the administered dose of Rufi reached the brain via direct *nose to brain* pathways, whereas in case of Rufi-Susp, only 31% of Rufi could reach the brain directly. This work demonstrated that the intranasal *in-situ* gel formulation Rufi is enhancing the overall brain exposure of Rufi compared to oral formulations.

To further enhance its direct nose to brain uptake Rufi nanocrystals (Rufi-NCs) were formulated by anti-solvent precipitation using the principle of DoE. Rufi-NCs were characterized for size, yield (%) and morphology. Rufi-NCs were loaded in a 2.0% w/v RXG

to form a nasal *in-situ* gel for direct nose to brain delivery of Rufi. The *in-situ* gel formulations were characterized for rheological properties, stability, *in vitro* drug release, and *in vivo* plasma and brain pharmacokinetics. Pharmacokinetic parameters were computed for aqueous suspension of nanocrystals (Rufi-NC-Susp) and *in-situ* gelling formulation for nanocrystals (Rufi-NC-RXG) and compared with the pharmacokinetic parameters of aqueous suspension of plain Rufi (Rufi-Susp). Rufi-NCs showed PS of 261.2 ± 2.1 nm, PDI of 0.28 ± 0.08, and yield (%) of 89.6 ± 2.0. The Rufi-NC-RXG formulation showed a gel transition temperature of 32 °C. The %DTP values for Rufi-Susp and Rufi-NC-RXG were 31.9 and 85.5, respectively. This indicates that the nanocrystal formulation further improved the drug delivery of Rufi to the brain.

In the next stage we have formulated Chitosan based nanoparticles for Rufi (Rufi-Ch-NPs). The Rufi-Ch-NPs were suspended in a solution of 2.0% w/v RXG to form a nasal *in-situ* gel for direct *nose to brain* delivery of Rufi. The Rufi-Ch-NPs were characterized for size, entrapment efficiency, zeta potential, morphology, and physical stability. The *in-situ* gel formulations were characterized for rheological properties, *in vitro* drug release, stability, and *in vivo* plasma and brain pharmacokinetics. Pharmacokinetic parameters were computed for aqueous suspension of nanoparticles (Rufi-NP-Susp) and *in-situ* gelling formulation for nanoparticles (Rufi-NP-RXG) and compared with the pharmacokinetic parameters of aqueous suspension of plain Rufi (Rufi-Susp). Brain targeting index %DTP value was calculated for all the formulations. The optimized nanoparticle formulation showed a size of 180 ± 1.5 nm, PDI of 0.29 ± 0.08, zeta potential of 38.3 ± 1.5 mV, entrapment efficiency of 75 ± 2.0 % and drug loading of 11 ± 0.3 %. The *in-situ* gelling formulation of nanoparticles showed a solution to gel transition temperature of 32 °C. The %DTP for Rufi-NP-Susp, Rufi-NP-RXG, and Rufi-Susp were 86.1, 91.5 and 31.9, respectively. This indicates that with Chitosan nanoparticles, the *nose to brain* uptake of Rufi increased further

Declaration

I hereby declare that the work carried out in this thesis titled '**Design, Optimization and Pharmacokinetic Evaluation of Rufinamide Nanoparticles Loaded Thermoresponsive In-situ Gelling Systems for Direct Nose-to-Brain Delivery'** is an original piece of research work carried out under the guidance of Prof. Punna Rao Ravi at BITS-Pilani, Hyderabad Campus, Hyderabad. India. This thesis has not been submitted by me for the award of any other degree of any other University/Institute.

Name: DALVI AVANTIKA VIJAY

Signature: 

Date: 03rd July 2021

Acknowledgements

It gives me pleasure in proclaiming that almost half a decade of studying, writing, experimenting, failing, learning has culminated into a meaningful research output encompassed by this thesis. Firstly, I praise Lord Dhanvantari, the Hindu god in ancient Indian Medicine. This thesis would not have been possible without the guidance, help, advice that I received from several people along the way. They say that 'too many cooks spoil the broth'. In my view, research is a special kind of broth, which requires help from as many cooks as it can get.

I have been associated with Prof. Punna Rao Ravi for almost seven years. He has taught me several courses during my master's degree. He was the supervisor for my master's and doctoral thesis. I consider myself truly fortunate to have known and worked with Prof. Punna Rao. He is a thorough researcher, and a wise person. He is a constant source of inspiration, and I always try to emulate his teaching and learning methods.

My sincere thanks to Prof. Souvik Bhattacharyya, Vice Chancellor, Prof. G. Sundar, Director, BITS Pilani, Hyderabad Campus, Mr. Ernest Samuel Ratnakumar J, Registrar, Prof. Venkata Vamsi Krishna Venuganti, Dean, Academic - Graduate Studies and Research, and Prof. Niranjan Swain, Dean, General Administration for providing necessary support to accomplish my research work.

I sincerely thank the examiners for my thesis- Prof. Vandana B. Patravale and Prof. Sanjula Baboota who agreed to review my thesis and gave their constructive comments and suggestions.

I also expressed my profound gratitude to Prof. Sajeli Begum, Professor and Head, Department of Pharmacy, for her support and extending the facilities to work at the institute.

I am deeply grateful to Prof. Swati Biswas and Dr. Murali Pandey who have acted as Doctoral Advisory Committee (DAC) members and provided their detailed constructive comments and support throughout this work.

I sincerely acknowledge the help provided by other faculty members, Prof. D. Sriram, Prof. P. Yogeeswari, Prof. V. V. Vamsi Krishna, Prof. Onkar Kulkarni, Dr. Balram Ghosh, Dr. Arti Dhar, Dr. Akash Chaurasiya, and Dr. Nirmal Jayabalan for sharing their vast experience and technical knowledge with me when needed.

I owe my warmest and humble thanks to Prof. Shrikant Y. Charde for his timely help, encouragement and boosting my confidence in the progress of my academics.

I want to extend a special thanks to Mr. Chandra Teja Uppuluri for being a constant support throughout my Ph.D. He is a quick witted, person with a curious mind and diverse interests. Tough times seemed less stressful with the company and help that I received from Mr. Uppuluri.

I would also like to thank Dr. Shailender Joseph for providing valuable guidance especially when I was at the crossroads of my career.

I am very grateful to my colleagues and lab mates, Rimpy, Ekta, Shareef, Radhika, Swagata, and many others for their advice, encouragement, help and cheerful moments spent with them at all times. They have helped in gaining a lot through mutual exchange of knowledge. Their

presence made the general work environment very pleasant and cheerful. I also thank my seniors Dr. Rimpy, Dr. Gangadhar, Mr. Radha Krishna and Mr. Pradeep Rawat who provided a lot of support and guidance during their stay in BITS-Pilani, Hyderabad Campus. I am very thankful to Dr. Vishnu Kiran, Dr. Shubhmita Bhatnagar for their professional guidance and advice. They have also been great friends of mine.

I am also grateful for the help provided by the non- teaching staff especially the lab technicians, Mrs. Saritha, Mrs. Rekha, Mrs. Sunita, Mr. Rajesh, and Mr. Srinivas and others including office, store, librarian, laboratory staff and security. I am thankful to the CAL technicians Mr. Uppalaiah, Mr. Mallesh, Mrs. Jyothi, Mr. Narasimha, and Mr. Kumar.

The postgraduate students of pharmacy department deserve a special mention here. Aashma, Ashwini, Shafik, Suvarna, Radhika, Sumeet, Vibha, Jyotsna, Shreyas, Chetan, and Rohit have been excellent students who have worked with me. Working with them was fun especially because of the camaraderie we share.

I acknowledge the help of Indian Council of Medical Research (ICMR) for providing financial assistance (Senior Research Fellowship) to pursue my Ph.D. work without any hindrance.

I would like to thank all my seniors, colleagues, and friends – Nikhila, Dr. Jaspreet, Dr. Shubham, Dr. Preeti, Dr. Himanshu, Dr. Onkar, Dr. Anup, Dr. Gangadhar, Dr. Priyanka Reddy, Dr. Prakruti, Dr. Santhosh, Dr. Mahibalan, Thirumalesh, Raghu, Yamini, Giridhari, Lokesh, Deepanjan, Sony Priyanka, Aasha, Kalyani, Kavita, Pravesh, Lavanya, Ashutosh, Samrun, Deepika, Srashti, Suresh, Trupti, Soniya, Sanjay, Milan, Ganesh, Sravani, Kirti, Pragya, Purbali, Sai, Dr. Sivakrishna, Madhu Rekha, Rida, and Parameswar.

I want to thank my parents Mr. Vijay Dalvi, and Mrs. Suchitra Dalvi for being patient throughout my doctoral degree and for being supportive of my career goals. A special thanks to my sister **Shubhangi** who has always talked me through difficult times and is my support for life.

List of Tables

List of Figures

List of Abbreviations

%RSD	Percentage relative standard deviation
°C	Degree Celsius
µg	Micro gram
µL	Micro litre
µm	Micro meter
Å	Angstrom
ACN	Acetonitrile
AEDs	Anti-epileptic drugs
ADME	Absorption, distribution, metabolism and elimination
ANOVA	Analysis of variance
AUC	Area under the curve
BBB	Blood-brain barrier
BBD	Box-Behnken design
Blank-RXG	Reacted Xyloglucan *in-situ* gel without Rufinamide
cm	Centimetre
C_{max}	Maximum plasma concentration of the drug
CCD	Central Composite Design
CNS	Central Nervous system
CYP	Cytochrome P450
DCM	Dichloromethane
DL	Detection limit
DMF	Dimethylformamide
DMSO	Dimethyl sulfoxide
DoE	Design of experiments
DSC	Differential scanning calorimetry
DTE	Drug transport efficiency
DTP	Drug transport percentage
EDTA	Ethylene diamine tetra acetic acid
EE %	Entrapment efficiency
EMA	European medicines agency
g	Gram

GAA	Glacial acetic acid
GIT	Gastrointestinal tract
G'	Elastic modulus
G"	Viscous modulus
h	Hours
HPLC	High-performance liquid chromatography
HQC	High quality control
IAEC	Institutional animal ethics committee
ICH	International council of harmonization
IS	Internal standard
i.v.	Intravenous
i.n.	Intranasal
Da	Dalton
kg	Kilogram
kV	Kilo volts
L	Litre
LLOQ	Lower limit of quantification
Log P	Logarithm of partition coefficient
LOQ	Limit of quantitation
LQC	Lower quality control
LVER	Linear viscoelastic region
mg	Milligram
min	Minute
mL	Millilitre
mM	Millimolar
mm	Millimetre
MCC	Mucociliary clearance
MiniRes	Minimum resolution design
MTT	Mucociliary transit time
MQC	Middle quality control
MRT	Mean residence time
MS/MS	Tandem mass spectrometry

mV	Millivolts
MW	Molecular weight
n	Number of replicates
ng	Nanogram
nm	Nanometre
NCs	Nanocrystals
NCA	Non compartmental analysis
NPs	Nanoparticles
N2B	Nose to brain
P-188	Poloxamer-188
P-407	Poloxamer-407
PBD	Placket-Burman design
PBS	Phosphate buffer saline
P	Calculated *P* value
PDA	Photo diode array
PDI	Polydispersity index
PEG 400	Polyethylene glycol 400
P-gp	P-glycoprotein
pH	Potential of hydrogen
PPF	Peak positive force
PS	Particle size
PVA	Polyvinyl alcohol
pXRD	Powder X-ray diffraction
QL	Quantitation limit
R^2	Regression coefficient
RH	Relative humidity
rpm	Rotations per minute
rcf	Relative centrifugal force
RT	Room temperature
Rufi	Rufinamide
RXG	Reacted Xyloglucan
Rufi-Ch-NPs	Rufinamide Chitosan nanoparticles

Rufi-NCs	Rufinamide nanocrystals
Rufi-Susp	Aqueous suspension of plain Rufinamide
Rufi-RXG	Plain Rufinamide suspended in RXG based *in-situ* gel
Rufi-NC-Susp	Aqueous suspension of Rufinamide nanocrystals
Rufi-NC-RXG	Rufinamide nanocrystals suspended in RXG based *in-situ* gel
Rufi-NP-Susp	Aqueous suspension of Rufinamide nanoparticles
Rufi-NP-RXG	Rufinamide nanoparticles suspended in RXG based *in-situ* gel
SD	Standard deviation
SEM	Scanning electron microscopy
Sol	Solution
STPP	Sodium tri poly phosphate
Susp	Suspension
$t_{1/2}$	Elimination half life
T_{max}	Time taken to reach maximum plasma concentration
TSX	Tamarind seed xyloglucan
$T_{sol \rightarrow gel}$	Sol to gel transition temperature
USP	United States Pharmacopoeia
UV	Ultraviolet
v/v	Volume by volume
w/v	Weight by volume
WHO	World health organization
α	Alpha
β	Beta
σ	Standard deviation of the intercepts

1 INTRODUCTION

Electricity is life but electricity also is an invisible fist punching up your spine, knocking your brains right out of your skull.

- Ray Robinson

1.1 Epilepsy and seizures

About less than two centuries ago, a British neurologist Hughlings Jackson defined epileptic seizures as phenomena resulting from sudden discharge of gray matter from the brain. This definition of epileptic seizures holds good even today. Epilepsy is a chronic neurological disease characterized by persistent seizures unprovoked by any insult to the central nervous system. Epilepsy syndrome is defined by a set of clinical characteristics which include, genetic basis, EEG findings, similar types of seizure, age of onset, similar responses to antiepileptic drugs (AEDs). The International League Against Epilepsy (ILAE) and the International Bureau for Epilepsy (IBE) in 2005, defined epilepsy as a brain disorder characterized by an enduring predisposition to generate epileptic seizures and by the neurobiological, cognitive, psychological, and social consequences of this condition [1,2]. Seizures are elements resulting from abnormal brain activity not necessarily related to epilepsy. Seizures that are provoked by reversible events like fever, trauma, hypoglycaemia are not classified as epileptic seizures. Epileptic seizures on the other hand, arise from abnormal firing of neurons. Seizures need to be diagnosed for determining the underlying brain abnormality and to treat/manage it. A definite diagnosis includes accurate description of a seizure/seizure like event, followed by confirmatory tests like an electroencephalogram (EEG), genetic studies, and neuroimaging. Epilepsy is typically diagnosed if there are 2 unprovoked seizures reported [1,2].

In 2010, IALE gave the most recent and revised classification of epileptic seizures. Epileptic seizures are mainly classified as generalized, focal (previously known as partial), and epileptic spasms. Generalized seizures originate in the bilateral

networks involving cortical and sub-cortical structures, while focal seizures originate in the neuronal networks of either of the cortex, and may become generalized. The subtypes of generalized seizures are absence seizures (previously known as petit mal seizures), tonic-clonic seizures (previously known as grand mal seizures), myoclonic and atonic seizures. Absence seizures involve staring with either nodding or blinking, unresponsive to external stimuli. Tonic-clonic seizures involve stiffening and jerking of muscles associated with limbs, often accompanied by loss of consciousness. In myoclonic seizures, the patient experiences lightning fast, sudden movements of the body without loss of consciousness. In case of atonic seizures, the patient loses the tone of the entire body causing a head drop or fall [3,4].

1.1.1 Incidence and prevalence of epilepsy

Epilepsy affects people of all races, ages, genders and geographical locations. A meta-analysis study done on a global level showed that the incidence for epilepsy was 61.4 per 1,00,000 person years. That means per year 61.4 people out of a hundred thousand people are reported as epilepsy patients. The incidence was reportedly higher in the lowest socioeconomic strata particularly in high income countries. It was higher in low to middle income countries than higher income countries [5].

Epilepsy is a huge burden and a grave problem in India. As of 2017, an estimated 12 million people in India suffered from epilepsy. The problem is even more common in rural India. 60% of the patients visit a doctor after an epileptic event in urban India, while it is just 10% in rural India [6–8]. A 2014 study revealed that there was a huge treatment gap in patients with epilepsy in India. Treatment gap arises because of lack of access to treatment options, or lack of patient adherence to therapy [8].

1.1.2 Lennox Gastaut Syndrome (LGS)

Lennox Gastaut Syndrome (LGS) is a form of childhood epilepsy. It was first described in 1950 by Lennox and Davis and later in 1966 by Gastaut. The ILAE has most recently classified LGS as age related epileptic encephalopathy. LGS starts in early childhood, affecting children at ages 3 to 5 which manifests in adulthood. Tonic clonic seizures are the most common feature of LGS. Seizures in LGS are accompanied by drops/falls resulting in severe injuries in patients with LGS. In patients with LGS, especially children, mental retardation is a common feature even before the seizures start showing up [2,9]. Children with LGS show impaired motor and cognitive skills. They need help with simple day to day activities like walking, crawling, eating etc. due to sudden loss in muscle tone [12].

LGS can be symptomatic or cryptogenic. Symptomatic LGS is when a specific cause can be attributed to the disease. These include head injury, trauma, radiotherapy, hypoxic ischemic encephalopathy, brain malformations and brain tumours. Family history/genetic mutations have been observed in 3 to 30% of LGS patients. On the other hand, a third of LGS patients are cryptogenic cases, where no specific cause can be identified [3,10].

1.1.3 Treatment of LGS

Treatment goals for LGS are same as other forms of epilepsy: reduced or no seizures, fewer side effects of medication, reduction in pill burden and ultimately an improved quality of life. Treatment and management of LGS is difficult because it is resistant to most of the currently available therapy. Valproic acid is the first line treatment for LGS. Clobazam is used when atopic seizures or drop attacks prevail. Other drug for LGS include lamotrigine, felbamate, Rufinamide. Non

pharmacological treatments include ketogenic diet, vagus nerve stimulation, and corpus callosotomy [3,11,12].

Recent studies have shown that Rufinamide is an effective medication added to the class of antiseizure drugs to treat LGS. Rufinamide has shown to reduce tonic and atonic seizures. Given its effectiveness in the management of LGS, it is likely to show a broad-spectrum activity in several other epilepsy syndromes. Overall, Rufinamide has shown a better efficacy and better safety profile than many other drugs used to treat epilepsy and LGS [13].

1.2 Rufinamide for the management of epilepsy and LGS

Rufinamide (Rufi) is a broad-spectrum AED that's chemically different from other AEDs. The chemical name of Rufi is 1-[(2,6-difluorophenyl) methyl]-1H-1,2,3-triazole-4 carboxamide. The structure for Rufi is given in Figure 1.1.

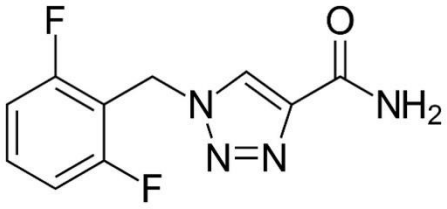

Figure 1.1 Chemical Structure of Rufi

Rufi was given the status of an orphan drug for treatment of LGS is 2004. Rufi was approved for marketing in Europe in 2007 under the trade name Inovelon®. In 2008, the US FDA approved it for treatment of LGS under the trade name Banzel® [2,14]. Rufi has also been indicated for use to treat partial seizures in adults.

1.2.1 Physicochemical properties of Rufi

Physicochemical properties of Rufi are given in Table 1.1. Rufi shows no ionizable groups in its structure. It has poor solubility in aqueous medium. Its solubility in 0.1 N HCl is approximately 63 mg/L and 59mg/L in simulated intestinal fluid. It shows

slight solubility in organic solvents like methanol and ethanol. This drug has four polymorphic forms viz A, A', B and C, among which polymorph A is most stable. Rufi shows poor flow properties due to needle shaped crystals. It is not susceptible to photo and thermal degradation; however, it requires storage below 30 °C [2,3,15].

Table 1.1 Physicochemical properties of Rufi

Parameter *	Description
Drug name and BCS class	Rufinamide, Class 4
Therapeutic class	Anti-epileptic drug
Chemical class	Triazole derivative
Chemical name	1-[(2,6-difluorophenyl) methyl]-1H-1,2,3-triazole-4 carboxamide
Chemical formula	$C_{10}H_8F_2N_4O$
Molecular weight	238.19 g/mol
Physical state	White to off-white, crystalline powder
Melting point	233 - 238 °C
Water solubility (at pH of ~ 7.0)	30.5 µg/mL
Hydrophobicity (Log P)	0.65
Ionization constant (pKa)	12.0
Hygroscopicity	Non hygroscopic

* *Data taken from available literature [16]*

1.2.2 Clinical pharmacology of Rufi

1.2.2.1 Mechanism of Action

The mechanism of action of Rufi has not been completely elucidated. Based on *in vitro* studies performed on a cortical neurons culture from immature rats, Rufi appeared to act on sodium channels (which are involved in normal and abnormal firing of neurons) by modulating their activity, mainly by prolonging the inactive state of sodium channels. Rufi slowed down the recovery of sodium channels significantly after a prolonged pre pulse. It reduced the sustained repetitive neuronal firing [17]. Studies have also shown that it may have an inhibitory action on glutamate receptor, subtype mguR5 at higher concentrations [2]. Its ED50 (dose required to produce 50% of the response against seizures) in mice MES model was found to be 23.9mg/kg. Results from animal models showed that Rufi had a broad-spectrum activity with broad therapeutic index [3].

1.2.3 Pharmacokinetics (PK) of Rufi

1.2.3.1 Absorption after oral administration

Rufi is well absorbed from the GIT, but the rate of absorption is slow. Some authors claim that food has a moderate positive effect on absorption of Rufi at doses lower than 400 mg. The main reason of its slow absorption is the slow dissolution rate. Although, the absolute bioavailability of the currently marketed formulation is not known, studies have reported that absorption of Rufi from the GIT is slow, with T_{max} of 4-6 h irrespective of the formulation used, or fed or fasted condition. Early clinical trials performed with 600 mg dose of Rufinamide filled in gelatin capsules showed that oral bioavailability of Rufinamide was around 85% when taken after a meal. It has also been reported that the oral bioavailability decreased with increasing dose. The oral bioavailability of the marketed formulation is unknown [18]. Several studies have been conducted to find the effect of different doses and multiple dose regimens on absorption. The studies revealed that at maximum dose of 3600 mg twice daily, the ratio of peak plasma concentration or the area under the curve over a 12 h period to the dose administered was half as that of the lowest dose studied i.e., 400 mg twice daily. As the dose increased, a less than proportional increase in the extent of absorption was seen [19]. This may be attributed to active transport mechanism of Rufi in the intestines which is indicated by some *in vitro* assays [15].

1.2.3.2 Distribution

Rufi has shown partitioning between plasma and erythrocytes equally and irreversibly in *in vitro* studies. The change in volume of distribution with respect to the fraction of drug absorbed was consistent with the observation that of lesser bioavailability with increase in dose [19]. Rufi crosses the Blood Brain Barrier

(BBB) rapidly and reversible. It shows no specific affinity to any particular organ or tissue [15].

1.2.3.3 Metabolism and Elimination

A mass balance study performed in healthy young males, showed that Rufi underwent extensive metabolism, by enzymatic hydrolysis. 70% of the metabolized product was excreted in urine, while 9.0% was excreted in faeces. Unchanged Rufi accounted for around 4.0% of the total dose administered, while a minor acyl-glucuronide metabolite accounted for around 7.0% of the total dose. The principal route of metabolism, reported from *in vitro* studies with liver microsomes was the hydrolysis of the carboxamide group. Both, the major and minor metabolites of Rufi are pharmacologically inactive. These studies also revealed that there was no involvement of the CYP (Cytochrome P450) system in the metabolism of Rufi. Also, Rufi does not show any inhibitory activity on the CYP family of enzymes [19,20].

The elimination half-life of Rufi in healthy subjects and epilepsy patients was 6-10 h. The principal route of excretion is through kidneys. Around 80% of the dose administered is excreted through kidneys. In a study conducted in healthy volunteers and epilepsy patients, the parameter Cl/F (Cl/F is the oral clearance value which is dependent on both oral bioavailability and Rufi clearance) was evaluated. The Cl/F value for a single dose of 400 mg was 4.8L/h and the (elimination half-life) $t_{1/2}$ were 10.3 h. A multiple dose study with 400 mg twice daily reported the Cl/F value to be 5.1 L/h. In a multiple dose study in patients with epilepsy, the $t_{1/2}$ was 6.9 h [19].

1.2.4 Adverse effects of Rufi

Adverse effects observed with Rufi were mild to moderate severity as reported by several clinical studies. Several studies also reported that the severity of adverse effects increased with increasing dose, within the therapeutic dose range [2]. The

most common side effects with patients with partial epilepsy were headache, dizziness, fatigue, nausea, somnolence. Double vision and trouble with balance were less common side effects. In case of patients with LGS, the most common side effects were vomiting and somnolence [21]. Other adverse events that were observed during clinical trials were classified according to the body systems and the frequency of the event- frequent (1 per 100 patients), infrequent (1 per 100 to 1 per 1000 patients) and rare adverse events (less than 1 per 1000 patients). [20].

1.2.5 Dosage administration and available dosage forms of Rufi

According to the US FDA, the starting dose of Rufi in patients with LGS from 1 to 17 years old is approximately 10mg/kg given as two equally divided doses. This can be increased to a maximum of 45mg/kg (not exceeding 3200 mg/day). In adults (beyond 17 years of age), the initiation dose is 400 mg/day, which can be increased by 400-800 mg every other day up to a maximum dose of 3200 mg/day.

Rufi is sold under the brand names Banzel® and Inovelon® in USA and Europe, respectively. Banzel® is available as 200 and 400 mg tablets and as a 40mg/mL oral suspension. Inovelon is available as 100, 200 and 400 mg tablets. In January 2021 US FDA approved Lupin Limited's generic medication Rufinamide Oral Suspension, to be used as an add-on therapy to control seizures in adults and children, ages 1 and older. In June 2021, Glenmark Pharma launched a new therapeutic equivalent of Banzel tablets, 200 mg and 400 mg in the US market.

1.2.6 Drawbacks of the currently available formulations of Rufi

Currently, Rufi is available as an oral tablet and an oral suspension. As mentioned in Section 1.2.3.1, Rufi shows low oral bioavailability. Also, its oral bioavailability increases in a non-proportional manner with increase in dose. Moreover, increase in the dose administered results in intensification of peripheral side effects. Once

absorbed into the systemic circulation, in order to reach the brain, drugs have to cross the tightly regulated blood-brain barrier (BBB). This further reduces the amount of drug reaching the brain.

1.2.6.1 The blood-brain barrier (BBB)

All organisms with a well-developed CNS have a BBB (Figure 1.2). The BBB is composed of blood capillaries that are morphologically similar to the capillaries from the other parts of the body, but are made up of specialized endothelial cells, astrocytes, pericytes and neuronal terminals [22]. The BBB proper is created at the level of the endothelial cells of cerebral blood capillaries. The tight junctions and the special nature of the endothelial cells help regulate substances crossing the BBB. The function of the BBB is to allow few, selective molecules to permeate across into the brain; this way it protects the brain from any toxins that may have entered the systemic circulation. Molecules move across the BBB by transcellular and paracellular transport by active or passive processes [23]. Solutes move through the paracellular pathway by passive diffusion and the movement is dependent on the electrochemical gradient, osmotic or hydrostatic gradient. Lipophilic and low molecular weight (<400 Da) solutes can permeate via this pathway.

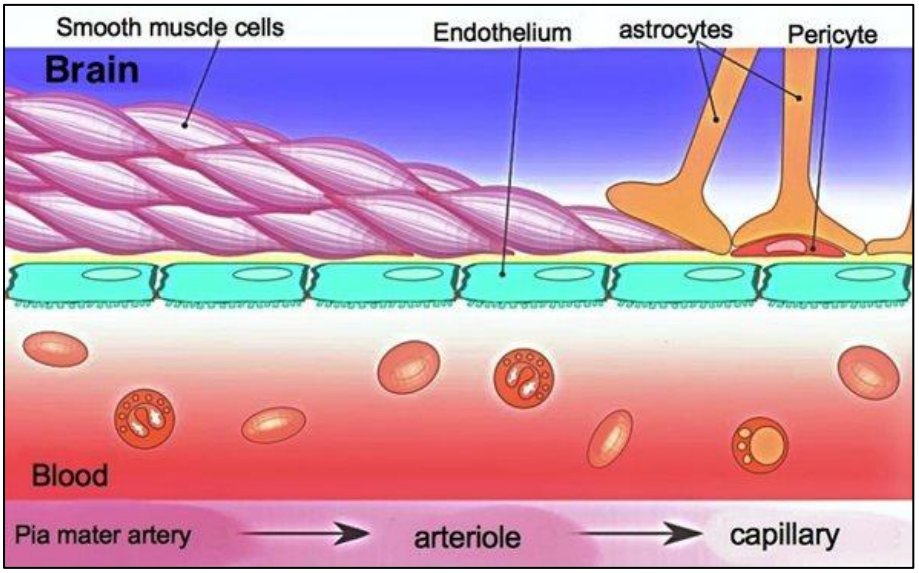

Figure 1.2 The blood-brain barrier (BBB)

Diagram of a micro vessel in the brain lined by the blood-brain barrier. The blood-brain barrier is a multicellular, compound structure composed of endothelial cells, pericytes and astrocytes in direct contact with brain tissue.
Source: https://commons.wikimedia.org/wiki/File:Blood_vessels_brain_english.jpg

1.2.7 Strategies to improve the bioavailability of Rufi in the brain

For more than a decade, drug delivery techniques to improve targeting to the brain have been the focus of several research groups. Viral vectors, altering the BBB permeability properties, stereotaxic injections into the brain are some of the strategies used to achieve brain targeted drug delivery [3]. These techniques, apart from being invasive, involve high risk, and seem impractical.

In recent times, efforts to deliver drugs to the brain and cerebrospinal fluid (CSF) by circumventing the BBB have gained momentum. Nose to brain drug delivery is one such technique that has shown promising results. Nasal delivery of drugs can circumvent all the problems associated with oral absorption and gastrointestinal (GI) side effects of the drugs administered through the oral route. Moreover, drugs administered through the intranasal (i.n.) route, if deposited in the appropriate region of the nose (olfactory region), reach CNS via several direct and indirect pathways.

1.3 Intranasal (i.n.) delivery of small molecules

Over the past decade, i.n. delivery to target the brain has been recognized as a non-invasive technique to deliver drugs to the brain. It has been considered as a better alternative to oral and i.v. delivery due to better reach to the brain, easy accessibility for administration, high surface area of nasal mucosa and avoidance of hepatic first pass metabolism [24].

1.3.1 Anatomy of the nose

The nose serves as an organ or the respiratory system in humans and other animals. Other than respiration, the nose also is a protective organ where it filters and humidifies the inhaled air before reaching the lungs. The nose is divided into two symmetrical halves by a septum; each half is divided into four regions based on their anatomical features and histology – the nasal vestibule, atrium, respiratory region and olfactory region. The nasal atrium is located between the respiratory region and the vestibule. It is covered with stratified columnar cells with small hair like projections called the 'microvilli'. The respiratory region has three sub regions – superior, middle and inferior turbinates. The turbinates extend from the lateral walls of the nose towards the septum. The nasal respiratory mucosa consists of three basic layers *viz* nasal epithelium which consists of pseudostratified columnar cells, the basement membrane and the lamina propria. The basal cells are found on the basolateral side of the epithelium and are adjacent to the basal lamina. The lamina propria has a network of blood vessels and nerves. The respiratory epithelium is innervated by the maxillary branch of the trigeminal nerve which goes right up to the brain stem. Goblet cells, basal cells and mucous secreting cells are a part of nasal epithelium [25]. The cilia have a special function of clearing the mucus towards the nasopharynx. The epithelial cell layer has a layer of mucus secreted by the goblet cells and secretory glands. The nasal mucus layer is approximately 5 μm thick and has an outer thicker, more viscous layer, with a more fluid layer underneath. The nasal mucus has several functions *viz* humidifying the inhaled air, providing enzymatic protection against foreign particles, toxins and drugs. The mucus layer owing to its high viscosity traps harmful particles, pathogens from the environment and the cilia on the epithelial cells keep beating to push the mucus layer towards the nasopharynx. This process is called the mucociliary clearance (MCC). The olfactory

region of the nose is located posterior to the respiratory region and covers the inferior surface of the cribriform plate. It extends slightly further on to the nasal septum and lateral walls till the end of superior turbinate of the respiratory region.

1.3.2 Nose to brain (N2B) pathways

Intranasally administered drugs can reach the brain via a direct and indirect routes *viz* from the nasal epithelium into the systemic circulation, and from the nasal cavity to the brain via different pathways. Therapeutic molecules travel from the nose to the brain mainly via three pathways *viz* olfactory neuronal pathway, trigeminal neuron pathway and the systemic circulation [3]. A schematic illustration of the N2B pathways is given in Figure 1.3. The molecules that travel through the olfactory neurons reach the cerebrum and those which travel via the trigeminal pathway, reach the pons, and then further get distributed to the brain [26].

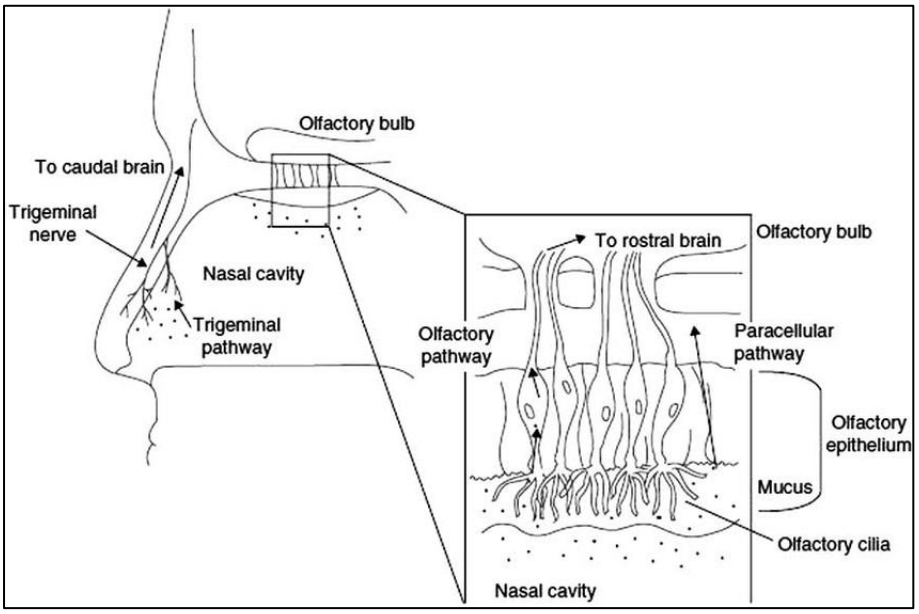

Figure 1.3 Schematic illustration of the N2B transport pathways

Source: Shinde, Rajshree & Jindal, Anil & Devarajan, Padma. (2011). Microemulsions and Nano emulsions for Targeted Drug Delivery to the Brain. Current Nanoscience. 7. 119-133. DOI: 10.2174/157341311794480282

1.3.2.1 Intracellular pathway

Intracellular uptake of molecules begins with its endocytosis by the neurons. The general process of endocytosis includes phagocytosis, pinocytosis and receptor mediated endocytosis [26,27]. Following endocytosis, molecules are enclosed within vesicles by the Golgi apparatus are transported along the soma (axon of the neuron). Following axonal transport, the vesicles containing molecules are exocytosed onto the post synaptic cleft of the olfactory bulb in the cerebrum, from the axon terminals. [28].

1.3.2.2 Extracellular uptake

The first step in extracellular mechanism of molecular transport is to cross the paracellular clefts between neurons and supporting cells of the nasal epithelium into the lamina propria. Molecule crossing the paracellular path must navigate the tight junctions (TJs) which act as the main barrier for paracellular transport. TJs are integral proteins which are attached to the actin cytoskeleton and an internal cell protein like zona occludins. The tightness/ permeability of the tissue is attributed to the TJs [29]. After reaching the lamina propria, the drug can reach many locations. To reach the CNS, the molecules diffuse through the perineural space which is anatomically in continuation with the subarachnoid space. This is one of the main pathways by which molecules can access the CNS. The transport of molecules via the perineural pathway is faster than intra-axonal transport [30].

Some molecules show uptake via N2B pathway, and some via nose to systemic circulation pathway. In 2019, Iwasaki *et al* showed that the drug's physiochemical properties played a role in preferentially getting absorbed by systemic circulation or via direct route [31].

1.4 Formulation strategies for N2B delivery of drugs

Over the years, several formulation strategies, excipients, and delivery devices to tailor delivery of molecules to the brain have been explored by researchers. All formulation strategies aim to address one or more distinct features of intranasal delivery – rapid clearance from the nasal cavity, poor permeability, high enzymatic activity, correct deposition of the formulation in the nose etc. Both conventional and non-conventional approaches have been used to enhance the transport of drugs to the brain via the nose. Different formulation strategies to enhance N2B delivery are briefly mentioned in the following sections:

1.4.1 Mucoadhesive systems

Mucoadhesive systems make use of mucoadhesive polymers like chitosan, Carbopol, pectin, polyacrylic acid etc. Mucoadhesive polymers act by delaying the clearance of formulations from the nose by interacting with the mucus. Mucoadhesive agents may also enhance permeation of molecules by facilitating the fluidization of the mucosal membrane [32].

1.4.2 Hydrogels and thermoresponsive drug delivery systems

Hydrogels are formed by crosslinked networks of hydrophilic, biodegradable polymers with a large amount of water. Hydrogels are biocompatible owing to their high-water content and their physicochemical properties, which show close resemblance to the native extracellular matrix. Hydrogels, due to their extensive crosslinking, show a viscosity high enough to delay their clearance from the nasal cavity.

Hydrogels can be formed in response to external stimuli such as temperature, pH, ions. Such hydrogels are called *in-situ* gels. *In-situ* gels are systems which undergo sol-gel transition at the site of administration. In addition to all the benefits offered

by hydrogels, *in-situ* gels have an additional benefit of precise dosing. During administration of the formulation, *in-situ* gels are in solution state. With a dose administration view point, liquid formulations are easier to administer than semisolid formulations [33].

1.4.3 Nanocarrier mediated N2B delivery

Over the last decade, tailoring of nanocarriers for delivery of molecules via N2B pathways has gained importance. It has been observed that both polymer and lipid-based formulations could help the drug transport through the nasal mucosa by increasing the retention time at the mucosal surface resulting in increased drug concentration at the site of interest. Nanocarriers can also protect susceptible drugs against metabolism by intranasal enzymes. Further, nanocarriers can be tuned to achieve desired release properties, desired retention time in the nasal cavity, and desired percent drug loading [32].

1.5 Problem definition and objectives of the research

Rufi is a BCS class 4 drug approved for the treatment of LGS in patients 1-17 years of age. Currently approved formulations of Rufi are oral tablets and oral suspension. Rufi suffers from moderately low oral bioavailability. This is due to its low dissolution rate and low solubility of Rufi in GI fluids [18]. At dosage <800 mg/day, oral bioavailability of Rufi was reported to be around 80%, which drastically dropped below 40% upon dose increment from 800 to 3200 mg/day [34]. Further, studies have reported that absorption of Rufi from the GIT is slow, with T_{max} of 4-6 h irrespective of the formulation used, or fed or fasted condition [18].

Once absorbed into the systemic circulation, in order to reach the brain, Rufi has to cross the BBB. This further reduces the amount of drug reaching the brain. To

overcome this problem, high doses of Rufi are being prescribed. This leads to intensification of peripheral side effects [2].

Rufi has been proven as an effective medication for management of LGS. Given its effectiveness in the management of LGS, it is likely to show a broad-spectrum activity in several other epilepsy syndromes. Overall, Rufi has shown a better efficacy and better safety profile than many other drugs used to treat epilepsy and LGS [13].

Considering the drawbacks of the currently available conventional formulations of Rufi, it is imperative to look for different formulations or a alternate routes for administration of Rufi. Extensive literature survey has shown that there have been no reports till now which aim to address the drawbacks of orally administered Rufi. N2B delivery is an attractive route, especially in case of molecules which suffer from problems with oral delivery.

The purpose of this research work was to improve the bioavailability of Rufi in the brain by administering it via i.n. route. Further, we wanted to compare different formulation approaches for delivering Rufi via i.n. route to the brain.

Therefore, the objectives of the current research work were envisaged as follows:

1. To develop and validate analytical and bioanalytical methods for the quantification of Rufi in various samples.

2. To formulate a nasal *in-situ* thermoresponsive gel for Rufi.

3. To design and optimize nanocarrier systems for Rufi using the concepts of design of experiments (DoE).

4. To perform physical and *in vitro* characterization for the optimized formulations of Rufi.

5. To carry out *in vivo* plasma and brain PK studies for the optimized formulations of Rufi administered via i.n. route and assess the direct uptake efficiency of various formulations.

2 DEVELOPMENT OF ANALYTICAL METHODS, THEIR VALIDATION, AND THEIR APPLICATION FOR QUANTIFICATION OF RUFINAMIDE IN DIFFERENT MATRICES

2.1 Introduction

Rufinamide (Rufi) is currently available as tablets and aqueous suspension, administered through oral route, for the treatment of LGS in patients in the age group of 1 to 17 years. Due to its low oral bioavailability and presence of BBB, a very small fraction of orally administered dose reaches the brain. In the current research it was envisaged to develop and optimize nano formulation loaded nasal *in-situ* gelling systems for improving delivery of Rufi to brain. In order to evaluate the physicochemical characteristics of the developed formulations like drug loading (DL), entrapment efficiency (EE), *in vitro* drug release, stability on storage etc., an aqueous HPLC method was developed and validated. To assess and compare the efficiency of the optimized formulations with conventional formulations, pharmacokinetic (PK) studies were planned to determine the brain time course and plasma time course of Rufi following the administration of optimized formulations and conventional formulations. For analysing the samples obtained from PK studies, a rapid, sensitive and precise bioanalytical method was developed and validated for accurate quantification of Rufi in both plasma and brain matrices.

For studying epilepsy, there is no single well-established animal model that describes it entirely. Few decades ago, cats and non-human primates were used to study antiepileptic drugs. In recent times, for *in vivo* assessment, rats and mice are the frequently used and also have become the default choice for antiepileptic drug (AED) testing [2]. There have been a few reported methods for analysis of Rufi in biological matrices. Few reports employing HPLC-UV method and LC-MS methods were published. M. Contin *et al*., have established a HPLC-UV method for estimation of Rufi along with other AEDs in human plasma and have reported the LOD and LOQ values as 0.5 μg/mL and 2.0 μg/mL respectively [35]. Z. Gáll *et al*.,

have worked on an LC-MS method for estimation of Rufi in rat, human, and rabbit plasma. The reported LC-MS method has several details to be monitored. Since the drug does not dissociate easily, its analysis using MS is challenging [36]. In addition to plasma, few researchers have gone further to analyse the drug in sparse matrices like dried blood spots. G la Marca *et al*., have worked on developing a spectrometric method for estimation of Rufi in dried blood spots [37].

Despite the advent of various detectors used for LC separation, UV detection still remains the most commonly used technique for bioanalysis. Moreover, it has also been reported that even though mass spectrometric techniques offer good sensitivity and selectivity, less expensive methods are generally preferred for routine analysis [38]. The biggest challenge faced by mass detectors is the analysis of neutral samples. In the work published by Z. Gáll *et al*., the authors have inferred that development of LC-MS methods for drugs that don't dissociate in the pH range between 2 to 9, like Rufi, is a major challenge [36]. Hence, it was necessary to develop in-house RP HPLC bioanalytical and analytical methods which would be rapid, sensitive and cost effective compared to the already reported methods.

Developing a robust, reproducible bioanalytical method involves monitoring and control of several variables right from the sample preparation stage to the analysis and detection stage. Traditionally, development of an analytical or bioanalytical method involves changing one factor/variable at a time when other factors/ variables remained constant (OFAT (one factor at a time) analysis). This was tedious, time consuming and rarely led to the optimal conditions for the developed method.

Design of Experiments (DoE) is a well-established concept in the pharmaceutical industry. Recently, researchers and regulatory bodies have urged the use of DoE in analytical method development. This came into effect when frequent method failures

arose during method transfers and in quality control departments. Failure of methods was largely attributed to the inadequate understanding between method variables and the method performance. Method performance of an analytical method includes parameters like selectivity, reproducibility, specificity, robustness etc. The purpose of implementing principle of DoE is to 1) identify the critical method variables affecting the method performance, 2) recognize a design space wherein the critical factors can be varied while still getting the desirable outcomes, and 3) find the optimum method conditions. Thus, DoE provides a deeper understanding of the effect of mix of variables on the desired level of method performance parameters, thereby avoiding the previously followed tedious OFAT analysis [37,39].

In the work presented in this chapter, we have described the development and optimization of a bioanalytical method for quantification of Rufi using Box Behnken Design (BBD), a response surface method (RSM). RSM is an advanced DoE technique in which changes in variables affecting a response of interest are represented in a 3D surface. This helps in finding the levels of variables that optimize one or more critical responses, and selecting the operating conditions to meet the specified responses. There are two kinds of RSMs – CCD (central composite design) and BBD (Box-Behnken design). BBD has fewer design points and consequently fewer experimental runs than CCD. Therefore, optimization using BBD involves less resources, less time and less cost for the same number of factors compared to CCD [40].

In this chapter, we have described the development and optimization of robust, reproducible and cost effective analytical and bioanalytical methods. The developed methods were validated as per the International Conference on Harmonization (ICH) and US FDA guidelines. To demonstrate the applicability of the developed

bioanalytical method, oral and intravenous (i.v.) PK studies of conventional formulations of Rufi were performed in male Wistar rats. The samples obtained from the PK studies were quantified to determine the plasma and brain time course of Rufi following oral and i.v. administration of the conventional formulations. The analytical method was used to analyse Rufi in samples obtained from DL and EE samples, *in vitro* studies and stability studies.

2.2 Materials and methods

2.2.1 Materials, chemicals and animals

Rufi and Piribedil (Internal standard (IS) for bioanalytical method) were gift samples from Glenmark Pharmaceuticals, Mumbai, India and Dr. Reddy's Laboratories, Hyderabad, India respectively. Acetonitrile (ACN) and methanol (MeOH) were purchased from Merck, Mumbai, India. Ammonium acetate and glacial acetic acid were purchased from SD Fine-Chem Limited, Mumbai, India and SRL Chemicals Ltd., Mumbai, India respectively. Throughout the analysis, high quality HPLC grade water obtained from our laboratory's Milli-Q water purification system (Millipore®, MA, USA) was used. All chemicals and solvents used were of HPLC grade. Male Wistar rats were procured from VAB biosciences (previously, Sainath Agencies) Hyderabad, India.

2.2.2 Instruments and chromatographic conditions

The HPLC system used was equipped with DGU-20A3R degasser, two solvent delivery LC-20AD pumps, a CTO-20AC column oven, a SIL- 20AC HT auto injector and an SPD-M20A photodiode array–UV detector (Shimadzu, Tokyo, Japan). LC Solutions, 1.25 version software was used to acquire and integrate data. Well calibrated, Eppendorf Research® Micropipettes (Eppendorf India Ltd.,

Chennai, India) were used during analysis. Measurement and adjustment of pH was done using pH meter (Model Eutech pH2700, Eutech Instruments, Mumbai, India). Vortex mixer (Model VX-200, Labnet International Inc., NJ, USA), sonicator (Model SONICA® 2200 MH, Soltec, Italy), refrigerated centrifuge (Model C- 24 BL, rotor head radius 70 mm, Remi, Mumbai, India), and deep freezer (Model BFS-345-S, Celfrost Innovations Pvt. Ltd., Mumbai, India), vacuum concentrator (SCANVAC Scan Speed 32, Labogne ApS, Lynge, Denmark) were used for sample preparation and storage during method development and validation. Throughout the analysis, the aqueous component of mobile phase was filtered through 0.22 μm filter membrane (Millipore®, MA, USA). Chromatographic conditions included a Phenomenex Kinetex C18 end-capped column (250×4.6 mm, 5 μm) maintained at 40 °C, with a mobile phase consisting of 10 mM ammonium acetate buffer (pH 4.7 ± 0.1, adjusted with HPLC grade glacial acetic acid) and HPLC grade ACN.

2.3 Method 1: Analytical method for quantification of Rufi in aqueous samples

2.3.1 Materials and instrument

Materials and instruments used were the same as described in sections 2.2.1 and 2.2.2.

2.3.2 Experimental

2.3.2.1 Development and optimization of method

The HPLC run conditions for the method were optimised based on system suitability test parameters *viz.* retention time, tailing factor and peak shape, theoretical plate number etc. For method optimization, factors like the ratio of aqueous to organic components of the mobile phase, pH of the aqueous component of mobile phase, and

other chromatographic conditions were varied to check their effect on the peak properties, sensitivity, and selectivity.

2.3.2.2 Chromatographic conditions

Chromatographic separation was optimized using a Phenomenex Kinetex C18 column (250 × 4.6 mm, 5 µm) maintained at 40 ºC. ACN was used as the organic component of the mobile phase while 10 mM ammonium acetate buffer of pH 4.7 constituted the aqueous component of the mobile phase. The ratio of ACN: buffer was 24:76% v/v. The mobile phase was run at 1 mL/min flow rate under isocratic conditions. Runtime of each sample was kept at 7 min. and the eluents were monitored at 220 nm using the PDA detector. The HPLC system was stabilized for about 1 h at 1 mL/min flow rate before actual analysis. The same was confirmed visually by baseline monitoring. The autosampler was set at 15 ºC and injection volume of 50 µL was used for all analysis.

2.3.2.3 Preparation of stock and standard solutions

Stock solution of Rufi was prepared at a concentration of 1 mg/mL in methanol. All subsequent dilutions were prepared using mobile phase as the solvent. The calibration standards were prepared with concentrations of Rufi ranging from 0.1 µg/mL to 10 µg/mL. Three quality control (QC) standards, lower quality control (LQC) = 0.35 µg/mL, middle quality control (MQC) = 0.75 µg/mL and higher quality control (HQC) = 8.5 µg/mL, covering lower, middle and higher concentrations within the selected linearity range were also prepared. Method validation parameters like precision, accuracy, and stability were assessed based on the replicate analysis of the three QC samples, LQC, MQC and HQC.

2.3.2.4 Method validation

2.3.2.4.1 Selectivity

The selectivity of the developed method was determined by spiking Rufi with the excipients used for the preparation of *in-situ* nasal gel and nanocarrier formulations. These samples were then vortexed for 5 min and centrifuged at 12000 rpm for 15 min. A clear supernatant was obtained which was diluted appropriately and analysed in HPLC. Further, blank samples (free of Rufi) were prepared and processed in a similar way and injected into HPLC system to check for the interference at the retention time of Rufi.

2.3.2.4.2 Linearity and range

The linearity plot was constructed for Rufi in the range of 0.1 to 10 µg/mL with seven concentrations (0.1, 0.25, 0.5, 1, 3, 7.5, and 10 µg/mL). Least-square regression analysis was performed for the mean peak area *vs* calibration standard concentrations of Rufi data six replicate (*n=6*) series. The coefficient of regression (R^2), slope and intercept values were determined and statistically evaluated. The least-square regression was used to determine the concentration of samples obtained in DL, EE, *in vitro* release studies and stability studies of the optimized nano formulation loaded *in-situ* gelling systems.

2.3.2.4.3 Sensitivity

LOD and LOQ can be used to define the sensitivity of the analytical method. LOD and LOQ are the minimum concentration of analyte that can be reliably detected and quantified respectively. LOD and LOQ were calculated by applying the following equations:

Equation 2.1

$$\mathbf{LOD} = \frac{\mathbf{3.3} \times \boldsymbol{\sigma}}{\boldsymbol{S}}$$

Equation 2.2

$$\mathbf{LOQ} = \frac{\mathbf{10} \times \boldsymbol{\sigma}}{\boldsymbol{S}}$$

Where '$\boldsymbol{\sigma}$' is the standard deviation of intercepts and '$\boldsymbol{S}$' is the mean of slopes obtained from *n=6* calibration curves.

2.3.2.4.4 Precision and accuracy

The accuracy and precision of the method were assessed by calculating intra-day and inter-day variations on three QC standards - LQC, MQC, and HQC. Accuracy was determined as per cent bias (%bias) and precision was determined as per cent relative standard deviation (%RSD). For intra-day repeatability, *n=3* replicates for each QC standard were analysed twice a day. For inter-day repeatability, similar samples were prepared and analysed on three consecutive days.

2.3.2.4.5 Stability

Stability of Rufi was assessed for three QC standards at autosampler conditions (autosampler maintained at 15 °C). Samples were prepared and stored separately in the autosampler. Samples were analysed for concentration of Rufi at 0 h (freshly prepared samples) and at 8,16 and 24 h after sample preparation. Per cent deviation (%deviation) of mean concentration of Rufi from freshly prepared samples was calculated and reported as %bias. Stability of the stock solution of Rufi (stored under refrigeration, 2-8 °C) was also assessed for a period of 30 days. All three QC standards were prepared from the stock solution of Rufi at 10, 20, and 30 days and their mean %deviation from 0^{th} day (freshly prepared and analysed) QC standard concentration was calculated.

2.3.3 Results and Discussion

2.3.3.1 Optimization of method conditions

During the preliminary method development trials, it was observed that the pH of the buffer had a minimal effect on the retention time and peak properties of Rufi. Given the pKa value of Rufi (Table 1.1), it undergoes very less ionisation in the pH range between 1-9. However, as the same chromatographic method conditions, with some necessary modifications, were planned to be used in bioanalytical method with Piribedil as the IS, 10 mM ammonium acetate buffer of pH 4.5 was selected as the aqueous phase in the aqueous analytical method.

For the selection of organic phase, both ACN and MeOH were tried. It was observed that with ACN the peak properties for Rufi were better than those obtained with MeOH. The proportion of organic phase in the mobile phase showed significant effect on the retention and peak properties of Rufi. With increase in organic phase component, the retention time of Rufi decreased. The method was optimized at the mobile phase composition of 75% v/v ammonium acetate buffer (10 mM, pH 4.7) and 25% v/v ACN. The flow rate of the mobile phase was optimised at 1 mL/min. At these chromatographic conditions, Rufi showed an average retention time of 6.06 ± 0.04 min. The injection volume for every sample was fixed at 50 µL. The peak parameters obtained for Rufi using the optimized method are given in Table 2.1. For further dilutions (from the stock solution of Rufi), it was observed that dilutions performed with pure organic solvent, either ACN or MeOH resulted in poor peak shape and peak properties. Dilutions prepared using solvent having the same composition as that of the mobile phase yielded the desired peak properties and good peak shape. Hence, all dilutions during sample preparation, were performed using optimised mobile phase composition as the diluent.

Table 2.1 Peak parameters for Rufi obtained for the analytical method

QC standard [a]	Retention time (min) (mean ± SD)	Tailing factor (mean ± SD)	Theoretical plate number (mean ± SD)	Peak Purity Index (mean)
LQC	6.07 ± 0.03	1.44 ± 0.10	18452 ± 1462	0.9994
MQC	6.05 ± 0.04	1.41 ± 0.08	20785 ± 2557	0.9995
HQC	6.05 ± 0.06	1.38 ± 0.10	21656 ± 1648	0.9994
Across all QC standards [b]	6.06 ± 0.04	1.41 ± 0.09	20297 ± 1656	0.9995

Note: standard deviation (SD); n=6 at each QC level.
[a] LQC = 0.35 µg/mL, MQC = 0.75 µg/mL, HQC = 8.5 µg/mL
[b] mean ± SD of the parameter for all QC samples (n=18)

2.3.3.2 Method validation

2.3.3.2.1 Selectivity

All spiked samples of Rufi showed a high peak purity index. Also, blank matrices showed no peak at the retention time of Rufi. Both these show the selectivity of the optimised method for quantification of Rufi. The overlaid chromatograms for Rufi are shown in Figure 2.1.

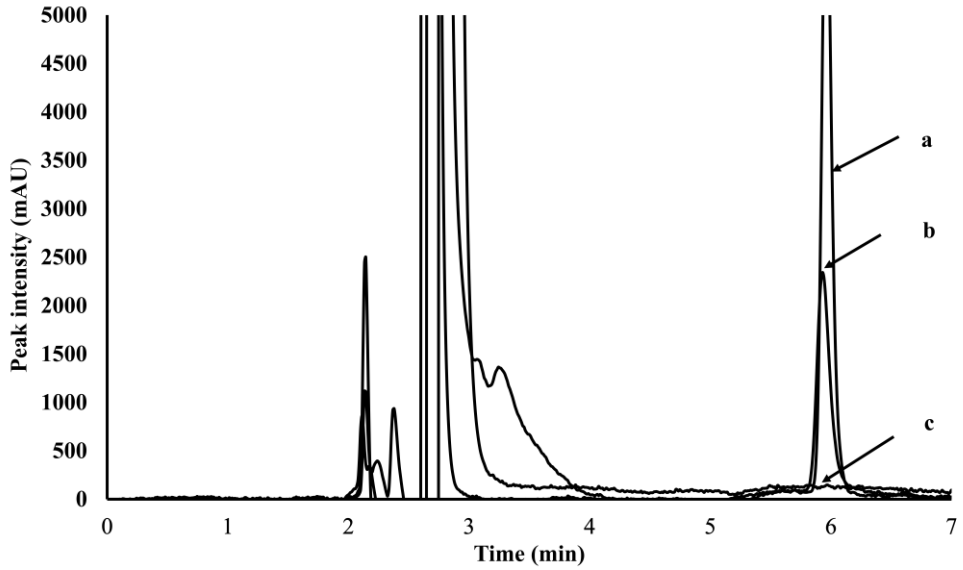

Figure 2.1 Overlaid chromatograms of a- Extracted Rufi from Rufi-Ch-NPs; b- pure Rufi (0.35 mcg/ml); c-extracted blank Rufi-Ch-NPs

2.3.3.2.2 Linearity and sensitivity

Calibration curves for Rufi were constructed using mean peak area vs calibration standard concentrations of six replicate series. The linear regression analysis was

performed on the average calibration curve (*n=6)*. The regression coefficient R^2 was observed to be 0.999. This indicates that the response (peak area) was linear in the concentration range of 0.1 to 10 µg/mL. The equation obtained from linear regression analysis of the mean calibration curve of six replicate series was: $\boldsymbol{Y = 124243.3 \times X + 1014.9}$, where '$\boldsymbol{X}$' and '$\boldsymbol{Y}$' are the concentration and the peak area of Rufi, respectively. The LOD and LOQ which were used as the measure of sensitivity of the method were 0.004 and 0.012 µg/mL respectively. The results for linear regression analysis and LOD and LOQ values are given in Table 2.2.

Table 2.2 Results obtained from linear regression analysis of the mean calibration and parameters indicating sensitivity of the analytical method

Parameter	Value [α]
Slope	124243.3 ± 1258.8
Intercept	1014.9 ± 161.6
CI of Intercept[#]	5414.96 to -5484.42
R^2	0.9995 ± 0.0007
F_{cal}	81857.99
Significance F	9.8991E-12
LOD	0.004 µg/mL
LOQ	0.012 µg/mL

Note: [a]Data is represented as 'mean ± SD' where appropriate. n=6 replicates of calibration curves.
[#]95% Confidence Interval (CI) of the intercept.
[*]F_{cal} value is greater than F_{tab} at 5% level of significance.

Mean %bias and %RSD were calculated for each concentration value using the standard calibration curve equation. The range of concentrations predicted by the equation, their mean deviation from the nominal concentration and their %RSD are given in Table 2.3.

Table 2.3 Linearity and range of Rufi using the standard calibration equation for the analytical method

Nominal concentration (µg/mL)	Range of predicted concentration[α] (µg/mL)	%RSD*	Mean %bias
0.1	0.090-0.096	1.9	5.9
0.25	0.237-0.243	0.8	3.8
0.5	0.495-0.500	0.3	0.2
1	0.958-0.985	1.1	2.9
3	3.00-3.096	1.1	-1.6
7.5	7.421-7.686	1.5	-0.4
10	9.851-10.078	0.8	0.4

Note: [α]Predicted concentration was calculated from the standard calibration equation (Section 2.3.3.2.2)
**Per cent Relative standard deviation (%RSD)*
#Accuracy is expressed as %bias. %bias was calculated as = [(predicted concentration – nominal concentration) × 100/nominal concentration].

2.3.3.2.3 Precision and accuracy

The variation in Rufi concentration measured by calculating %RSD for inter-day and intra-day precision was found to be not more than 2% and 4% respectively. Accuracy of the method was established by calculating the mean %bias (or mean %deviation of the predicted values from the actual values). The mean %bias was found to be not more than 2% for all QC samples. This indicates the accuracy and precision of the developed aqueous HPLC method for quantifying Rufi within the given concentration range. The data for accuracy and precision is given in Table 2.4.

Table 2.4 Accuracy and Precision for the analytical method

QC	Intra-day precision α (%RSD)			Inter-day precision* (%RSD)	Predicted concentration# (µg/mL) (mean ± SD)	Mean %biasβ
	Day 1	Day 2	Day 3			
LQC	3.12	0.73	1.63	1.92	0.35 ± 0.01	1.70
	2.13	0.57	0.57			
MQC	0.85	0.64	0.82	1.12	0.74 ± 0.02	-0.94
	0.82	1.66	0.45			
HQC	0.94	0.73	0.64	1.06	8.4 ± 0.10	-0.20
	0.64	0.78	1.05			

Note: [α]Intra-day repeatability was assessed by replicate analysis (n = 3) twice a day at each QC level
[*]Inter-day repeatability was assessed by replicate analysis (n=18) of each QC samples over three days
[#]Predicted concentrations were calculated from the best-fit regression equation (Section 2.3.3.2.2)
[β]Accuracy is expressed as %bias. %bias was calculated as = [(predicted concentration – nominal concentration) × 100/nominal concentration].

2.3.3.2.4 Stability

Autosampler stability for all QC samples showed less than 2% mean %bias from freshly prepared samples for a period of 24 h. In case of stock solution stability, all QC standards prepared from the stock solution of Rufi showed less than 2% mean %bias from freshly prepared stock solutions at the end of 30 days when stored at refrigerated conditions (2-8 °C). The results obtained from stability studies are shown in Figure 2.2.

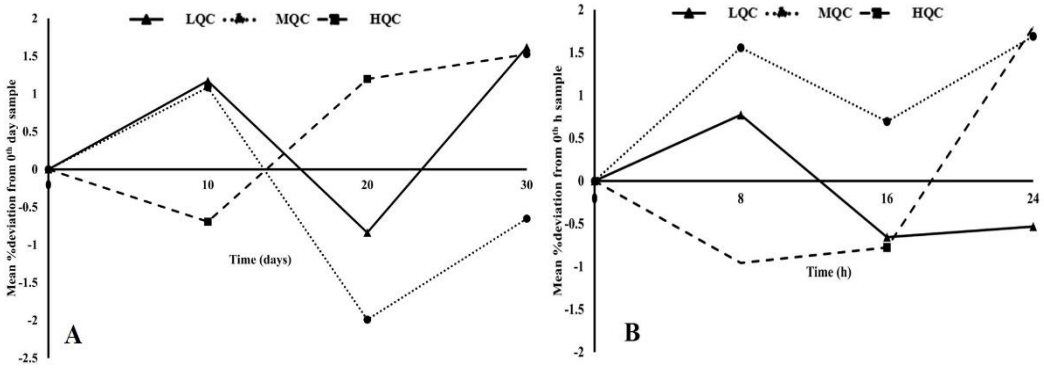

Figure 2.2 Stability data for Rufi, A: Stock solution stability over 30 days when stored at 2-8 ºC; B: Autosampler (maintained at 15 ºC) stability over a period of 24 h

2.4 Method II: Bioanalytical method for quantification of Rufi from plasma and brain samples

2.4.1 Materials and instrument

Materials and instruments mentioned in Sections 2.2.1 and 2.2.2 were used for bioanalytical method for quantification of Rufi.

2.4.2 Method development

2.4.2.1 Experimental design

Bioanalytical method for quantification of Rufi using HPLC with PDA detector was optimised using DoE. Critical factors affecting the method were identified from the literature and based on the preliminary trials performed. (Table 2.5). Peak area ratio of Rufi/IS ($\boldsymbol{Y_1}$) and theoretical plate number of the analyte (Rufi) peak ($\boldsymbol{Y_2}$) were taken as the critical responses. Optimization was carried out by employing Box Behnken design (BBD) using Design Expert software (Version 10.0.3, Stat-Ease Inc., Minneapolis, MN).

Table 2.5 Critical factors and their levels in optimization of bioanalytical method conditions

Factor Code	Critical factors	Levels		
		-1	0	+1
$\boldsymbol{X_1}$	pH of buffer	4	4.5	5
$\boldsymbol{X_2}$	wavelength for detection (nm)	215	220	225
$\boldsymbol{X_3}$	Proportion of buffer (% v/v)	82	85	88

Experiments runs were carried out in a randomized order to avoid bias. The goal of optimization was to achieve a maximum peak area ratio of analyte/IS which depicts sensitivity of the method (response $\boldsymbol{Y_1}$), and a good, sharp, well resolved drug peak indicated by theoretical plate number of the analyte (Rufi) peak (response $\boldsymbol{Y_2}$). The experiments were performed in a single block with a total of 17 runs which included 5 centre point runs. The mathematical models were expressed in the following form:

Second order polynomial equation:

Equation 2.3

$$\boldsymbol{R_i = b_0 + b_1X_1 + b_2X_2 + b_3X_3 + b_4X_1X_2 + b_5X_1X_3 + b_6X_2X_3 + b_7X_1^2 + b_8X_2^2 + b_9X_3^2}$$

And, third order polynomial equation:

Equation 2.4

$$\boldsymbol{R_i = b_0 + b_1X_1 + b_2X_2 + b_3X_3 + b_4X_1X_2 + b_5X_1X_3 + b_6X_2X_3 + b_7X_1^2 + b_8X_2^2 + b_9X_3^2 + b_{10}X_1X_2X_3 + b_{11}X_1^2X_2 + b_{12}X_1^2X_3 + b_{13}X_1X_2^2 + b_{14}X_1X_3^2 + b_{15}X_2^2X_3 + b_{16}X_2X_3^2 + b_{17}X_1^3 + b_{18}X_2^3 + b_{19}X_3^3}$$

Where, '$\boldsymbol{b_0}$' is the intercept, $\boldsymbol{R_i}$ is the response, '$\boldsymbol{b_i}$' (i = 1, 2, 3...n) are coefficients of individual linear, quadratic and cubic effects as well as their interactions and $\boldsymbol{X_1}$, $\boldsymbol{X_2}$, and $\boldsymbol{X_3}$ are the critical factors in the design.

2.4.2.2 Statistical treatment of data

The experimental data were analysed using regression analysis by employing Design Expert software. The statistical significance of the model was tested using the F test and lack of fit test at 5% level of significance ($\boldsymbol{\alpha}$=0.05). The F test was also applied to determine the significance of the regression coefficients obtained. Factor interactions having statistically insignificant coefficients were disregarded as model terms. R^2 and adjusted R^2 values were used to decide the quality of fit of the model equation.

2.4.2.3 Diagnostic plots, response surface plots and desirability function

Diagnostic plots like the residual plot and predicted response versus observed (actual) response plots were used to evaluate the model's predictive ability. Further, 3D response surface graphs were plotted for response variations against three factors.

For the purpose of finding the best possible conditions for both the responses, the desirability function was used. The experimental conditions yielding the highest desirability value were chosen as the optimized chromatographic conditions.

2.4.2.4 Collection of brain tissue and plasma from rats

Prior approval was obtained from the Institutional Animal Ethics Committee (IAEC) for all experiments involving animals (IAEC no.: BITS-Hyd/IAEC/2017/19). Blood was collected from retro-orbital plexus of male Wistar rats (240-260 g) using a rat bleeding capillary. Blood was collected into centrifuge tubes containing disodium EDTA solution (4.5% w/v) as the anticoagulant. For each unit volume of blood collected, 10% v/v disodium EDTA solution was added (i.e., for 200 µL of blood collected, 20 µL anticoagulant solution was added). Plasma was separated by centrifuging the blood samples in a cooling centrifuge at 3,500 rpm for 10 min at 4 °C and the supernatant (plasma) was carefully collected and stored at -20 °C until further use.

For collection of brain, the animals were anesthetised and exsanguinated via the abdominal artery in order to render the brain free of blood. Immediately the whole brain was collected, blotted to remove any residual blood or excess fluid, weighed and stored at -20 °C until further use.

2.4.2.5 Processing of brain and plasma samples from rats

Protein precipitation method was used to extract both Rufi and IS from both, plasma and brain matrices. To 90 µL of plasma, 10 µL of Rufi and 10 µL of IS working standards were added and vortexed for 2 min. Stock solution of both Rufi and IS were prepared in MeOH and ACN respectively. Any further dilutions from the stock solutions were made using the mobile phase. To the plasma spiked with Rufi and IS, 400 µL of MeOH (as precipitating agent) was added and vortexed for 2 min. This

was followed by centrifugation at 12,000 rpm for 10 min at 4 °C. The supernatant was transferred into a fresh microfuge tube (1.5 mL) and evaporated to dryness under vacuum. The dry sample was reconstituted with 100 µL of mobile phase, vortexed for 2 min and transferred into a sample loading vial and injected on to the column.

Tissue homogenization was employed as sample pre-treatment technique for processing rat brain samples. To the pre-weighed brain tissue (fresh or thawed), water was added at a level of 3 mL/g of brain tissue and homogenised at 12500 rpm for 3 min. The obtained brain homogenate was treated in the same way as plasma, except that protein precipitation was achieved with 200 µL of MeOH for 100 µL of homogenate (instead of 400 µL of MeOH as in the case of plasma).

2.4.2.6 Calibration curve and quality control standards

Stock solutions of 1 mg/mL for Rufi and IS were prepared separately in MeOH and ACN respectively. In order to study the absolute recovery from plasma and brain samples, working standard solutions were prepared from the above stock solutions using mobile phase as the solvent. For plasma and brain matrices, seven non-zero calibration standards of Rufi in the range of 0.1 – 2.0 µg/mL and 0.3 to 6.0 µg/g respectively, were prepared using aforementioned sample preparation procedure with IS at 1.0 µg/mL for plasma and 3.0 µg/g for brain tissue. For plasma, 0.15, 0.85, 1.85 µg/mL and for brain, 0.45, 2.55, 5.55 µg/g were considered as lower, medium and higher quality control samples (LQC, MQC and HQC) respectively.

2.4.2.7 Method validation

Methods developed for both matrices were validated according to the guidelines prescribed by the ICH and US FDA [41,42]. Selectivity, linearity, sensitivity, accuracy, precision, recovery, and stability were established for the method as a part

of validation using the QC standards. Selectivity of the method was shown by comparing chromatograms of blank (without Rufi and IS) plasma and brain homogenates against Rufi and IS spiked plasma and brain homogenate samples. The linearity of the method was assessed by plotting ratios of peak areas of Rufi/IS against the nominal concentration of Rufi. Unweighted linear regression analysis was used to fit the calibration curves. LOD and LOQ, the indicators of sensitivity of a method, were determined using the standard deviation of the y-intercepts and the average of the slopes of the six calibration curves (n=6). Accuracy, precision and intermediate precision were assessed for all QC standards for both matrices. Per cent bias was determined for assessing accuracy of the method. The observed concentration computed from area ratios using mean regression equation from the nominal concentration *(n=6)* was used to calculate %bias. As a measure of precision of the method, percentage relative standard deviation (%RSD) was computed by replicate analysis. Intra-day and inter-day precision were determined by analysing samples in triplicates, two times a day and on three different days, respectively. Recovery of the drug was assessed at all three QC levels in triplicates by comparing the peak area ratios of Rufi/IS obtained from extracted biological samples (from both matrices) against the areas obtained for analytical standards at the same nominal concentration.

Stability of Rufi in both plasma and brain matrices was evaluated under three different stress conditions: post-preparation auto-injector storage, freeze-thaw and long-term storage. Stability was determined by triplicate analysis at all QC levels in each of the abovementioned conditions. Post-preparative auto-injector stability (maintained at 15 °C) was assessed by analysing the same set of samples at 0, 8, 16 and 24 h. Three freeze-thaw cycles (stored at -20 °C) were performed on three

consecutive days and one set of samples were analysed after each cycle. Long-term stability was determined by analysing one set of samples that were stored at -20 °C on 9^{th}, 18^{th}, 27^{th} day after sample preparation. The %deviation from the mean concentrations observed at zero time was calculated.

2.4.2.8 Single dose intravenous and oral pharmacokinetic (PK) study

Male Wistar rats weighing 240-260 g were used for the study *(n=4)*. Before conducting any study, all animals were housed in cages, and allowed to accustom to the animal house of the institute which is maintained at 22 ± 1 °C room temperature; 55 ± 10% relative humidity; 12 h light/dark cycle. Food and water were provided *ad libitum*. 12 h prior to dosing, all the animals were kept in fasted conditions in separate cages. Rats being coprophages, (animals that feed on their own faeces) they were mounted on a platform inside the cage to prevent coprophagy. 4 h after dosing, rat chow diet was provided ad libitum. The intended dose of Rufi for intravenous (i.v.) pharmacokinetic study, was solubilized (at a level of 0.25 mg/mL) in an optimized solvent mixture of N-Methyl-2-pyrrolidone (NMP), Polyethylene glycol (PEG 400), and water at volume ratios of 0.5:6.5:3 just before the commencement of study. Injection of the dose was done through tail vein in rats. Rufi was administered at a dose of 0.5 mg/kg, at a dose volume of 2 mL/kg. For oral dosing, a suspension of plain Rufi was prepared in 0.2% w/v methyl cellulose (grade 400 cp). Retro-orbital puncture technique was employed for blood collection. Blood was collected in centrifuge tubes, containing disodium EDTA (4.5% w/v) as an anticoagulant, at 0 (before administration of the drug), and 5, 15, 30, 60, 120, 240, 360, 480,720, 1200, and 1440 minutes following i.v. bolus administration of Rufi. Blood was withdrawn at the same time points after oral administration also. 200 µL of blood was collected from every animal at each time point. Time points for collecting brain samples after

i.v. dosing, were decided on the basis of i.v. plasma concentration versus time profile of Rufi. At 30, 60, 240, and 480 min post dosing, following blood sampling, four animals at each time point were sacrificed and brain tissues were collected from all the animals. At the same time points brains were harvested after oral administration. The developed and validated method as described in the previous sections was used for processing and analysing all the samples. A plasma concentration versus time profile was obtained after analysing the samples. In order to determine the compartment model followed by Rufi, PK data from the study was fit into different compartmental models. PK parameters like C_{max}, $t_{1/2}$, $AUC_{0\text{-}tlast}$, V_{ss} were computed using non-compartmental analysis in Phoenix WinNonlin software (Version 7.0, Pharsight Corporation, NC, USA).

2.4.3 Results and discussion

2.4.3.1 Experimental design

The factor levels and experimental results obtained for BBD are shown in Table 2.6. The data was analysed using Design Expert software. The data for responses were fitted in several models. For each response, model showing the highest F_{cal} value was chosen and validated using ANOVA.

Table 2.6 Actual composition of the 17-runs generated by BBD and their observed responses, peak area ratios and theoretical plates of analyte peak

Run*	pH of buffer (X_1)	Wavelength of detection (X_2), (nm)	Proportion of buffer (X_3), (% v/v)	Peak area ratio# (Y_1)	Theoretical plate number^ (Y_2)
1	4.5	225	82	0.404	23011
2	4	215	85	0.501	25613
3	4	220	82	0.281	23761
4	4.5	215	88	0.543	25479
5	4.5	220	85	0.586	26118
6	4.5	220	85	0.547	26283
7	5	225	85	0.436	19105
8	4.5	220	85	0.581	26009
9	5	220	82	0.465	23405
10	4	225	85	0.401	26831
11	4.5	215	82	0.577	22882
12	4.5	220	85	0.572	25699
13	4.5	225	88	0.384	26527
14	4.5	220	85	0.557	25996
15	4	220	88	0.426	27201
16	5	215	85	0.706	14752
17	5	220	88	0.445	24035

*Note: * The run order was randomized by the software before performing the experiments;*
 # peak area ratio of analyte/IS (Rufi/IS);
^ theoretical plate number of analyte (Rufi) peak.

2.4.3.2 Statistical treatment of data

Statistical evaluation and fit of the model for both the responses is shown in Table 2.7. In case of drug peak area ratio (response $\boldsymbol{Y_1}$) quadratic model was found to be significant with F value of 43.14 (P<0.0002). While a cubic model was found to be a better fit in the case of drug peak theoretical plate number (response $\boldsymbol{Y_2}$) with F value of 185.15 (P<0.0002) indicating that both the models were a good fit for the corresponding responses. An additional test that is often used to check if the obtained model is adequate in predicting the responses in the experimental space is the 'lack of fit 'test. As shown in the Table 2.7, the F_{cal} values and P values for lack-of-fit were 5.49 and 0.0667 for response $\boldsymbol{Y_1}$ and 4.63 and 0.0977 for response $\boldsymbol{Y_2}$, respectively. Insignificant 'lack-of-fit' values indicate that the model equation obtained is adequate in predicting responses. Adjusted R^2 value tests the goodness of fit of the model. Higher the value, better is the correlation between values predicted

by the model and actual values. The Adjusted R^2 value for response $\boldsymbol{Y_1}$ was 0.927 and for response $\boldsymbol{Y_2}$ was 0.992. The significance of each coefficient was determined by the *P* value. Terms showing $P<0.05$ were included in the model equation. The model equation for responses in terms of coded factors is given below.

Equation 2.5

$$\textbf{Peak area ratio } (Y_1) = 0.57 + 0.056X_1 - 0.088X_2 + 0.009X_3 - 0.042X_1X_2 - 0.041X_1X_3 - 0.065{X_1}^2 - 0.099{X_3}^2$$

Equation 2.6

$$\textbf{Theoretical plate number of analyte peak } (Y_2) = 26021 - 880.5X_1 + 1528.4X_3 + 783.8X_1X_2 - 702.5X_1X_3 - 2160.1{X_1}^2 - 2285.7{X_2}^2 + 739.6{X_3}^2 + 1392.7X_1^2X_2 - 510.9X_1^2X_3 - 3766.2X_1X_2^2 + 294.4X_2X_3^2$$

Table 2.7 Regression coefficients and statistical analysis for Box Behnken design for bioanalytical method

Source	Peak Area Ratio ($\boldsymbol{Y_1}$)			Theoretical plate number ($\boldsymbol{Y_2}$)		
	SS	df	P value	SS	df	P value
Model	0.163	7	6.08E-06	1.60E+08	11	8.53E-06
$\boldsymbol{X_1}$	0.0247	1	0.000143	3.10E+06	1	0.001511
$\boldsymbol{X_2}$	0.062	1	3.81E-06			
$\boldsymbol{X_3}$	0.0007	1	0.332701	9.34E+06	1	0.000113
$\boldsymbol{X_1X_2}$	0.007	1	0.007901	2.46E+06	1	0.00254
$\boldsymbol{X_1X_3}$	0.007	1	0.009202	1.97E+06	1	0.004086
$\boldsymbol{X_1^2}$	0.0178	1	0.000472	1.96E+07	1	1.85E-05
$\boldsymbol{X_2^2}$				2.20E+07	1	1.4E-05
$\boldsymbol{X_3^2}$	0.0412	1	1.96E-05	2.30E+06	1	0.002927
$\boldsymbol{X_1^2X_2}$				7.76E+06	1	0.000177
$\boldsymbol{X_1^2X_3}$				5.22E+05	1	0.049787
$\boldsymbol{X_1X_2^2}$				2.84E+07	1	7.49E-06
$\boldsymbol{X_2X_3^2}$				3.47E+05	1	0.090007
Residual	0.005616	9		3.94E+05	5	
Lack of Fit	0.004573	5	0.123833	2.11E+05	1	0.097672
Pure Error	0.001043	4		1.83E+05	4	
Cor Total	0.168556	16		1.61E+08	16	

2.4.3.3 Response surface plots and desirability function

3D response surface plots (Figure 2.3) are a graphical representation of the regression equation. Effect of independent variables on the responses can be visualized easily using such plots. Figure 2.3A shows interaction between pH and wavelength with respect to its effect on drug peak area. From the 3D response surface plots, it can be observed that from pH 4.6 to 5 for wavelengths 215 to 218 nm the peak area is maximum. In case of number of theoretical plates (Figure 2.3 B), high number of theoretical plates was observed for pH 4 to 4.8 and buffer proportion 85.0% to 88.0%.

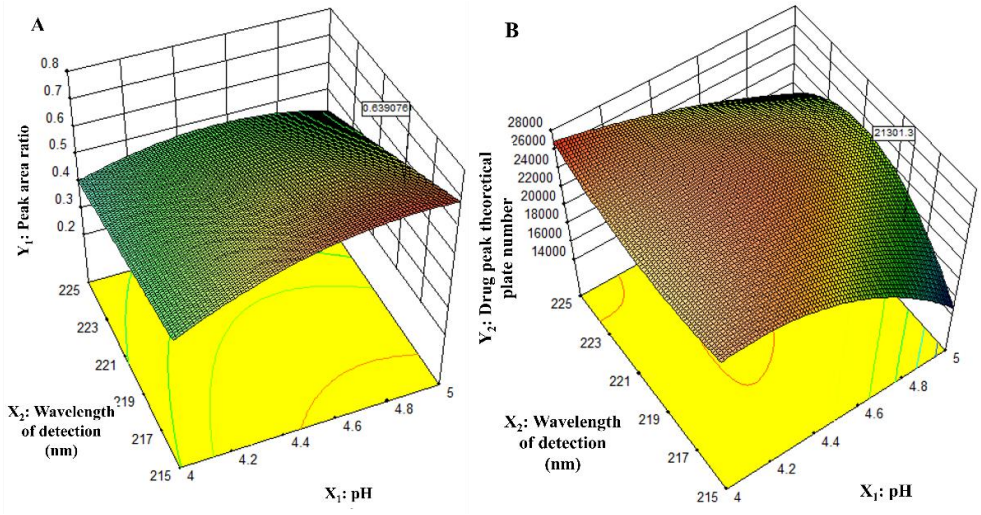

Figure 2.3 3D response surface plots showing the effect of significant critical factors on responses, (A) Peak area ratio ($\boldsymbol{Y_1}$) and (B) Theoretical plate number of analyte ($\boldsymbol{Y_2}$).

2.4.3.4 Determination of optimized method and its validity

A high desirability function (0.971) was obtained for the optimized method. The optimal conditions for critical factors for obtained the desired responses were as follows: pH of buffer: 4.7, wavelength of detection: 215 nm, buffer proportion: 84.7% v/v. Based on the optimised conditions suggested by the desirability function, the method was validated again according to ICH guidelines as described in section 2.4.2.7 and used for further analysis of pharmacokinetic and stability samples. Six

trials were performed with the optimized conditions and the responses in terms of peak area ratio ($\boldsymbol{Y_1}$) and theoretical plate number of analyte ($\boldsymbol{Y_2}$) were determined. Predicted responses were obtained by substituting the values of the critical factors suggested by desirability function in the corresponding regression models. The observed data was compared with predicted data using Wilcoxon signed rank test. The mean values of peak area ratio ($\boldsymbol{Y_1}$) and theoretical plate number of analyte ($\boldsymbol{Y_2}$) were not significantly different than the values predicted by the model (P >0.05).

2.4.3.5 Sample preparation and drug extraction

Protein precipitation, liquid-liquid extraction (LLE) and solid phase extraction (SPE) are the most commonly used extraction techniques for small molecules from plasma [43]. Protein precipitation was thought to be an appropriate method for extracting Rufi from plasma. Given its low log P value of 0.65, rather than SPE and LLE, protein precipitation is a better, and a greener option that uses lesser organic solvents for drug extraction. It is also inexpensive and fast. Trials with protein precipitation were done using MeOH and ACN as protein precipitating agents for extracting Rufi and IS form plasma and brain matrices.

Initial trials were carried out with 1:2, 1:3 and 1:4 ratios of plasma: MeOH. Broad peaks were observed with ACN as precipitating agent at all three volume ratios and hence was not considered as suitable precipitating agent. When MeOH was used at plasma: MeOH ratios of 1:2 and 1:3 the mean recoveries obtained were 75% and 80% respectively. Recoveries greater than 85% were observed with 1:4 volume ratio of plasma to MeOH. However, the peak shape was poor, which may be because of some MeOH soluble impurities interfering with the analyte peak. Moreover, after adding 1:4 of plasma: MeOH, the sensitivity of the method decreased due to dilution of the analyte with higher amount of MeOH. Hence, evaporating the sample and

reconstituting it with mobile phase (100 µL) was tried. Peak shape and sensitivity were found to be good. Hence, protein precipitation with 1:4 volume ratio of plasma: MeOH, followed by evaporating and reconstituting the samples with mobile phase was selected as the final plasma sample preparation method.

Literature review had revealed that distribution of Rufi into the brain is uniform and not concentrated to any specific part of the brain [2]. Therefore, for analysis, the whole brain was collected and processed. Subsequently, brain tissues were homogenised using high quality water and further subjected to processing. Since brain is a soft tissue, a rotating blade homogeniser was sufficient to break it down. Homogenisation was done in water because of its ease of preparation and its lysing effect on cells due to low osmotic pressure. Lysing effect of water, coupled with mechanical forces of the homogeniser, yielded a fine, uniform suspension of both intracellular and intercellular components of brain [44]. Hence, water was used for brain homogenisation. Few trials for optimization of quantity of water for homogenisation were carried out with 2, 3 and 5 ml/g of brain tissue. With a volume of 2 ml water per gram of brain tissue, the homogenate obtained was coarse and viscous and hence difficult to process, leading to low and variable recoveries (in the wide range of 55-85%). The homogenate obtained with 1:3 brain tissue to water ratio was found to be fine, uniform and less viscous. Recoveries for QC samples were assessed at 1:4 and 1:2 volume ratio of brain homogenate: MeOH (precipitating agent). Recoveries were high and reproducible with both 1:4 and 1:2 volume ratio of brain homogenate: MeOH, but the peak shape was not good which may be because of some MeOH soluble impurities interfering with the analyte peak. Therefore, MeOH was evaporated and the residue obtained was reconstituted using mobile phase. Hence, the same was adapted for further studies. Protein precipitation with

1:2 volume ratio of brain homogenate to MeOH, followed by evaporation and reconstitution with mobile phase was used as the method for extraction of Rufi and IS from brain tissue. For choosing an internal standard for the method, drugs like Telmisartan, Cilnidipine, Piribedil were tried. Piribedil was selected as the IS because, at the given chromatographic conditions, IS eluted after the drug and just before the run ended which is a desired property while using an internal standard. Secondly, the technique (protein precipitation followed by evaporation and reconstitution) for sample processing, yielded recoveries greater than 85% for both, Rufi and IS.

2.4.3.6 Method validation

2.4.3.6.1 Selectivity

Protein precipitation method followed by evaporation and reconstitution of samples was found to be effective and reliable for the estimation of Rufi in plasma and brain matrices. No interfering peaks were seen at the retention times of Rufi or IS in both the matrices. Figure 2.4 shows overlays of chromatograms for both plasma and brain of their respective blanks, QC standards, and *in vivo* pharmacokinetic samples.

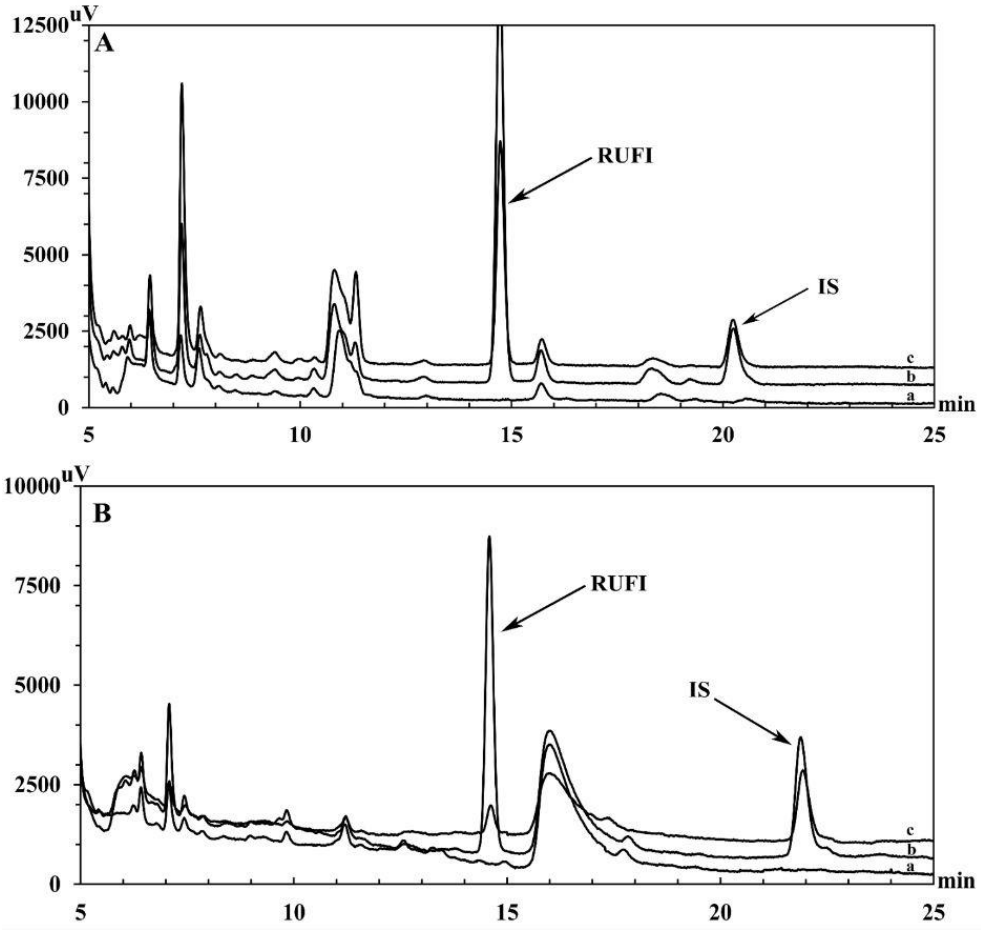

Figure 2.4 Overlaid chromatograms of A: plasma, B: brain a: blank matrix; b: QC standard; c: *in vivo* pharmacokinetic sample.

2.4.3.6.2 Linearity and sensitivity

The calibration curves were linear in the selected concentration range of 0.1 – 2.0 µg/mL and 0.3 to 6.0 µg/g for plasma and brain matrices respectively, with IS at 1.0 µg/mL for plasma and 3.0 µg/g for brain tissue (mean regression coefficient, R^2=0.9985). Calibration curves were constructed with peak area ratios of Rufi/IS on vertical-axis and concentration (µg/mL in case of plasma and µg/g in case of brain) of Rufi on horizontal-axis. From the linear regression analysis, slope, intercept and R^2 values were determined and the results are summarized in Table 2.8. SEE (Standard Error of Estimate) shows low error values, indicating that the developed methods were highly precise. In both the cases, the F_{cal} values were found to be

significantly greater than the F_{crit} (6.608 at α=0.05), further indicating that the regression was good.

LOD (Equation 2.1) and LOQ (Equation 2.2) were used to indicate the sensitivity of the method. The LOD value for Rufi in plasma and brain was found to be 0.019 µg/mL and 0.037 µg/g respectively while the LOQ value for Rufi in plasma and brain was found to be 0.060 µg/mL and 0.111 µg/g respectively (Table 2.8). Thus, the lower limit of quantification values i.e., 0.1 µg/mL and 0.3 µg/g for plasma and brain respectively can be considered to be reliable, accurate and reproducible. Also, the LLOQ values were adequate enough to estimate Rufi in a pharmacokinetic study performed in rats.

Table 2.8 Results obtained from linear regression analysis of calibration curves, LOD and LOQ for Rufi

Parameter	Plasma	Brain
Slope (mean ± SD)	1.24 ± 0.018	0.56 ± 0.025
Intercept (mean ± SD)	0.024 ± 0.008	0.012 ± 0.002
R^2	0.9985	0.9984
SEE	0.02	0.091
95% CI of Intercept	-0.05 to 0.02	-0.15 to 0.13
F_{cal}^{α}	4922	3991
LOD	0.019 µg/mL	0.037 µg/g
LOQ	0.060 µg/mL	0.111 µg/g

Note: Standard deviation (SD), regression coefficient (R^2), standard error of estimate (SEE). n = 6 in all cases.

[α] The F_{cal} value is significantly greater than F_{crit} (F_{crit} = 6.608, at α = 0.05), implying a good regression.

[β] LOD = 3.3 × (SD of intercepts/mean value of slopes); LOQ = 10 × (SD of intercepts/mean value of slopes).

2.4.3.6.3 Accuracy and Precision

In both matrices, the QC samples in all cases had %bias ranging from -0.19 to 0.67 indicating that the method was accurate in quantification of Rufi (Table 2.9). In the repeatability study, the %RSD for intra-day precision was not more than 5.90, and that for inter-day precision was less than 6.38 across all samples (Table 2.10). %RSD

values were within acceptable limits, thereby indicating the intermediate precision of the methods for plasma and brain.

Table 2.9 Accuracy, precision and absolute recovery data of proposed methods for Rufi

QC level*	Predicted concentration[α]			Mean %bias[β]	%Recovery[γ]	
	Range	mean ± SD	%RSD		mean ± SD	%RSD
Plasma (µg/mL)						
LQC	0.142 – 0.175	0.150 ± 0.007	4.66	0.38	89.64 ± 2.01	2.24
MQC	0.803 – 0.873	0.846 ± 0.028	3.30	-0.45	90.21 ± 3.64	4.04
HQC	1.725 – 1.943	1.861 ± 0.086	4.62	0.62	88.37 ± 1.81	2.05
Brain (µg/g)						
LQC	0.432 – 0.469	0.449 ± 0.014	3.11	-0.19	90.37 ± 2.17	2.40
MQC	2.486 – 2.617	2.567 ± 0.042	1.63	0.67	87.16 ± 3.24	3.72
HQC	5.446 – 5.622	5.528 ± 0.062	1.12	-0.39	91.03 ± 2.81	3.08

Note: Standard deviation (SD), Per cent relative standard deviation (%RSD), n = 6 samples in all cases.

**For plasma, LQC, MQC, HQC are 0.150, 0.850, 1.850 µg/mL and IS = 1.0 µg/mL. For brain, LQC, MQC, HQC are 0.450, 2.550, 5.550 µg/g and IS = 3.0 µg/g.*

[α] Predicted concentrations of Rufi were calculated using linear regression equation, given in µg/mL for plasma and µg/g for brain.

[β] Accuracy is given as %bias = [100 × (predicted concentration – nominal concentration)/nominal concentration].

[γ] %Recovery = [(Peak area of plasma standard/peak area of aqueous analytical standard of same concentration) ×100].

Table 2.10 Results for intermediate precision study for bioanalytical method

Matrix	QC level*	Intra-day repeatability (%RSD) (*n* = 3)			Inter-day repeatability (%RSD) (*n*=18)
		Day 1	Day 2	Day 3	
Plasma	LQC	4.27	1.54	5.20	6.38
		1.50	2.14	5.90	
	MQC	2.03	1.13	1.39	3.87
		2.25	2.69	3.98	
	HQC	3.08	0.43	2.17	4.86
		3.30	3.18	3.37	
Brain	LQC	1.52	2.49	1.46	4.28
		0.88	1.36	2.96	
	MQC	2.16	0.43	2.06	4.05
		1.64	2.86	1.52	
	HQC	1.91	0.97	1.95	3.41
		2.58	1.03	2.43	

Note: Per cent relative standard deviation (%RSD); Intra-day repeatability was assessed by replicate analysis (n=3) twice a day at each QC level. Inter-day repeatability was assessed by replicate analysis (n=18) of each QC samples over three days. For plasma, LQC, MQC, HQC are 0.150, 0.850, 1.850 µg/mL and IS = 1.0 µg/mL. For brain, LQC, MQC, HQC are 0.450, 2.550, 5.550 µg/g and IS = 3.0 µg/g

2.4.3.6.4 Recovery

The absolute recovery of Rufi was shown with all QC samples. Drug peak areas from plasma and brain matrices spiked with Rufi at all QC levels were compared against equivalent aqueous samples. The %recovery was within 87.16 to 91.03% with %RSD not more than 4.04 in all cases (Table 2.9). Mean recovery of IS was found to be 92.36% with %RSD less than 2.37. Thus, the extraction efficacy of the method and MeOH as a protein precipitating agent was elucidated by high mean recovery values.

2.4.3.6.5 Stability

The stability of Rufi in both the matrices was evaluated using QC samples under different stress conditions. The results are shown in Figure 2.5. No significant degradation of Rufi in plasma samples was observed under all three stress conditions i.e., freeze thaw (-20 °C) stability studied for 3 cycles on 3 consecutive days, long term stability (-20 °C) for a period of 27 days and auto-injector stability (at 15 °C) study of the processed plasma samples over 24 h post-preparation. The deviation from zero-time samples in all the stress conditions was observed to be in the range of -2.87 to 3.01%.

Rufi spiked brain samples showed no degradation with auto-injector over 24 h, with %deviation from zero-time samples in the range of -1.98 to 2.65%. In case of freeze-thaw stability and long-term stability studies, the %deviation with respect to zero-time samples was between -1.65 to 3.53% up to 1st freeze-thaw cycle and 18th day samples. However, the samples showed interfering peaks and noise around the retention times of both Rufi and IS with rest of the 2 freeze-thaw cycles and the 27th day long-term stability samples. Hence, it can be concluded that when stored at -20

ºC, the rat brain samples were stable for one freeze-thaw cycle, over a period of 18 days. At room temperature, the stock solution was stable for a period of 48 h.

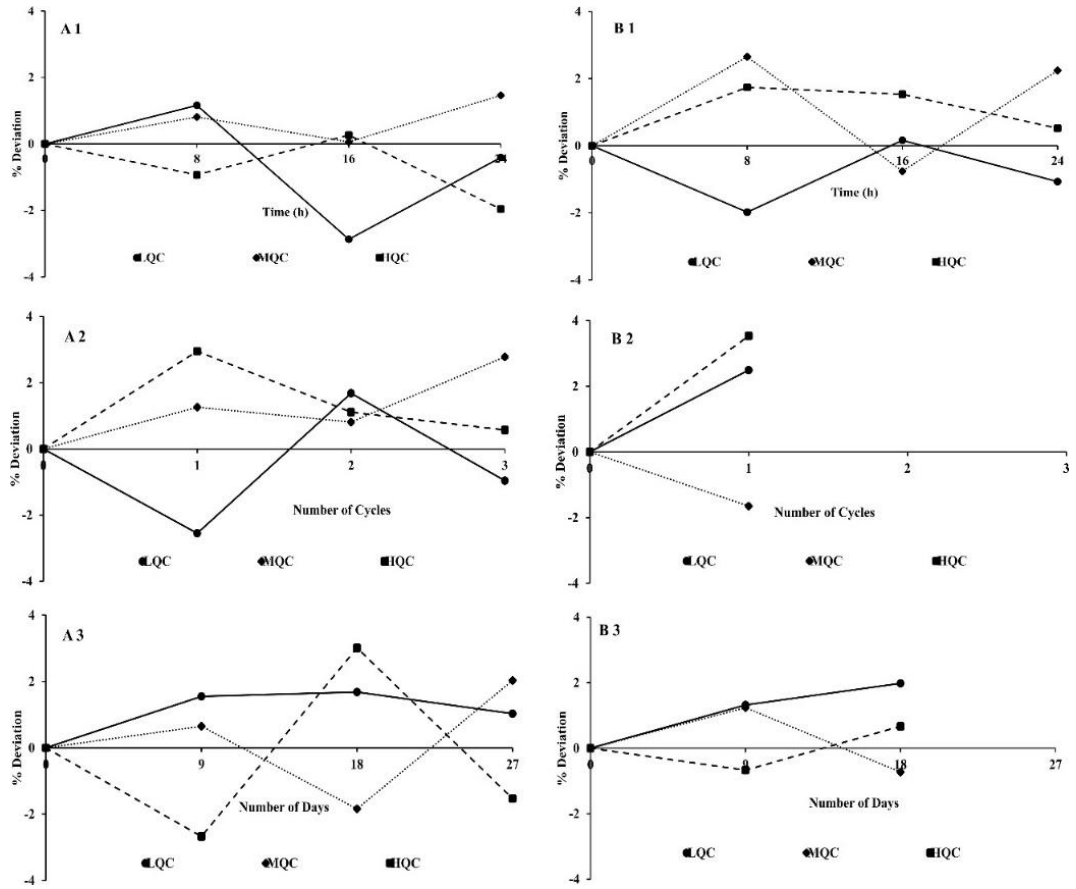

Figure 2.5 Stability of biological QC samples

A1 and B1: Autosampler stability in plasma and brain respectively; A2 and B2: Freeze thaw stability in plasma and brain respectively; A3 and B3: Long term stability in plasma and brain respectively Single dose i.v. bolus and oral pharmacokinetics of Rufi in male Wistar rats

2.4.4 *In vivo* PK studies of Rufi in rats

Plasma time course of Rufi obtained from a single i.v. bolus dose (0.5 mg/kg) was found to follow a mono exponential equation, $\boldsymbol{C = 0.844 \times e^{-0.0011t}}$ with R^2 value of 0.996. Where '$\boldsymbol{C}$' is the concentration of drug in the plasma at any time '$\boldsymbol{t}$'. Also, the predicted and observed values for one compartment model were in close agreement. In the residual plots, the residuals were found to be randomly scattered on both sides of the zero line with no specific pattern. This indicates that the drug

follows one compartment open model in male Wistar rats as determined by the software. The plasma and brain distribution profiles on single i.v. bolus dose administration is shown in Figure 2.6. The pharmacokinetic parameters obtained by non-compartmental analysis (Table 2.11) were ($AUC_{0\text{-}tlast}$) = 607.47 µg/mL*min, mean retention time (MRT) = 607.2 min, elimination half-life ($t_{1/2}$) = 332.3 min. The $AUC_{0\rightarrow tlast}$ in plasma was found to be 91.9% of $AUC_{0\text{-}\infty}$. This indicates that the developed analytical method is very sensitive and can capture almost the entire time course of Rufi in rat plasma at the given dose. The $AUC_{0\rightarrow tlast}$ of orally administered Rufi was 2071.0 ± 169.8 min×(µg/mL). The absolute bioavailability of Rufi was 34.1%, and the brain bioavailability was 31.3%.

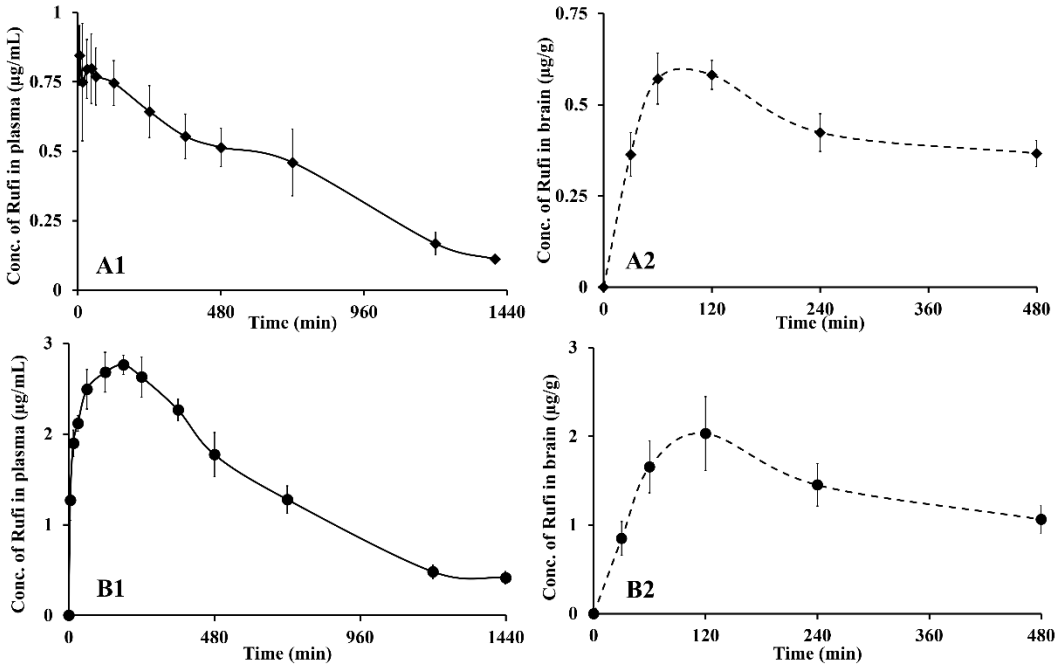

Figure 2.6 I.v. and oral PK profiles for Rufi

A1 and A2: Rufinamide PK profiles for plasma and brain respectively following i.v. administration (0.5 mg/kg); B1 and B2: Rufinamide PK profiles for plasma and brain respectively following oral administration (5 mg/kg); All data points are represented as mean ± SD of n=4 observations; n=4 animals were used for plasma PK, and for brain PK n=4 animals' brains were used at every time point.)

Table 2.11 PK parameters of Rufi following i.v. bolus administration (0.5 mg/kg) and oral administration (5 mg/kg) in rats

Matrix	PK Parameter	Units	Route of administration	
			i.v. bolus	oral
Plasma	$AUC_{0\rightarrow tlast}$	min×(µg/mL)	607.47 ± 90.2	2071.0 ± 169.8
	C_{max}	µg/mL	0.844 ± 0.17	0.82 ± 0.11
	T_{max}	min	5	180-240
	MRT	min	607.2 ± 9.0	478.5 ± 14.2
Brain	$AUC_{0\rightarrow tlast}$	min×(µg/g)	214.8	671.36
	C_{max}	µg/g	0.58	2.03
	T_{max}	min	120	120

Note: All values are given as mean ± SD of n=4 replicates. The plasma data is represented as mean ± SD. The brain data is represented as single values. The time points in the brain PK profile were an average of the pooled concentration data obtained from 4 animals. the average brain concentration profile was constructed from the pooled concentration data and hence, PK parameters like $AUC_{0\rightarrow tlast}$ *and MRT were calculated as single values without standard deviation.*

2.5 Conclusion

Simple, rapid and sensitive HPLC analytical method was developed for quantification of Rufi from various *in vitro* studies. The analytical method was rapid with short run time of 10 min. It was validated in the concentration range of 0.1-10 µg/mL. The current chapter also describes the development and validation of rapid, sensitive and a cost-effective method for analysis of Rufi in rat plasma and brain matrices. Statistical tools and the design of experiments concept facilitated in finding the critical factors that affected the method, and their optimization which eventually led to the precise conditions required for desired responses. Further, the method was found to be accurate, precise, linear, selective, and highly sensitive. I.v. and oral PK studies were performed as an application of the method. The drug's course in the brain on i.v. and oral dosing was also elucidated. Altogether, the method can be used for routine estimation of Rufi in rat plasma and brain matrices owing to its simple, cost -effective, yet highly sensitive nature. This method was further employed in analysing samples obtained from *in vivo* PK studies performed for evaluating the *in vivo* performance of different formulations given in the subsequent chapters.

3 RUFINAMIDE LOADED THERMORESPONSIVE NASAL *IN-SITU* GELLING SYSTEMS: DESIGN, OPTIMIZATION, *IN VITRO* AND *IN VIVO* EVALUATION

3.1 Introduction

Over the last two decades, researchers have shown promising results with direct nose to brain delivery of small molecules. Nasal delivery of drugs can circumvent all the problems associated with oral absorption and gastrointestinal (GI) side effects of the drugs administered through the oral route. Drugs administered through intranasal (i.n.) route, if deposited in the appropriate region of the nose (olfactory region), reach the central nervous system (CNS) via several direct and indirect pathways. The direct pathway of nose to brain delivery is thought to be mediated predominantly by olfactory neurons, circumventing the blood-brain barrier (BBB) and delivering the drugs directly into the brain [45–47]. Several studies (preclinical and clinical) show evidence that suggests the feasibility of a direct olfactory pathway to deliver drugs to the brain. Some studies have also proven the superiority of nose to brain (N2B) route over intravenous (i.v.) route for CNS targeting [3,47,48]

Nevertheless, delivery of formulations through i.n. route is challenging due to the anatomical structure and physiological conditions of the nasal cavity. The greatest barrier to i.n. delivery is the low residence time of the formulation especially in case of liquid formulations. Once administered, the formulation can get cleared by either draining out of the nose or by drainage via the nasopharynx by a process called mucociliary clearance (MCC). The mucociliary apparatus of the nose is composed to cilia (hair like protrusions) on the surface of epithelia cells. It is an important defence mechanism against foreign particles entering the nose. The goblet cells in the epithelial surface, continuously secrete mucus which is cleared from the nasal cavity by MCC process. The mucus in the nose is constantly being pushed towards the caudal side (away from the nostrils, towards the nasopharyngeal duct) of the nasal cavity approximately every 15-20 min [49,50].

If the clearance of the formulations from the nasal cavity is delayed, it leaves more time for the drug molecule to get absorbed via the epithelium. To overcome the problem of rapid clearance, several formulation approaches have been explored. Some examples include: use of mucoadhesive polymers, *in-situ* nasal gelling systems and use of ciliostatic compounds [51]. Ciliostatic compounds act by chelating calcium ions, by inhibiting enzymes responsible for ciliary movement. Isotonic solutions are sometimes responsible for inhibition of ciliary activity. Such compounds if used for a prolonged time, may lead to irreversible toxic damage to the ciliary apparatus. Studies have shown evidence which advocates against the use of ciliostatic compounds especially for formulations intended for chronic use [51]. Another comparatively harmless approach to delay clearance of formulations from the nasal cavity is the use of mucoadhesive polymers. Mucoadhesive polymers adhere to mucosal membranes by penetrating the tissue crevices and by intertwining with mucus present on the surface of mucosal membranes. Subsequently the mucoadhesive remains attached to the mucosal membranes by forming hydrogen bonds or by hydrophobic interactions. Natural polymers (such as xanthan gum, guar gum and chitosan), semisynthetic and synthetic derivatives of cellulose are a few examples of mucoadhesive polymers. Even better approach for nasal delivery of drugs is the *in-situ* nasal gel. *In-situ* nasal gelling systems are liquid at room temperatures, and turn to a gel by polymer crosslinking once they come into contact with a biological tissue/cavity. The stimulus for the conversion from liquid to gel can be because of temperature or pH, or ionic composition of the fluids on the biological surface or cavity. When compared to mucoadhesive formulations and hydrogels for i.n. delivery of drugs, *in-situ* gels offer advantages like precise dosing (due to their

liquid state while administering intranasally) and instantaneous gel formation resulting in delayed clearance from the nasal cavity [51].

This chapter describes the formulation of a nasal *in-situ* gelling system for Rufinamide (Rufi). Appropriate *in vitro* tests were carried out for characterization of the gel. Also, *in vivo* pharmacokinetic studies were performed to assess the distribution of Rufi to the blood and the brain when administered as an *in-situ* gel. The *in-situ* gel for Rufi was prepared using tamarind seed xyloglucan (TSX). TSX is a branched, natural polysaccharide with a back-bone chain of β (1→4) linked glucopyranose residues. It has a molecular weight of 700–880 kDa. TSX is a biocompatible mucoadhesive polymer and therefore has found applications in the food and pharmaceutical industry. Native TSX is not thermoresponsive. Enzymatic modification of TSX yielded a thermoresponsive form of TSX [52–54].

3.2 Materials and methods

3.2.1 Chemicals and reagents

Tamarind seed Xyloglucan (TSX) was a gift sample from Encore Natural Polymers Pvt. Ltd. Ahmedabad, India. Rufinamide (Rufi) and Piribedil (Internal Standard, IS) were gift samples from Glenmark Pharmaceuticals, Mumbai, India and Dr. Reddy's Laboratories, Hyderabad, India, respectively. β-Galactosidase from *Aspergillus oryzae* was purchased from Sigma Aldrich, Mumbai, India. Thiomersal was procured from SRL Chemicals Pvt. Ltd., Mumbai, India.

Acetonitrile (ACN) and Methanol (MeOH) were purchased from Merck, Mumbai, India. Ammonium acetate and glacial acetic acid were purchased from SD Fine Chemicals Limited, Mumbai, India and SRL Chemicals Pvt. Ltd., Mumbai, India respectively. High-quality HPLC grade (Milli-Q) water obtained from our

laboratory's Milli-Q water purification system (Millipore®, MA, USA) was used for the analysis of samples. All chemicals and solvents used were of RP-HPLC grade. Male Wistar rats were procured from VAB Biosciences, Hyderabad, India.

3.2.2 Analytical method

Aqueous RP-HPLC method described in Chapter 2, Section 2.3 was used for analysis of formulations samples (for drug content estimation), *in vitro* drug release samples and stability studies samples. The pharmacokinetic (PK) samples obtained from i.v. and i.n. administration of different formulations were analysed using the validated bioanalytical RP-HPLC method described in Chapter 2, Section 2.3.

3.2.3 Purification of TSX

The TSX provided by the industry had a small percentage of fat and protein impurities. Hence, TSX was treated using organic solvents and heat to remove such impurities. To remove the fat impurities, 15 g of isopropyl alcohol (IPA) was added to 5 g of TSX taken in a 50 mL graduated centrifuge tube [55]. The dispersion was vortexed for 15 min, centrifuged at 5,000 rpm for 10 min at 10 °C and the supernatant was discarded. The same was performed for the second cycle and the sediment was dried at 50 °C. To remove the protein impurities, the procedure described by Kochumalayil *et al.*, 2010, was partly adapted [54]. Defatted TSX was dispersed in distilled water under continuous stirring at a concentration of 3.0% w/v and was refrigerated for 12 h for its complete hydration. Later, the dispersion was heated to 60 °C for 2 h, allowed to cool down to room temperature, centrifuged at 5,000 rpm for 10 min. The supernatant was collected and the same procedure was repeated for one more cycle (heating followed by centrifugation). The resultant supernatant was collected and precipitated with thrice its volume of 95% v/v ethanol

under continuous stirring. The precipitate was collected by centrifugation (5,000 rpm for 10 min) and dried at 50 °C. The dried polymer was stored in a desiccator until further use.

3.2.4 Modification of TSX

TSX was treated with an enzyme – β-galactosidase from *Aspergillus oryzae* – to partially remove galactoside residues in order to render it thermoresponsive. The procedure described by Kochumalayil et al., 2010 was followed [54]. Briefly, 3.0% w/v solution of purified TSX was prepared in 10 mM sodium acetate buffer (adjusted to pH 5.0 using glacial acetic acid) and was refrigerated for 12 h for complete hydration of the polymer. To this, β- galactosidase from *Aspergillus oryzae* was added at a level of 7.4 U/mL and the mixture was mildly stirred at 35 °C for 18 h. At the end of 18 h, the enzyme was inactivated by heating the reaction mixture to 90 °C for 30 min. The enzyme reacted tamarind seed xyloglucan (RXG) was obtained by precipitating with 95% v/v ethanol, followed by drying at 50 °C.

3.2.5 Formulation of thermoresponsive RXG gels

Thermoresponsive polymer solutions were prepared by adding weighed quantity of RXG to Milli-Q water and allowing the polymer to undergo complete hydration under refrigerated conditions for 48 h. After hydration, the polymer dispersions were mixed uniformly using a magnetic stirrer. Thiomersal, a bacteriostatic and fungistatic preservative, was added at a level of 0.01% w/w to the polymer dispersions. Rufi with particle size ranging from 75-90 μm was added to the prepared polymer dispersions (Rufi-RXG), to yield a dose strength of 50 mg/mL (5.0% w/v) (the selected dose for *in vivo* pharmacokinetic studies in Wistar rats was 1 mg/kg and the

dose volume was 20 μL/kg) and uniformly dispersed using magnetic stirring. The formulations were stored under refrigeration (2-8 °C) until further use.

3.2.5.1 Preliminary evaluation of thermoresponsive RXG gels

Blank-RXG (RXG solution without Rufi) with varying polymer concentrations (between 1.0 and 4.0% w/v) were prepared as per the above procedure. Initial screening for determination of gelation temperature of Blank-RXG solutions was done using the 'vial tilting' method. Blank-RXG solutions showing gelation below 35 °C were taken up further for optimization.

3.2.5.2 Determination of sol-to-gel transition temperature using a rheometer

The sol-to-gel transition temperature was evaluated for both Blank-RXG and Rufi-RXG (RXG solution loaded with Rufi at the required dose strength) formulations. Rheological properties were evaluated using a rheometer (Anton Paar MCR 302, Graz, Austria). Measurements were performed in the oscillatory mode using temperature sweep experiments from 20 to 40 °C using a parallel plate geometry. The temperature sweep for the samples was performed in their respective linear viscoelastic regions (LVER). Gelation temperature ($T_{sol \rightarrow gel}$) and the strength of gel formed were assessed using a plot depicting the storage modulus (G′) vs temperature.

3.2.5.3 Determination of gel strength using Texture Analysis

Texture Analysis (Stable Microsystems TA. XT plus C, Surrey, U.K.) was performed to support the results obtained from rheological analysis. The $T_{sol \rightarrow gel}$ was determined based on the cohesive strength of Rufi-RXG formulations at different temperatures. Rufi-RXG formulations containing varying concentrations of polymer (RXG) were divided into aliquots of 5 g and dispersed into glass beakers of the same dimensions (23 mm and 34 mm diameter and height respectively). The formulations

were stored under refrigerated conditions for at least 24 h before evaluation to allow for the removal of any entrapped air bubbles. Before the test, aliquots of each formulation were separately equilibrated at specific temperatures: 25, 27, 29, 31, 33 and 35 ºC. The peak positive force (PPF) experienced by the probe from the formulation, which is indicative of the hardness (strength) of the formulation was recorded for each formulation at different temperatures. The formulation samples were kept under the probe and the test was run at the conditions specified in Table 3.1. The test was repeated thrice for every sample at each temperature mentioned above. A plot of PPF vs temperature was constructed. A steep increase in the PPF with temperature was considered as the gelation temperature of the formulation. Formulations showing gelation at temperatures below 35 ºC were considered for further evaluation and development.

Table 3.1 Test specifications set for determining gel strength of *in-situ* gel formulation by Texture Analyser

Specification	Value
Pre-test speed	0.1 mm/s
Post-test speed	0.1 mm/s
Test speed	0.05 mm/s
Trigger force	24.5 mN
Probe diameter	0.5 inch
Load cell capacity	50 kg

3.2.6 *In vitro* drug release studies

The traditional dissolution apparatus available as on date are not capable of creating the conditions of the nasal cavity for testing of thermoresponsive gels. Therefore, *in vitro* drug release study was carried out by membrane-less method using an apparatus designed in our laboratory. Dissolution was carried out in 250 mL beakers, all of the same dimensions. At the base of the beaker, an aluminium pan was glued at the centre. The beakers were pre equilibrated at 34 ± 1 °C for around 30 min. 50 µL

of Rufi-RXG formulations (all containing 2.5 mg of Rufi) were carefully dropped into the aluminium pan which was glued to the beaker. Within 2 min of addition of the formulations, 125 mL of dissolution medium, (simulated nasal electrolyte solution (SNES)) pre-equilibrated at 34 ± 1 °C was carefully poured into the beakers. The beakers were left in the incubator orbital shaker (REMI instruments Pvt. Ltd. Mumbai, India) at 34 °C, 100 rpm. Samples of 2 mL were withdrawn at predetermined time points (15, 30, 60, 120, 240, 360, 480, and 720 min) and replaced with 2 mL of fresh dissolution medium. The *in vitro* drug release study was carried out for Rufi-RXG formulations and for aqueous suspension of Rufi (Rufi-Susp). Samples were analysed using a validated RP-HPLC analytical method. The results from the *in vitro* study were fitted into different mathematical models *viz.* zero order, first order, Higuchi and Korsmeyer-Peppas model. The mechanism of drug release was determined based on the value of 'n' obtained from the Korsmeyer-Peppas model. Similarity factor (f2) was used for pair-wise comparison of the dissolution profiles of 2.0, 2.5 and 3.0% w/v Rufi-RXG formulations.

3.2.7 *In vivo* studies of the developed RXG *in-situ* gel formulations of Rufi

In vivo studies included the measurement of mucociliary transit time (MTT), PK studies, and nasal toxicity evaluation. *In vivo* studies were performed for optimized Rufi-RXG formulation and Rufi-Susp both containing Rufi at a dose strength of 50 mg/mL. Aqueous suspension of Rufi (Rufi-Susp) was prepared by dispersing Rufi uniformly in water containing 0.2% w/v methylcellulose as a suspending agent. Male albino Wistar rats (*n=4*) weighing 240-260 g were used in all the *in vivo* studies. All animals were housed in cages and were left to acclimatize to the institute's animal house (maintained at 22 ± 1 °C room temperature, 55 ± 10% relative humidity, and 12 h light/dark cycle) for at least 10 days before carrying out any experiments on

them. Food and water were provided *ad libitum*. All procedures carried out as a part of *in vivo* studies were approved by the Institute Animal Ethics Committee (Approval number- BITS-Hyd/IAEC/2017/19).

3.2.7.1 Administration of nasal formulation to rats

Formulations were administered intranasally using a 10 µL micropipette tip attached with a soft cannula of length 1.3 cm (Figure 3.1). Animals were anaesthetized using isoflurane anaesthesia. 5 µL of formulation was carefully pipetted out and administered in one of its nostrils. Following the administration of the formulation, the animal was kept in supine position till it recovered from the anaesthesia. The same dosing procedure was followed for all *in vivo* studies.

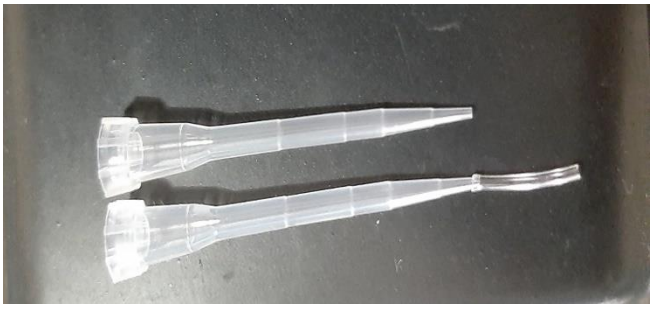

Figure 3.1 Cannula microtip setup for i.n. administration of formulation to rats

3.2.7.2 Dosing precision studies

Dosing precision study was carried out for Rufi-RXG formulations and Rufi-Susp. Using the set up for nasal dosing as mentioned in Section 3.2.7.1. 5 µL of formulation was pipetted out and analysed for Rufi after suitable dilutions. This was repeated 6 times for each formulation, and the per cent Relative Standard Deviation (%RSD) for Rufi delivered each time was calculated.

3.2.7.3 Measurement of mucociliary transport time (MTT) of formulations

MTT was assessed for optimised Rufi-RXG formulation and Rufi-Susp. With slight modifications, the method reported by Ravi *et al*., was followed for assessing MTT

[56]. Formulations were administered to rats as mentioned in section 3.2.7.1 Post administration, the oropharyngeal cavity of rats was swabbed with cotton buds at predetermined time points till 300 min. Rats were not given food for 2 h after commencement of the study. The samples collected at different time points were suitably diluted and analysed for Rufi in each swab using a validated RP-HPLC method as described in Chapter 2. The time point at which Rufi appeared in the oropharyngeal cavity was recoded for respective formulations.

3.2.7.4 In vivo PK studies

PK studies were performed for optimised Rufi-RXG formulations and Rufi-Susp. Dosing of formulation was done using the set up and procedure described in section 3.2.7.2 Rufi was administered at a dose of 1 mg/kg, at a dose volume of 20 µL/kg in one of the animals' nostrils. Retro orbital puncture technique was used to collect blood samples. To finalise the sampling time points for PK studies, pilot PK studies were conducted for i.n. administration of aqueous Rufi-Susp based on the sampling time points of i.v. bolus study (Chapter 2, Section 2.4.4). It was observed that sampling time points followed in case of i.v. bolus PK study were appropriate for i.n. PK studies as well, since we could obtain good absorption and distribution phases. At every time point, 200 µL of blood was collected in centrifuge tubes containing disodium EDTA (4.5% w/v solution in water) as an anticoagulant, at time intervals of 0 (pre dose), 5, 15, 30, 45, 60, 120, 240, 480 min post dosing.

Time points for collecting brain tissue samples after i.n. administration was decided based on previously done brain distribution study with Rufi administered intravenously (i.v.). Brain tissue samples (n=4 at every time point) were harvested at time points: 30, 60, 120, 240 min after dosing. Processing and analysis of biological samples was done using a previously developed and validated RP-HPLC method

described in Chapter 2, Section 2.4. PK parameters viz. $AUC_{0\rightarrow tlast}$ and MRT were determined by non-compartmental analysis (NCA) using Phoenix WinNonlin (Version 8.0, Pharsight Corporation, NC, USA). In order to assess and compare the brain uptake of Rufi following i.n. administration of optimized Rufi-RXG formulation and Rufi-Susp, two parameters- %DTE (Direct Targeting Efficiency percentage) and %DTP (brain drug-direct-transport percentage) were calculated according to Equation 3.1, Equation 3.2, and Equation 3.3.

Equation 3.1

$$\%\boldsymbol{DTE} = \left(\frac{(\boldsymbol{AUC_{brain}/AUC_{blood}})_{\boldsymbol{in}}}{(\boldsymbol{AUC_{brain}/AUC_{blood}})_{\boldsymbol{i.v}}}\right) \times \mathbf{100}$$

Equation 3.2

$$\%\boldsymbol{DTP} = \frac{\boldsymbol{B_{i.n.}} - \boldsymbol{B_x}}{\boldsymbol{B_{i.n.}}} \times \mathbf{100}$$

Equation 3.3

$$\boldsymbol{B_x} = \frac{\boldsymbol{B_{i.v.}}}{\boldsymbol{P_{i.v.}}} \times \boldsymbol{P_{i.n.}}$$

Where $B_{i.n.}$ is the brain $AUC_{0\rightarrow tlast}$ following i.n. administration of a given formulation, $B_{i.v.}$ is the brain $AUC_{0\rightarrow tlast}$ following i.v. administration of the drug and $P_{i.n.}$ is the blood $AUC_{0\rightarrow tlast}$ following i.n. administration of a given formulation, $P_{i.v.}$ is the blood $AUC_{0\rightarrow tlast}$ following i.v. administration of the drug and B_x is the brain $AUC_{0\rightarrow tlast}$ fraction contributed by the systemic circulation through the BBB following i.n. administration of a given formulation. Positive and higher values of %DTE and %DTP are suggestive of more efficient drug delivery to the brain. More specifically, %DTE includes total drug transported to the brain, directly from the nose, and also from the systemic circulation, while %DTP value signifies the percentage of drug reaching the brain directly via the nose to brain pathways.

3.2.8 Nasal toxicity evaluation

Nasal toxicity evaluation of the optimised Rufi-RXG formulation was carried out on excised goat nasal mucosa according to the method mentioned by Ruby and Pandey [57]. Goat nasal tissue was freshly procured from the local slaughterhouse. Immediately after procurement, the nasal mucosa was carefully separated from the underlying cartilage using a scalpel and forceps, cut into pieces of equal dimensions, and placed in a Petri plate. Prior to treatment, the nasal mucosa was gently cleaned using PBS pH 6.4. The excised nasal mucosa was treated with negative control (PBS pH 6.4), a positive control (IPA), and optimized Rufi-RXG formulation for a period of 4 h. After the study, the samples were carefully rinsed with PBS pH 6.4 and stored in 4.0% v/v formalin solution for 12 h and then subjected to further processes of sectioning and H and E staining. The stained sections were examined for the intactness of the epithelial lining and the appearance of goblet cells.

3.2.9 Statistical analysis of data

Data obtained from physical characterization studies, *in vivo*, and *in vitro* studies were represented as mean ± SD. One-way analysis of variance (ANOVA) was performed to compare *in vivo* PK data from different treatment groups at 5% significance level. If there was a significant difference obtained in ANOVA, the data were further compared using a suitable post hoc test at 5% level of the significance.

3.3 Results and discussion

3.3.1 Purification of TSX

Tamarind seed polysaccharide supplied by the industry had fat and protein impurities. From the literature it is known that removal of protein and fat impurities from TSX yields better, elastic gels. The powder was washed with IPA to remove fat

impurities. To get rid of protein impurities, the proteins were precipitated by applying heat, followed by separation using centrifugation. The pure TSX devoid of fat and protein impurities was used for further processing [55].

3.3.2 Modification of TSX

Xyloglucan is a major structural polysaccharide in higher plants. It is found in endosperm of tamarind tree (*Tamarindus indica*) seed. 'Xyloglucans' is a general term applied to non-starch polysaccharides that have a β (1→4)-linked glucan backbone (similar to cellulose molecules) substituted with α (1→6)-linked xylose, some of which are β-D-galactosylated [53]. TSX gels majorly via hydrophobic interactions between its backbone chains. In the case of native/unmodified TSX, the hydrophobic parts of the polymer chain are masked/hindered by the presence of galactose groups. This makes it difficult for native TSX to form strong gels [52]. According to literature, thermoreversible TSX gels are formed upon heating when a fraction (approximately 40%) of the galactose residues are removed using a β-galactosidase enzyme. Therefore, to remove at least ~40% of galactose residues, TSX was treated with β-galactosidase enzyme at conditions mentioned in Section 3.2.4 and shown in Figure 3.2. The enzymatically reacted TSX (RXG) was dissolved in water to yield dispersions of different concentrations which were subjected to further evaluation [58]. To ensure batch to batch consistency of the RXG obtained by reacting TSX, we have repeated the modification reaction in triplicates. Rheological analysis (determination of G' value) for three samples from every lot was performed to ensure within lot and across lot consistency. For all samples, within and across lots, the %RSD of G' values was less than 5%.

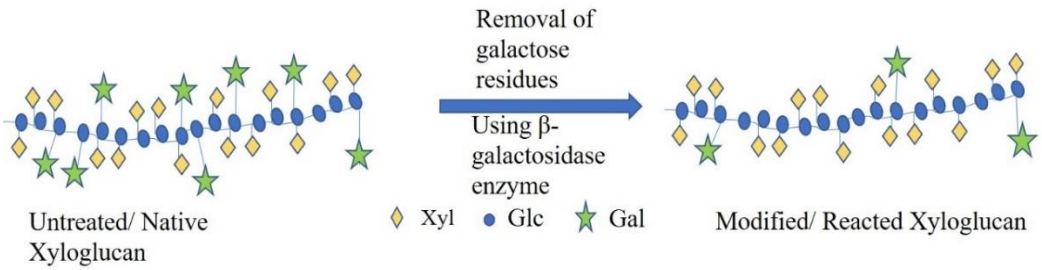

Figure 3.2 Reaction on native TSX/Xyloglucan to remove galactoside groups

Xyl- xylose group; Glc- glucose groups; Gal- galactose residues

3.3.3 Optimization of nasal *in-situ* gel

During the initial few trials, a simple vial tilt method was used to evaluate the gelation properties of the formulations. Gelation and flowability (in the sol state) were checked for Blank-RXG formulations with RXG at levels of 1.0 to 4.0% w/v. It was observed that polymer dispersions containing RXG at concentration greater than 3.0% w/v were highly viscous in the sol state and were barely flowing. In case of polymer dispersions with less than 2.0% w/v RXG, the $T_{sol \rightarrow gel}$ was found to be greater than 37 °C. Hence, for further optimization, *in-situ* gel formulations (both blank and drug suspended) containing RXG at level of 2.0, 2.5 and 3.0% w/v were used. The selected *in-situ* gel formulations were assessed for their rheological properties, gelation temperature, *in vitro* drug release, and *in vivo* PK studies.

3.3.3.1 Determination of sol-to-gel transition temperature using rheometer

Polymer rheology is an intricate state to understand and needs measurements to be made delicately. Majority of the polymers used for drug delivery application in pharmaceutical sciences exhibit viscoelastic properties. In case of polymeric solutions, their microstructure (microstructure here indicates the way in which the polymer molecular chains are arranged around each other) is the state of equilibrium. Any disturbance in this state causes the thermodynamic forces to restore the structure. The energy spent in this restoration is the elastic component of the material

(it is also called the ‘storage’ energy) and is characterized by the ‘storage’ modulus (G'). Similarly, any disturbance to the system also causes some energy to be dissipated (not restored). This part of the energy constitutes the viscous component of the fluid. It is characterized by ‘loss’ modulus (G"). The range of shear stress values in which this microstructure of the polymer, characterized by G' and G" is not disturbed, is called the linear viscoelastic region (LVER). Measurements within the LVER of the formulations helps in preserving the internal microstructure of the samples. This enables accurate estimation of sol-to-gel transition process in terms of transition temperature and gel strength [59].

LVER for the formulations was identified by varying the percentage amplitude strain at a constant angular frequency. Based on the LVER, all formulations were tested at 0.5% amplitude strain and 10 rad/s angular frequency using a temperature sweep (the temperature was varied from 20 to 40 °C with 1 °C rise per minute). The results were recorded as G' values vs temperature plots (Figure 3.3). In case of hydrogels, the transition from sol-to-gel is noted as the crossover of G' and G" curves, and the temperature at the crossover point is recorded as the $T_{sol \rightarrow gel}$ [60]. In case of both Blank-RXG and Rufi-RXG formulations, even in the sol state, G' values were higher than G" values. This is because, even in the sol state, all the formulations exhibited a fairly strong microstructure. Hence, for all formulations, instead of crossover point of G' and G", the temperature at which the G' values saw a significant increase was noted as their $T_{sol \rightarrow gel}$. The $T_{sol \rightarrow gel}$ values for each formulation (Blank-RXG and Rufi-RXG) along with the G' value at $T_{sol \rightarrow gel}$ (indicative of the gel strength) is shown in Table 3.2. As can be seen from the table, the $T_{sol \rightarrow gel}$ for Rufi-RXG formulations was lesser than the Blank-RXG formulations. The Rufi-RXG formulation with 3.0% RXG showed very high viscosity in its sol state itself, which

seemed impractical from dosage administration point of view. Rufi-RXG formulations containing 2.5 and 2.0% w/v of RXG were still flowing at the sol state and turned to gel at their respective $T_{sol \rightarrow gel}$. For Blank-RXG and Rufi-RXG formulations, drug suspended gels, it can be seen that an increase in the polymer concentration caused an increase in the viscosity at the sol state and also resulted in higher gel strength. All the three Rufi-RXG formulations (with 2.0, 2.5 and 3.0% w/v RXG) were taken further for evaluating their *in vitro* release behaviour.

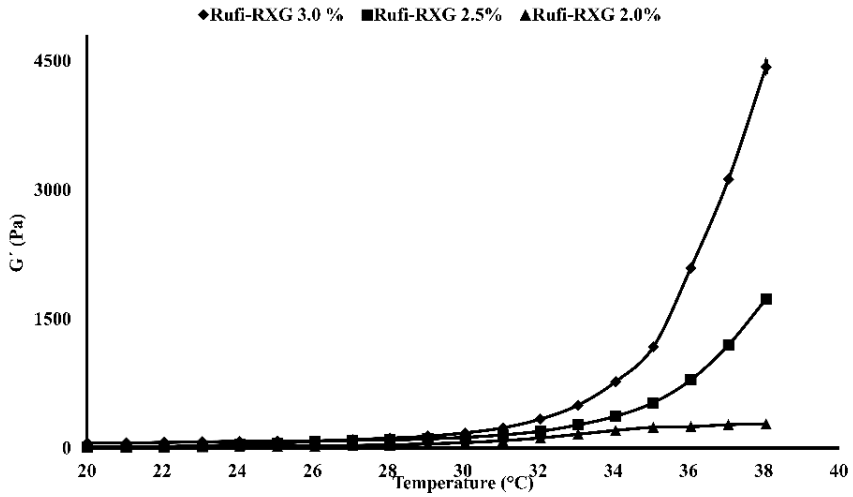

Figure 3.3 Rheological evaluation for determination of sol-to-gel transition temperature ($T_{sol \rightarrow gel}$) of various Rufi-RXG *in-situ* gelling formulations shown using a plot of (storage modulus) G' values vs temperature *(Each data point is represented as mean ± SD of n=3 determinations)*

Table 3.2 Sol-to-gel transition temperature ($T_{sol \rightarrow gel}$) of various Rufi-RXG and Blank-RXG *in-situ* gelling formulations evaluated using rheometer.

Formulation	$T_{sol \rightarrow gel}$ (°C)	G' (Pa)			
		20 °C	33 °C	35 °C	37 °C
3.0% Blank-RXG	34	7.9 ± 0.2	58.8 ± 0.7	100.4 ± 3.0	174.2 ± 5.3
2.5% Blank-RXG	34	3.9 ± 0.2	9.9 ± 0.8	20.4 ± 1.3	40.5 ± 1.9
2.0% Blank-RXG	34	1.5 ± 0.1	6.2 ± 0.9	14.8 ± 0.8	29.2 ± 2.6
3.0% Rufi-RXG	31	59.6 ± 1.0	500.4 ± 9.0	1175.3 ± 15.6	3122.7 ± 22.5
2.5% Rufi-RXG	32	16.7 ± 1.5	270.2 ± 8.6	528.4 ±14.4	1199.8 ± 24.2
2.0% Rufi-RXG	32	9.6 ± 0.5	161.8 ± 4.2	242.7 ±2.1	273.1 ± 2.6

Note: Statistical comparison of G' of blank gels against drug loaded gels for different polymer concentrations at 33 and 35 °C showed that there was a significant difference (P<0.001) between drug loaded and blank gels at both 33 and 35 °C. Concentration of RXG given in % w/v; Each measurement given as mean ± SD of n=3 determinations.

3.3.3.2 Determination of gel strength using Texture Analysis

As a confirmatory study, Texture Analysis of all three (with 2.0, 2.5 and 3.0% w/v RXG) Rufi-RXG formulations was carried out. The hardness value of formulations at different temperatures (at 27, 29, 31, 33, 35ºC) was measured. A single compression cycle provides basic properties like hardness and fracturability of a gel. During the single compression measurement, hardness of the sample was defined as the peak compression force or a PPF obtained from a force vs displacement curve [61]. Profiles with PPF at different temperatures are shown in Figure 3.4. The temperature at which the PPF showed a significant increase (almost 2 times rise in PPF) was taken as the $T_{sol \rightarrow gel}$ transition temperature. The Rufi-RXG formulation with 3.0% w/v RXG gelled at 31 ºC, while those with 2.5% w/v and 2.0% w/v RXG gelled at 32 ºC. In line with the observation from rheological studies, it can be clearly seen that the PPF at all temperatures increased with increase in the RXG concentration. Values for PPF for all three Rufi-RXG formulations are shown in Table 3.3. Both rheological and texture profile analysis confirmed that all three Rufi-RXG formulations gelled at temperatures between 31 to 35 ºC.

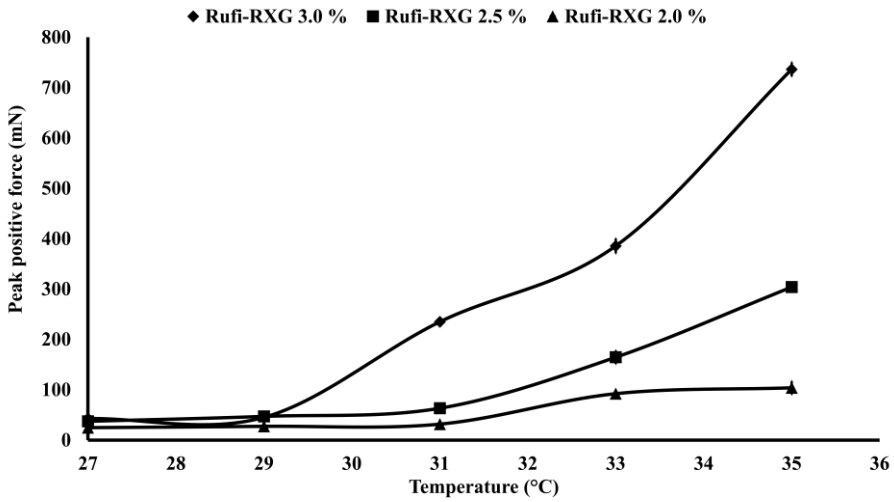

Figure 3.4 Texture analysis for determination of sol-to-gel transition temperature ($T_{sol \rightarrow gel}$) of various Rufi-RXG formulations shown using a plot of peak positive force (PPF) Vs temperature (*Each data point is represented as mean ± SD of n=3 determinations)*

Table 3.3 Sol-to-gel transition temperature ($T_{sol \rightarrow gel}$) of various Rufi-RXG formulations evaluated using Texture Analyzer

Formulation	PPF (mN)				
	27 °C	29 °C	31 °C	33 °C	35 °C
3.0% Blank-RXG	25.0 ± 3.9	30.9 ± 2.7	174.9 ± 8.9*	275.6 ± 31.1	562.9 ± 34.7
2.5% Blank-RXG	-	-	-	104.5 ± 5.6	250.5 ± 21.7
2.0% Blank-RXG	-	-	-	74.6 ± 3.5	77.2 ± 5.7
3.0% Rufi-RXG	42.9 ± 1.5	45.2 ± 4.9	234.9 ± 5.7[a]	385.6 ± 14.7	736.3 ± 14.1
2.5% Rufi-RXG	37.4 ± 6.7	47.2 ± 6.3	63.4 ± 3.6	132.6 ± 9.5[a]	303.9 ± 9.3
2.0% Rufi-RXG	24.8 ± 0.5	27.4 ± 6.5	31.7 ± 3.2	92.2 ± 2.3[a]	103.9 ± 13.2

[a] *$T_{sol \rightarrow gel}$ transition temperatures of respective formulations*

Note: Statistical comparison of PPF of blank gels against drug loaded gels for different polymer concentrations at 33 and 35 °C showed that there was a significant difference (P<0.05) between drug loaded and blank gels at both 33 and 35 °C. Concentration of RXG given in % w/v; Each measurement is given as mean ± SD of n=3 determinations

3.3.4 *In vitro* drug release study

The *in vitro* drug release profiles (Figure 3.5) clearly indicated that the drug release rate decreased with increase in polymer concentration from 2.0% to 3.0% w/v. As the polymer concentration increased, the number of RXG molecules increased, thereby forming a dense gel network. As the tortuosity of the polymer chain increases, the gel strength increases. This makes it more difficult for drug to dissolve

and diffuse, resulting in slower release rates. The data obtained from *in vitro* drug release studies was fit into various kinetic models to determine the release kinetics. The results obtained are summarized in Table 3.4, with R^2 values for every model. From the R^2 values, it can be seen that all three Rufi-RXG formulations follow first order release kinetics. The 'n' values for Korsmeyer-Peppas model are also shown in the Table 3.4. This value for all the three formulations was greater than 1 indicating that the mechanism of drug release was a 'Super Case II transport'. For systems showing Super Case II transport, the prevailing mechanisms of drug release are the relaxation of polymer matrix and solvent crazing (i.e., development of microcracks in the polymer network because of the drug movement, and acceleration in an attempt to diffuse through the gel network) [62]. The results of the *in vitro* release study align with the observations from the gel strength studies (Section 3.3.3), supporting that the release rate is inversely proportional to the gel strength. From the results of gel strength studies and *in vitro* drug release studies, it was evident that the drug release from Rufi-RXG formulation with 3.0% w/v RXG was very slow, and hence Rufi-RXG formulations with 2.5 and 2.0% w/v RXG were taken forward for *in vivo* studies.

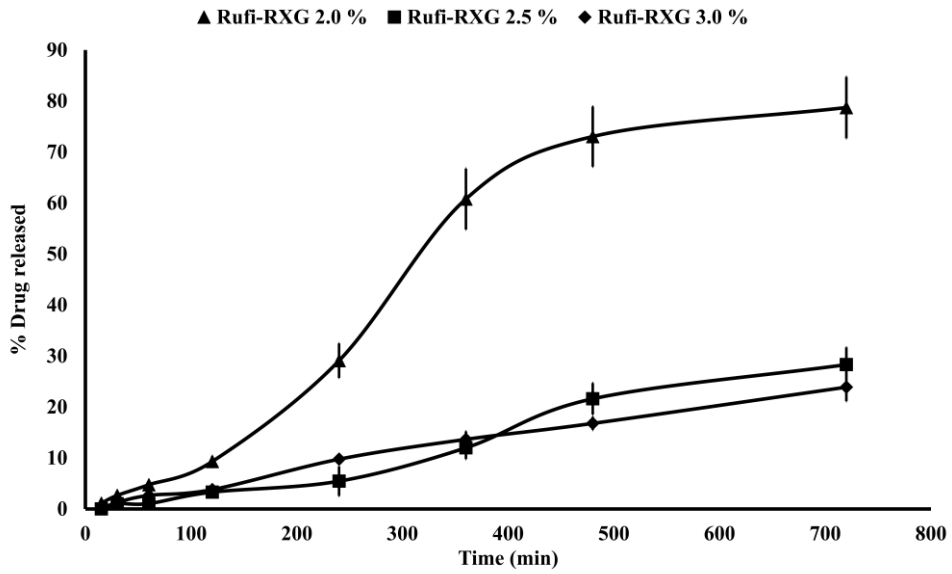

Figure 3.5 In vitro drug release profiles of different Rufi-RXG formulations (Each data point is represented as mean ± SD of n=3 determinations)

Table 3.4 Results obtained from modelling the *in vitro* drug release data of Rufi-RXG formulations in various kinetic models

Formulation	Kinetic Models			
	Zero order (R^2)	First order (R^2)	Higuchi (R^2)	Korsmeyer-Peppas (n), (R^2)
2.0% Rufi-RXG	0.962	0.973	0.908	1.56, 0.85
2.5% Rufi-RXG	0.994	0.997	0.922	1.27, 0.81
3.0% Rufi-RXG	0.991	0.996	0.949	1.09. 0.82

n = exponent of release in function of time 't' (related to drug release mechanism)
Note: Dissolution profiles for 2.0, 2.5 and 3.0% w/v drug loaded gels have been compared using the similarity factor (f2) method. The f2 values were calculated for 2.0% w/v Vs 2.5% w/v, 2.5% w/v Vs 3.0% w/v, and 2.0% w/v Vs 3.0% w/v. This showed that only dissolution profiles of 2.5% w/v and 3.0% w/v drug loaded gels were similar, and rest other comparisons showed dissimilarity of dissolution profiles. Concentration of RXG given in % w/v; Drug release study was performed in triplicates for each formulation, and the model fitting was done using the mean dissolution profile.

3.3.5 *In vivo* studies

There is no well-established model for studying epileptic syndrome. Few decades ago, cats and non-human primates were widely used to study the efficacy and mechanism of action of anti-epileptic drugs. Recently, researchers started exploring rodents (rats and mice) for studying epilepsy. Over the last decade, rats and mice

have become the default choice for anti-epileptic drug testing [63]. Therefore, *in vivo* PK studies and mucociliary transport study were performed in male Wistar rats.

3.3.5.1 Administration of nasal in-situ gel formulation to rats

I.n. dosing in rats required optimization of two aspects *viz.* site of delivery of formulation in the nasal cavity and dose volume. Site specific deposition of formulation into the nose affects the pathway via which the drug gets taken up. One of the main strategies to enhance direct N2B drug delivery is to deposit the drug at the olfactory region of the nose which is marked by the beginning of the superior turbinate [50,64]. The olfactory region is situated deeper into the nasal cavity. To find out the precise length of the delivery setup needed to reach the olfactory region, three animals (240–260 g) were sacrificed, and their noses were harvested. The noses were cut open longitudinally, along the nasal septum in the middle, and the region of the nose above the superior turbinate was identified as the olfactory region (shown in Figure 3.6). The distance from the nostril to the olfactory region was measured to be approximately 1.3 cm. A simple microtip was initially used to deposit the formulations into the nose. Since the polypropylene microtip was hard, it posed the risk of injury to the rat's nose, and hence was not used further. Finally, a soft and flexible cannula of length 1.3 cm attached to a microtip was used to deliver the formulations into the animal's nose. The setup is shown in Figure 3.1.

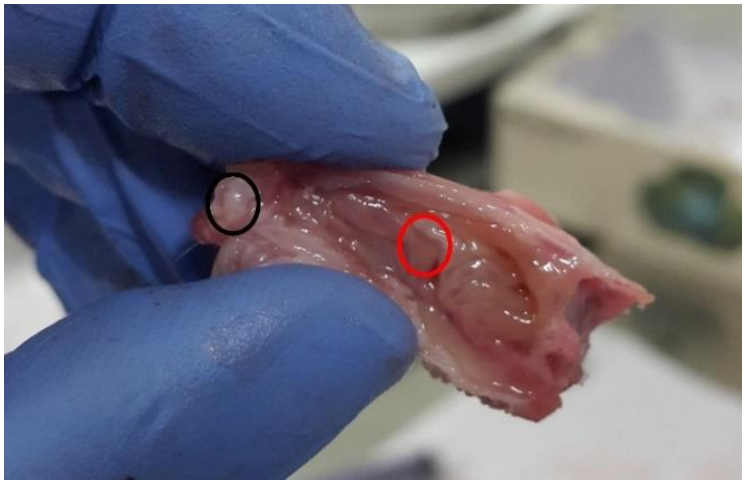

Figure 3.6 Rat nose cut open along the septum; Black circle: nostril (rostral side); Red circle: beginning of olfactory region; the site of deposition of formulation (caudal side)

It is known that the nasopalatine duct connects the oral cavity and the nasal cavity, while the nasopharyngeal duct connects the nasal cavity and the trachea. Drainage of formulation via nasopalatine duct is due to passive leakage of the formulation from the nasal cavity. Hence to optimize the dose volume, the leakage from the nasopalatine duct into the rat's mouth was checked for volumes ranging from 10 – 100 µL/kg [65]. To ensure that the formulation did not appear in the oral cavity via the nasopalatine duct, a dye (amaranth) was mixed in the formulation and was administered using the abovementioned setup. It was visually observed (in *n*=3 rats) that there was no appearance of the dye even at 30 min after administration of the formulation, at a dose volume of 20 µL/kg. The drainage of the formulation via the nasopharyngeal duct was assessed by mucociliary transport studies (mentioned in section 3.2.7.3).

3.3.5.2 Dosing precision studies

Precise dosing with the microtip cannula setup was critical for all *in vivo* studies. In order to rule out the possibility of variability arising because of the dose administration, dosing precision studies were carried out. The %RSD value of doses

delivered using the same setup were less than 5.0% indicating that the dosage administration was precise.

3.3.5.3 Measurement of mucociliary transit time (MTT) of formulations

The mucociliary clearance (MCC) process is an innate defence mechanism of the body to clear away inhaled pathogens or nasal irritants. The inhaled pathogens are trapped in the mucus secreted by goblet cells of the respiratory epithelium and pushed towards the pharynx. The action of 'pushing' the mucus is caused by the continuous beating of cilia (tiny hair like protrusions on the surface of epithelium). [50,65]. In case of nasally administered formulations, it is pertinent that the formulation is retained in the nasal cavity for sufficiently long time to allow for maximum absorption of the drug. In such cases, the MCC may prematurely clear the formulation from the nasal cavity. Hence, MCC was compared for Rufi-Susp, 2.0 and 2.5% w/v Rufi-RXG formulations. From the results (Table 3.5) it is evident that for the Rufi-RXG *in-situ* gel formulations with 2.0, 2.5% w/v RXG, the 'time of appearance' was significantly greater ($P<0.05$) than the Rufi-Susp. This observation can be attributed to the gel formed once inside the nose. Under the influence of i.n. temperature, the formulations converted to gel, thereby resisting the clearance process, and stayed in the nasal cavity for a longer time. Rufi-RXG formulations with 2.0 and 2.5% w/v RXG were taken further for PK evaluation.

Table 3.5 Mucociliary Clearance (MCC) time of Rufi-Susp and Rufi-RXG formulations

Sample	Time of appearance (min) (mean ± SD)
Aqueous Rufi-Susp	11.6 ± 2.8
2.0% w/v Rufi-RXG gel	36.6 ± 5.7
2.5% w/v Rufi-RXG gel	51.7 ± 4.9

Note: MTT was determined for each formulation in n=3 animals; Each value is given as mean ± SD of n=3 replicate analysis

3.3.5.4 In vivo PK studies for Rufi in rats

I.n. PK studies for Rufi-Susp and the Rufi-RXG formulations (2.0 and 2.5% w/v RXG) were carried out. In case of Rufi-RXG formulation with 2.5% w/v RXG, concentrations of Rufi in both the matrices (blood and brain) were below quantifiable limit (BQL) at all sampling time points. This can be attributed to the higher gel strength of 2.5% w/v RXG *in-situ* gel formulation, which made it difficult for the drug to diffuse through the gel network and hence it did not get taken up either by the brain or through the systemic circulation. The plasma and brain time course profiles of Rufi-Susp and Rufi-RXG formulations with 2.0% w/v RXG (optimized formulation) (dosed at 1 mg/kg Rufi) are shown in Figure 3.7. In the same figures, the plasma and brain time course of Rufi following i.v. bolus administration are also shown (dosed at 0.5 mg/kg). PK parameters *viz*. $AUC_{0\rightarrow tlast}$, C_{max}, T_{max} and MRT (Mean Residence Time) for Rufi-Susp and 2.0% w/v Rufi-RXG formulation are listed in Table 3.6.

Table 3.6 PK parameters of optimized Rufi-RXG formulation and Rufi-Susp in brain and plasma

Matrix	PK Parameter	Units	Treatments		
			Rufi-RXG	Rufi-Susp	i.v. bolus of Rufi
Plasma	$AUC_{0\rightarrow tlast}$	min×(µg/mL)	114.4 ± 9.0	200.75 ± 74.4	607.47 ± 90.1
	C_{max}	µg/mL	0.32 ± 0.02	1.16 ± 0.53	0.844 ± 0.17
	T_{max}	min	120	120	5
	MRT	min	136.3 ± 12.2	147.4 ± 9.4	607.2 ± 6.4
Brain	$AUC_{0\rightarrow tlast}$	min×(µg/g)	201.8	104.28	214.8
	C_{max}	µg/g	1.48 ± 0.09	0.79 ± 0.11	0.58 ± 0.03
	T_{max}	min	60	120	120

Note: n=4 animals were used for plasma PK, and for brain PK, n=4 animals' brains were used at every time point; The plasma data is represented as mean ± SD. The brain data is represented as single values. The time points in the brain PK profile were an average of the pooled concentration data obtained from 4 animals. the average brain concentration profile was constructed from the pooled concentration data and hence, PK parameters like $AUC_{0\rightarrow tlast}$ and MRT were calculated as single values without standard deviation

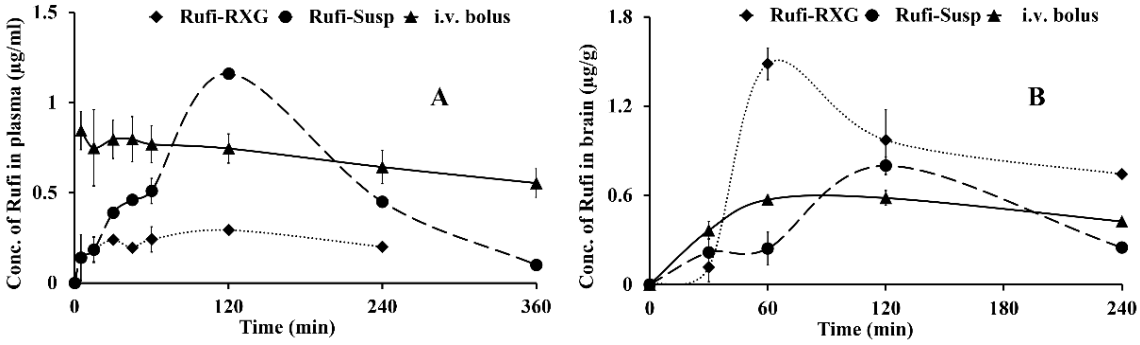

Figure 3.7 Mean concentration-time profiles obtained following i.n. administration of optimized Rufi-RXG formulation, Rufi-Susp, and i.v. bolus administration of Rufi- A: in plasma, and B: in brain

The i.v. bolus dose was 0.5 mg/kg, the i.n. dose was 1.0 mg/kg at 20 µL/kg dose volume in one nostril; n=4 animals were used for plasma PK, and for brain PK n=4 animals' brains were used at every time point. Each data point is a mean ± SD of n=4 replicates

The plasma $AUC_{0\rightarrow tlast}$ of the optimized Rufi-RXG formulation was about 4 times lesser than that obtained with Rufi-Susp. While the brain $AUC_{0\rightarrow tlast}$ for the same was approximately 2 folds higher than that with Rufi-Susp. This indicates that the optimized Rufi-RXG formulation delivered significantly higher amount of Rufi towards the brain but lesser amount of Rufi towards systemic circulation as compared to aqueous Rufi-Susp when administered through i.n. route.

Statistical analysis of the plasma data obtained following different treatments (Table 3.6) showed that plasma $AUC_{0\rightarrow tlast}$ is the order of i.n. Rufi-RXG formulation < i.n. Rufi-Susp < i.v. bolus Rufi (P<0.05; using one-way ANOVA test followed by Tukey's Multiple Range post-hoc test) [66,67].

The brain PK time course for each treatment was constructed by sacrificing n=4 animals at each time point. Each time point in the brain PK profile was an average of the pooled concentration data obtained from 4 animals, the underlying assumption being that inter-individual differences accounted for residual variability rather than the inherent differences in PK process of different treatments. As we could only construct the average brain concentration profile from the pooled concentration data,

PK parameters like $AUC_{0\rightarrow tlast}$ and MRT were calculated as single values without standard deviation. Therefore, unlike the plasma profile, statistical analysis was not done for brain data. Nonetheless, comparisons of brain exposure of Rufi from different treatments were carried out for the concentrations in brain at 60, 120, and 240 min. Statistical comparison of brain concentrations of all three treatments at different time points revealed that the optimized Rufi-RXG formulation performed better than the Rufi-Susp and i.v. bolus administration of Rufi (Table 2.11).

Direct nose to brain uptake can be assessed by calculating mathematical indices like %DTE and %DTP. %DTE compares the fraction of drug reaching the brain (either directly from nose to brain or via systemic circulation to brain, or both) when given as an i.n. formulation and i.v. bolus [68]. Out of the total drug reaching the brain when administered i.n., the fraction of drug reaching the brain directly via nose to brain pathways (and not via systemic circulation) is indicated by %DTP. The %DTE values for Rufi-RXG formulation and Rufi-Susp were 498.8 and 146.88 and the %DTP values were 79.9 and 31.91, respectively. The %DTP values indicate that almost 80% of the Rufi-RXG formulation was transported directly to the brain as compared to 31% direct transport seen with Rufi-Susp.

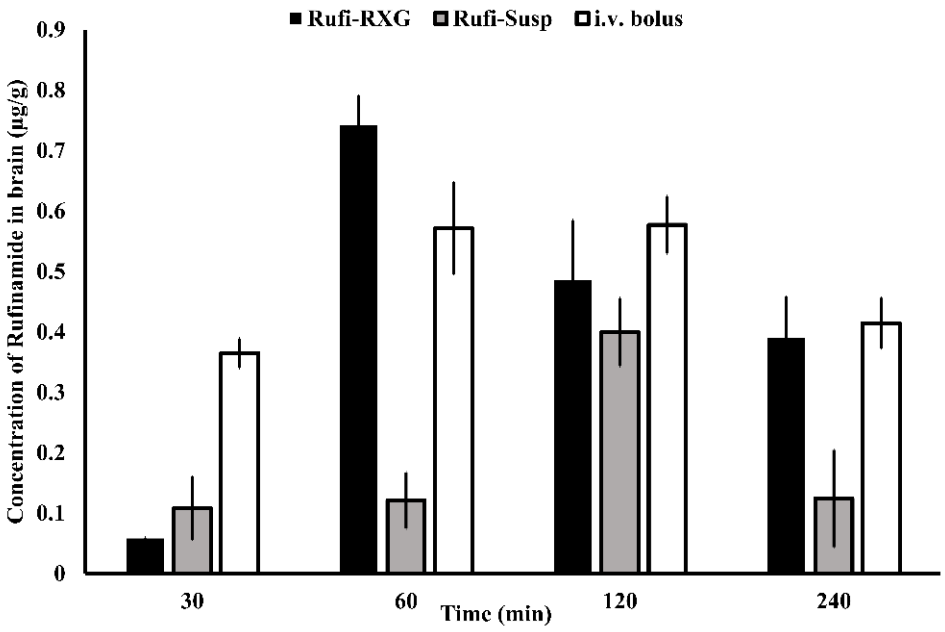

Figure 3.8 Comparison of concentration of Rufi in brain following i.n. administration of optimized Rufi-RXG formulation and Rufi-Susp and i.v. bolus administration of Rufi at four different brain sampling points

*NS= no significant difference, *P<0.05; The i.v. bolus dose was 0.5 mg/kg, the i.n. dose was 1.0 mg/kg at 20 µL/kg dose volume in one nostril; n=4 animals were used for brain PK at every time point; Each bar represents brain concentration of Rufi as mean ± SD of n=4 replicates*

3.3.6 Nasal Toxicity Evaluation of the developed RXG *in-situ* gels

Photographs of the treated and stained tissues obtained from nasal toxicity studies are shown in Figure 3.9. As evidenced by the pictures, the positive control (IPA) (Figure 3.9B) caused damage to the epithelial cell lining. The epithelium appeared diffused and necrotized. Atrophy of the submucosal glands was reported. The tissue treated with the optimized Rufi-RXG *in-situ* gel formulation (Figure 3.9A) appeared similar to the tissue treated with negative control (Figure 3.9C). Based on the results obtained, we can infer that the optimized Rufi-RXG formulation caused minimal damage to the tissue.

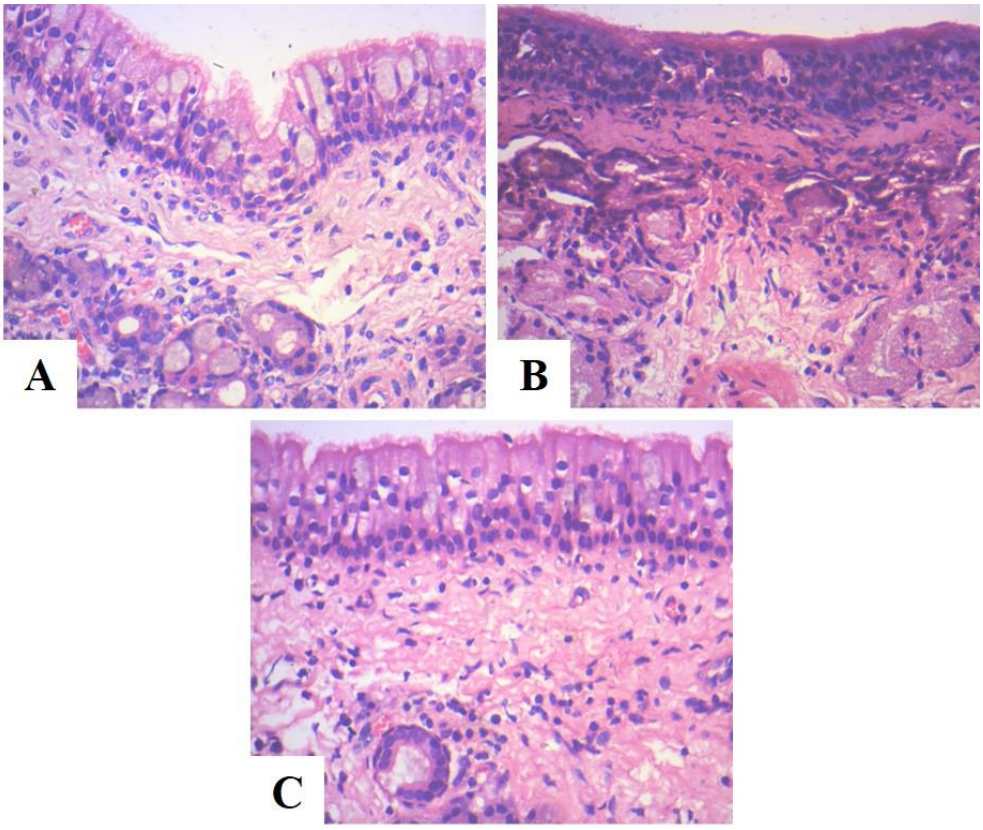

Figure 3.9 H and E-stained tissue images from nasal toxicity studies. Nasal epithelium treated with- A: optimized Rufi-RXG formulation; B: positive control (IPA); C: negative control (PBS pH 6.4)

3.4 Conclusion

Up until recent times, poloxamers have been widely used to formulate nasal thermoresponsive *in-situ* gels, be it for systemic or direct nose to brain delivery of drugs. To achieve thermoresponsive gelation at body temperatures, high amounts of different grades of poloxamers (9% to 30%) have been used in formulations. Poloxamers are synthetic polymers consisting of repetitive polyoxypropylene (POP) and polyoxyethylene (POE) units. Xyloglucan on the other hand, is a natural biodegradable polymer which has GRAS approval. In the present work, a nasal *in-situ* gelling system was successfully formulated for delivering Rufi to the brain. Xyloglucan, a biodegradable polymer obtained from natural sources was used as the thermoresponsive polymer. The concentration of Xyloglucan used had a great effect

on the gel strength, drug release and the pharmacokinetic results. From the brain distribution studies in rats, it was evident that with administration of Rufi as a thermoresponsive nasal *in-situ* gel, almost 80% of the total drug amount reaching the brain was transported directly via nose to brain pathway. The systemic exposure of the drug with optimised nasal *in-situ* gel was four times lesser than the aqueous suspension of Rufi which would result in lesser peripheral side effects. The research findings from this work suggest that the distribution of Rufi towards brain is higher with intranasal administration of *in-situ* gelling systems of Rufi compared to intranasal administration of conventional formulations of Rufi (aqueous suspension of Rufi) compared to oral administration of conventional formulations of Rufi. However, the optimised formulations have to be evaluated in human subjects to determine their clinical efficacy.

4 DESIGN, OPTIMIZATION, PHYSICAL CHARACTERIZATION, AND *IN VIVO* EVALUATION OF RUFINAMIDE NANOCRYSTALS LOADED IN XYLOGLUCAN BASED THERMORESPONSIVE NASAL *IN-SITU* GELLING SYSTEMS

4.1 Introduction

Several formulation approaches have been used to improve the delivery of drugs having low distribution to the brain. Nano formulations have been recently explored as an efficient strategy to delivery drugs via nose to brain (N2B) pathways [32]. Several nano formulations *viz.* solid-lipid nanoparticles, polymeric nanoparticles, liposomes, NCs (nanocrystals) etc. can be used to enhance the permeability of drugs via the nasal epithelium. Among several nano formulations, NCs have an advantage in that they can carry a higher drug load than the other kind of nano formulations. NCs contain near to 100% drug which is stabilized using polymers and surfactants [69]. Increased dissolution rate and increased solubility are major advantages that NCs offer over other kind of nano formulations. Size reduction of drug particles from micrometre to nanometre range drastically improves the surface area and in turn the rate of dissolution. Drug powder with particle size (PS) size less than 1 µm show a drastic change in its saturation solubility compared to PS greater than 1 µm [70]. When administered through nasal route, NCs are reported to be taken up/ internalized by cells/ neurons of the N2B pathway directly, particularly when the PS of the NCs is less than 100 nm. NCs with PS between 100 to 300 nm are internalised by the cells via pinocytosis, while NCs with PS greater than 500 nm are taken up by phagocytosis when administered through nasal route for N2B delivery [71].

The preparation methods of NCs can be broadly classified into two categories- top down and bottom-up approaches. The top-down approach is an energy intensive process where larger particles are broken down into smaller particles by using high pressure homogenization (HPH) or wet ball milling (WBM). More recently, Jet-Stream Homogenization (micro fluidization) is being widely employed for the formulation of NCs [70,72]. The bottom-up approach of preparation of NCs can be

broadly called as the antisolvent-precipitation technique. The principle here is to precipitate drug particles from a supersaturated drug solution. A near saturated drug solution is added to an antisolvent under suitable processing conditions in the presence of stabilizers. Simplicity, low processing cost, and ease of scale-up are the advantages of a bottom-up approach. However, several variables need to be controlled/optimized to get the desired PS using this technique. Solubility of the drug in the solvent, and the solvent-antisolvent (S-AS) mixture, the S-AS ratio, viscosity of the solvent and anti-solvent, temperature, type of stabilizers, are some of the parameters which can affect the properties of the NCs [73–75].

In this work, we have formulated NCs for Rufinamide (Rufi-NCs) using an antisolvent-precipitation technique. The preparation of NCs depends on several factors, and is mostly empirical. Extensive preliminary trials were performed to identify stabilizers, solvents (alone and in combination), processing conditions with the lower and upper limits for each of those factors. Further, a screening and an optimization design were used to formulate Rufi-NCs. Formulations prepared based on the screening and optimization design experimental runs Rufi-NCs were characterized for their PS, Zeta potential (ZP) and yield (%). The optimized Rufi-NCs were suspended in previously developed RXG based nasal *in-situ* gelling system. The Rufi-NCs loaded *in-situ* gel was evaluated for rheology, gel strength, *in vitro* release and *in vivo* brain and plasma pharmacokinetics (PK) in male Wistar rats.

4.2 Materials and methods

4.2.1 Materials

Rufinamide (Rufi) was obtained from Glenmark Pharmaceuticals, India. Piribedil (PBD) (used as Internal Standard (IS) in bio-analytical RP-HPLC method) was a gift sample from Dr. Reddy's Laboratories, Hyderabad, India. Tamarind seed Xyloglucan (TSX) was a gift sample from Encore Natural Polymers Pvt. Ltd. Ahmedabad, India. β-Galactosidase from Aspergillus oryzae was purchased from Sigma Aldrich, Mumbai, India., India. Mannitol, poloxamer 407, and N-methyl – 2 – pyrrolidone (NMP) were obtained from Sigma-Aldrich, Mumbai, India. Hydroxy propyl methyl cellulose E5 LV (HPMC) (Methoxyl: 28-30%, Hydroxypropoxyl: 7-12%, Viscosity of 2% w/v in water at 20 °C: 4-6 cp) was procured from Molychem, Mumbai, India. HPLC grade methanol, acetonitrile (ACN), glacial acetic acid (GAA), ammonium acetate, and thiomersal were procured from SRL Chemicals Pvt. Ltd., Mumbai, India. For all experimental processes and analysis, HPLC grade Milli-Q water from our in-house water purification unit (Millipore®, MA, USA) was used. Male Wistar rats were procured from VAB Biosciences Pvt. Ltd., Hyderabad, India.

4.2.2 Preparation of Rufi-NCs

A bottom-up approach using antisolvent-precipitation technique was used to prepare Rufi-NCs. In the preliminary trials, various stabilizers and processing conditions were tried to control the crystal growth of NCs. HPMC (E5 LV grade) and poloxamer 407 were selected as the stabilizers in the preparation. Briefly, 50 mg Rufi along with poloxamer 407 (amount varied as per the design) were dissolved in NMP (volume varied according to the design). HPMC solution (percentage varied according to the design) was prepared in a separate beaker. The Rufi-poloxamer

solution was added to the HPMC solution using a syringe under high-speed homogenization (Polytron PT 3100D, Kinemetica, Lucerne, Switzerland). Thereafter, the homogenate was subjected to ultrasonication process (Vibra cell, Sonics, Connecticut, USA). All the processing was carried out at controlled temperature conditions. The obtained nanosuspension was centrifuged at 12,000 rpm 10°C for 30 min. The pellet obtained was redispersed in Milli-Q water containing mannitol as a cryoprotectant and freeze dried.

4.2.3 Experimental design for preparation of Rufi-NCs

Rufi-NCs were designed based on the principles of design of experiments (DoE). PS of NCs are an important property which can affect their uptake via the neuronal pathways. ZP is an important property of nano formulations affecting their stability and interaction with biological membranes. Yield (%) of NCs is an important property which defines the dose of NCs. Hence, PS (nm), ZP (mV), and yield (%) of the NCs were identified as critical quality attributes (CQAs) or responses. Based on the literature review and preliminary trials, a total of 8 factors (involving material attributes and process parameters) affecting the CQAs of Rufi-NCs were identified. Plackett-Burman design (PBD) was used to screen the 8 factors to determine the statistically significant/critical factors affecting the responses of Rufi-NCs. Each factor was studied at three levels, which were chosen based on preliminary trials performed for the preparation of NCs. The factors and their levels screened using PBD are given in Table 4.1.

Table 4.1 Factors and their levels selected for screening using PBD for formulation of Rufi-NCs

Factor Code	Actual factors	Levels		
		-1	0	+1
X_1	HPMC concentration (% w/v)	0.1	1.05	2.0
X_2	Ultrasonication time (min)	5	10	15
X_3	Processing temperature (°C)	5	10	15
X_4	Amount of poloxamer (mg)	5	15	25
X_5	Homogenization time (min)	5	10	15
X_6	Homogenization speed (rpm)	7000	11000	15000
X_7	Ultrasonication amplitude (%)	25	32.5	40
X_8	Volume of NMP (µL)	1500	2250	3000

Based on the results obtained from PBD, HPMC concentration, ultrasonication time and processing temperature were found to have a statistically significant effect on the responses of Rufi-NCs. Further, a high-resolution central composite design (CCD) was applied to understand the effect of the three critical factors on the responses and to optimize the preparation of Rufi-NCs. CCD is a type of a response surface design, used to obtain a second order polynomial equation to optimize a formulation by performing very few experiments. The CCD consisted of 20 runs (inclusive of 6 centre runs to check reproducibility) for 3 factors. The second order polynomial equation generated from CCD is of the following form:

Equation 4.1

$$Y = \beta_0 + \beta_1 X_1 + \beta_2 X_2 + \beta_3 X_3 + \beta_{12} X_1 X_2 + \beta_{23} X_2 X_3 + \beta_{13} X_1 X_3 + \beta_{11} {X_1}^2 + \beta_{22} {X_2}^2 + \beta_{33} {X_3}^2$$

Where, Y is the dependent variable, $\beta_0$is the arithmetic mean response of the 20 runs and $\beta_{ii}'s$ $(i = 1-3)$ are coefficients of individual linear and quadratic effects of the factors respectively and $\beta_{ij}'s$ $(i,j = 1-3;\ i < j)$ are coefficients of the effect of interaction between i^{th} and j^{th} factor.

4.2.4 Desirability function and model validation

The optimum values for the three critical factors were given by the Design Expert software (Version 11, Stat-Ease Inc., Minneapolis, MN) based on the desirability function criteria. The desirability function was calculated based on the constrains set for the responses: Maximizing the yield (%) and minimizing the PS. In order to validate the regression model obtained from CCD, six different batches (n=6) of Rufi-NCs were prepared based on the optimized experimental conditions predicted by the regression model and were characterized for their PS and yield (%). Wilcoxon signed rank test was performed to check if there was any significant difference between experimental (or observed) and predicted values for both the responses given by the model.

4.2.5 Preparation of Rufi-NCs loaded in reacted xyloglucan (RXG) based gel

Reacted xyloglucan (RXG) *in-situ* gel was prepared using the method given in Sections 3.2.4 and 3.2.5 in Chapter 3. Briefly, a 3.0% w/v solution of tamarind seed xyloglucan (TSX) prepared in 10 mM sodium acetate buffer (pH 5.0) was treated with β-galactosidase enzyme obtained from Aspergillus oryzae to partially remove galactoside residues. The reaction was kept at 35 °C for 18 h. To terminate the reaction, the entire reaction mixture was heated to 90 °C for 30 min. RXG was obtained by precipitation using 95% v/v ethanol followed by drying in an oven at 50 °C. The formulation development and optimization were based on several parameters which are discussed in detailed in Chapter 3, Section 3.3. The optimized, freeze dried Rufi-NCs (equivalent to the selected dose of Rufi) were dispersed in 2.0% w/v solution of RXG gel using a magnetic stirrer to form Rufi-NCs loaded in reacted xyloglucan based *in-situ* gelling formulation (Rufi-NC-RXG). To the Rufi-

NC-RXG formulation, thiomersal was added at a level of 0.01% w/v as a preservative.

4.2.6 Characterization of formulations

4.2.6.1 Measurement of PS and ZP

PS was measured using dynamic light scattering principle. Zetasizer instrument (Nano ZS, Malvern Instruments Ltd., Worcestershire, UK) was used to measure the PS, polydispersity index (PDI), and ZP of the Rufi-NCs. The intensity of the scattered light was measured at a backscatter angle of 173°. All measurements were performed at 25 °C and an equilibration time of 2 min was set for all samples before the measurements were made.

4.2.6.2 Determination of yield (%) of Rufi-NCs

The yield (%) was measured using a direct method. The freshly prepared Rufi-NCs suspension was centrifuged at 12,000 rpm, at 10 °C for 30 min, and the supernatant was discarded. The pellet obtained at the bottom of the tube was vacuum dried using a centrifuge for speed vacuum concentrator (SCANVAC Scan Speed 32, Labogne ApS, Lynge, Denmark). The dried pellet was then dissolved in a suitable solvent and diluted further for analysis using a validated HPLC method. The yield (%) was calculated as follows:

Equation 4.2

$$\boldsymbol{Yield}(\%) = \frac{\boldsymbol{W_{Rufi\ in\ pellet}}}{\boldsymbol{W_{total\ Rufi\ added}}} \times \mathbf{100}$$

Where, $\boldsymbol{W_{total\ Rufi\ added}}$ is the amount of Rufi used in the preparation of Rufi-NCs and $\boldsymbol{W_{Rufi\ in\ pellet}}$ is the amount of Rufi present in the pellet obtained after centrifugation of the Rufi-NCs suspension.

4.2.6.3 Morphological analysis of Rufi-NCs

Scanning electron microscope (FE-SEM, FEI, Apreo LoVac, TermoFisher Scientific, MA, USA) consisting of sputter coater (Leica EM 200, Wetzlar, Germany) was used for analysing the shape and size of Rufi bulk particles and Rufi-NCs. 50 µL of sample was drop cast on an aluminium stub, spread evenly and left to dry under vacuum for 12 h. Sputter coating was achieved with gold under an inert (Argon gas) environment. The sputter coated sample was kept in a vacuum chamber to capture images at an acceleration voltage of 5 kV.

4.2.6.4 Thermal analysis using differential scanning calorimetry (DSC) and Powder X-ray diffraction studies

Differential scanning calorimetric analysis (DSC 60; Shimadzu Corporation, Kyoto, Japan) was performed for Rufi-NCs, pure Rufi (bulk drug), and the physical mixture of Rufi with all the excipients used in the preparation of Rufi-NCs. For the analysis, weighed samples (5 mg) were taken in aluminium pans and crimp sealed. A sealed empty aluminium pan was used as a reference. The sample and reference pans were placed in the DSC sample chamber and allowed to equilibrate at 25 °C before the run. The thermograms were obtained in the temperature range of 10 to 300 °C with a heating rate of 10 °C/min in an inert (Nitrogen) environment.

The powder X-ray diffraction (pXRD) study was carried out for freeze dried Rufi-NCs, physical mixture of constituents of Rufi-NCs, and pure Rufi to characterize the physical state of the samples with Rigaku, Ultima IV diffractometer (Texas, USA). The samples were illuminated with a Ni-filtered Cu-Kα radiation (λ = 1.54 Å) at a voltage of 40 kV and a current of 30 mA. The analysis was performed for a 2θ range of 10-80° at a scanning rate of 2 degree/min.

4.2.7 Rheological evaluation of Rufi-NC-RXG formulation

A rheometer (Anton Paar MCR 302, Graz, Austria) was used to determine the sol-to-gel transition temperature ($T_{sol \rightarrow gel}$) and the gel strength in terms of the storage modulus (G') of Rufi-NC-RXG. The $T_{sol \rightarrow gel}$ for Rufi-NC-RXG was compared with that of Blank-RXG. The linear viscoelastic region (LVER) of the sample was first determined using an amplitude sweep. All measurements were performed in the LVER of the samples. The change in storage modulus (G') with change in temperature was plotted for both Blank-RXG and Rufi-NC-RXG.

4.2.8 *In vitro* drug release study from Rufi-NC-Susp and Rufi-NC-RXG formulations

In vitro drug release study was carried out by membrane-less method for Rufi-NC-Susp and Rufi-NC-RXG formulations. Dissolution was carried out in 250 mL beakers, all the same dimensions. At the base of the beaker, an aluminium pan was glued at the centre. The beakers were pre equilibrated at 34 ± 1 °C for around 30 min. Formulation quantity equivalent to 2.5 mg of Rufi were carefully dropped into the aluminium pan which was glued to the beaker. Within 2 min of addition of the formulations, 125 mL of dissolution medium, (simulated nasal electrolyte solution (SNES)) pre-equilibrated at 34 ± 1 °C was carefully poured into the beakers. The beakers were left in the incubator orbital shaker at 34 °C, 100 rpm. Samples of 2 mL were withdrawn at predetermined time points (15, 30, 60, 120, 240, 360, 480, and 720 min) from each beaker kept separately at different time points. Samples were analysed using a validated RP-HPLC analytical method (Chapter 2, Section 2.3). The results from the *in vitro* study of Rufi-NC-RXG formulation were fitted into different mathematical models *viz*. zero order, first order, Higuchi and Korsmeyer-Peppas model. The mechanism of drug release was determined based on the

exponent value 'n' obtained from the Korsmeyer-Peppas model. Similarity factor (f2) was used for pair-wise comparison of the dissolution profiles of Rufi-RXG (profile obtained from Chapter 3, Section 3.3.4) and Rufi-NC-RXG formulations.

4.2.9 Stability of Rufi-NCs

Stability was evaluated for both freeze-dried Rufi-NCs and Rufi-NC-RXG. Freeze-dried Rufi-NCs were stored separately in airtight vials (*n*=3) at room temperature conditions (25 ± 2 °C and relative humidity of 60 ± 5%), and Rufi-NC-RXG was stored separately in refrigerated conditions (2-8 °C) as the *in-situ* gelling system is recommend being stored at temperatures from 2-8 °C (as given in Chapter 3). Samples were collected after every 15 days and evaluated for their PS, yield (%), and ZP.

4.2.10 *In vivo* studies in male Wistar rats

Adult male Wistar rats weighing 240-260 g were used for *in vivo* studies. Prior approval was obtained from the institute's animal ethics committee (Approval number- BITS-Hyd/IAEC/2017/19) for all the procedures carried out during animal experimentation. Brain and plasma PK studies and mucociliary clearance (MCC) studies were performed for Rufi-NC-RXG and aqueous suspension of freeze dried Rufi-NCs (Rufi-NC-Susp) following i.n. administration of the formulations in rats. The plasma and brain PK parameters of both the nanocrystal formulations were compared with the PK parameters of aqueous suspension of plain Rufi (Rufi-Susp). During the *in vivo* studies, animals were housed in our institute's animal housing facility in a controlled environment maintained at a temperature of 22 ± 1 °C with 55 ± 10% relative humidity and 12 h light dark cycle. Food and water were provided to the rats, ad libitum, except during *in vivo* studies. Prior to the day of the experiment,

the rats were fasted overnight with free access to water till 4 h post-dosing of the formulations on the day of the experiment.

4.2.10.1 Administration of formulations in rats through i.n. route

A microtip-canula setup as mentioned in Section 3.2.7.1, Chapter 3 was used for administration and deposition of i.n. formulations. 10 µL of formulation was administered to the animal in one of its nostrils using the cannula-microtip set up, while maintaining the animal under isoflurane anaesthesia. After i.n. dosing of the formulations, the animal was kept in a supine position till it recovered from the anaesthesia.

4.2.10.2 Dosing precision studies

Dose precision studies were conducted by pipetting out 10 µL of formulation (Rufi-NC-RXG/ Rufi-NC-Susp), six times (n=6), using the cannula-microtip set up. The amount of Rufi present in the volume pipetted out was analysed using the HPLC method. Dose precision was expressed in terms of the relative standard deviation (%RSD) for the amount of Rufi present in six repetitions of a given formulation.

4.2.10.3 Assessment of mucociliary transport time (MTT)

The MTT for both Rufi-NC-Susp and Rufi-NC-RXG formulations was based on the method as given in Section 3.2.7.3, Chapter 3. 10 µL of a formulation was administered through i.n. route into one nostril of the rat using cannula-microtip set up. Post dosing, the oropharyngeal cavity of rats was swabbed using a cotton swab at predetermined time points till 360 min post dosing. Rats were not given access to water/ food up to 2 h post dosing. The cotton swabs were analysed for Rufi by using a suitable extracting solvent. Rufi was quantified using a previously developed and

validated HPLC method. The study was performed in *n*=3 animals for each formulation.

4.2.10.4 Brain and Plasma PK analysis

In the PK study, for both the treatments, formulation equivalent to Rufi dose of 1 mg/kg with a dose volume of 40 µL/kg was administered to the rats. Retro orbital puncture technique was used to withdraw blood samples at pre-determined time points: pre dose, 5, 15, 30, 45, 60, 120, 240, 360, 480, and 600 min. Around 200 µL of blood was collected at each time point in centrifuge tubes containing 4.5% w/v solution of EDTA sodium salt (EDTA solution was used at 10% v/v of blood collected). Brain tissue from animals was harvested at pre-determined time intervals post dosing: 30, 60, 120, 240, and 480 min (*n*=4 rats were used at every time point). Plasma and brain samples were processed and analysed using a validated RP-HPLC method described in Section 2.4, Chapter 2. PK parameters were computed using Phoenix WinNonlin software version 8.1 by employing NCA analysis of the data. The results obtained from plasma and brain distribution PK studies of Rufi-NC-RXG and Rufi-NC-Susp were compared with aqueous suspension of plain Rufi (Rufi-Susp) (taken from Section 3.3.5.4, Chapter 3).

4.2.10.5 Quantifying direct N2B uptake

Two parameters viz. % DTE (Direct transport efficiency) and %DTP (nose to brain direct transport percentage) were computed to quantify and compare the brain uptake of Rufi-NC-Susp and Rufi-NC-RXG formulations. These values were computed using Equation 3.1, Equation 3.2, and Equation 3.3 given in Section 3.2.7.4, Chapter 3. A higher DTE value indicates higher overall transport to the brain, both via the

direct N2B pathways and via nasal to systemic to brain pathway. The %DTP value indicates the percentage of transport via direct N2B pathways.

4.2.11 Statistical analysis

To determine statistically significant/critical variables affecting the response variables, Analysis of Variance (ANOVA) was performed for the data obtained from the experimental runs conducted based on the PBD. In case of the optimization design using CCD, the regression model for each response variable was tested and validated based on various diagnostic plots. In addition, the significance of the regression model for each response variable was evaluated based on the results obtained from ANOVA, Adjusted R^2 and Predicted R^2 values. In case of *in vivo* PK studies and *in vitro* characterization, the data was expressed as mean ± SD. One-way ANOVA was used to compare PK data obtained from different experimental groups at 5% level of significance. If the ANOVA results showed statistically significant difference, a suitable post hoc test was applied to further compare the groups.

4.3 Results and discussion

4.3.1 Preliminary trials for preparation of Rufi-NCs

Prior to the identification of critical factors using a screening design, a few preliminary trials were performed to choose the appropriate combination of stabilizers, solvents for dissolution of Rufi, appropriate S-AS, and processing conditions for the preparation of Rufi-NCs using anti-solvent precipitation technique. Solubility of Rufi was checked in several organic solvents like ethanol, NMP, dimethyl sulfoxide (DMSO), MeOH, ethyl acetate, dimethyl formamide (DMF), and acetone. Amongst all the solvents, the solubility of Rufi was found to be highest in DMF and NMP. Further, few trials were performed with a combination of

steric stabilizers (viz. methyl cellulose, HPMC, hydroxy propyl cellulose of different viscosity grades) and amphiphilic surfactants (different grades of Pluronics). The final formulation consisted of HPMC E 5LV and poloxamer 407 as a stabilizer system for the preparation of Rufi-NCs. NMP was used as a solvent for dissolving Rufi.

In this work, Rufi-NCs were prepared using an antisolvent-precipitation technique. The basic steps in this process are - mixing of drug solution and antisolvent → creation of supersaturation → nucleation → growth by coagulation → agglomeration (in case the particle growth is not controlled using stabilizers). The PS of the NCs in this technique mainly depends on two factors- the degree of supersaturation, and how effectively the stabilizers control the particle growth. The degree of supersaturation can be given as:

Equation 4.3

$$\boldsymbol{S = \frac{C}{C^*}}$$

Where $\boldsymbol{C}$ is the actual concentration of the drug in a solvent, and $\boldsymbol{C^*}$ is the concentration of the drug in the mixture of solvent and anti-solvent. It has been widely known that high degree of supersaturation results in greater extent of nucleation leading to formation of many particles with controlled growth [76,77].

In order to achieve high supersaturation, solvents in which Rufi exhibited highest solubility – DMF and NMP were chosen for preliminary trials. In the final formulation, NMP was used to dissolve Rufi. NMP shows very low acute toxicity in animals and is expected to show no hazardous effects on the environment. DMF is listed as a CMR (Carcinogenic, Mutagenic, and Reprotoxic) solvent, and its use is limited to cases where any other solvents like acetonitrile cannot be used [78].

Hence, considering the better safety profile of NMP compared to DMF, NMP was used as a solvent to dissolve Rufi.

Another important aspect in controlling the particle growth, is the choice of stabilizer. Several reports state that the choice of stabilizers is made solely based on experimentation. Khan *et al.,* reported that there is no defined relationship between the drug's physicochemical properties, crystal surface properties and the choice of stabilizer [76]. Toumela A *et al*., has also reported that the factors determining the stabilization effect of stabilizers are not fully understood and that the selection of stabilizer for drug NCs is mostly empirical [79]. For achieving rapid supersaturation, it is imperative that the solubility of Rufi in the S-AS mixture should not be increased due to the presence of stabilizer. Hence, stabilizers which did not increase the solubility of Rufi in the S-AS mixture were considered for further trials. Vitamin E TPGS, Poloxamer 407, poloxamer 108, PEG 400, PEG 6000, lecithin, SLS, Tween 80, PVA, methyl cellulose (grades 400 and 1500 cp), HPMC (100000 cp, 15000 cp, and 5 cp) were screened. Out of the abovementioned polymers, Poloxamer 407, poloxamer 108, methyl cellulose, and HPMC did not affect the solubility of Rufi. Further experimentation revealed that a combination of poloxamer 407 and HPMC 5 cp resulted in a lesser PS and PDI. Hence, they were taken up for optimization using DoE.

4.3.2 Screening and optimization design for preparation of Rufi-NCs

From the preliminary trials, a total of eight independent factors were identified with their upper and lower limits. A PBD screening design with resolution III was used to identify the critical effects. Out of the eight factors (Table 4.1), three factors *viz* factor $\boldsymbol{X_1}$- HPMC concentration (% w/v), factor $\boldsymbol{X_2}$: ultrasonication time (min), and

factor $\boldsymbol{X_3}$: processing temperature (°C) were found to be critically affecting the responses. Hence, these factors were taken up further for optimization design. An inscribed CCD was used for optimization of the three critical factors in order to achieve desired responses for Rufi-NCs. In the screening design (PBD), the ZP and yield (%) did not show much change with the experimental run conditions. Hence, for the optimization design only one response, PS (nm) was evaluated. The standard run order of experimental runs of the design, with the levels of each factor in their original scale, and the responses obtained are given in Table 4.2.

Table 4.2 Randomized run order of the CCD experimental design for Rufi-NCs

Run No.	HPMC conc. (X_1), (% w/v)	Ultrasonication time (X_2), (min)	Processing temperature (X_3), (°C)	PS (Y_1), (nm)	%Yield
1	1.05	15	10	383.3	86.4
2	1.05	10	10	444.8	91.6
3	1.6	12.9	7.0	583.3	91.2
4	1.6	12.9	12.9	550.7	87.0
5	1.6	7.0	12.9	595.8	90.4
6	1.05	10	15	449.3	90.6
7	1.05	5	10	480.9	86.9
8	1.05	10	10	500.3	85.1
9	0.48	7.0	7.0	299	91.0
10	1.05	10	10	474.2	91.2
11	0.48	12.9	7.0	256.8	90.8
12	1.6	7.0	7.0	601.2	86.5
13	1.05	10	10	468.5	86.2
14	0.1	10	10	234.1	89.3
15	2	10	10	910	86.0
16	0.48	7.0	12.9	314	88.9
17	0.48	12.9	12.9	261.5	89.4
18	1.05	10	5	475.8	87.1
19	1.05	10	10	510.9	89.2
20	1.05	10	10	518.8	87.7

The sum of squares, 'F_{cal}' value and 'P' value for the factorial terms having a significant effect on the PS are given in Table 4.3. The factors with 'P' values less than 0.05 were considered to have statistically significant effect on the response. Table 4.3 also shows the 'F_{cal}' values for lack-of-fit, pure error and model terms for

the response. The regression equation for PS in the coded form after deleting the insignificant factor coefficients from the model is as follows:

Equation 4.4

$$\boldsymbol{PS\ (Y_1) = 486.73 + 171.08X_1 - 23.57X_2 - 30.86{X_2}^2}$$

Table 4.3 Statistical output (ANOVA) for regression analysis of optimization model for PS of Rufi-NCs

Source	PS (Y_1)		
	SS	df	P value
Model	4.213E+005	3	< 0.0001
X_1	3.997E+005	1	< 0.0001
X_2	7584.68	1	*0.0859
${X_2}^2$	13973.18	1	0.0244
Residual	36214.35	16	< 0.0001
Lack-of-fit	32171.45	11	0.0835
Pure error	4042.89	5	
Total	4.575E+005	19	

*Note: SS represents Sum of Squares; *Even though the 'P' value is more than 0.05 for the term, it is included in the regression model to preserve hierarchy of the model*

The PS of the NCs was affected by HPMC concentration and the ultrasonication time. A quadratic model was suggested by the software for defining the relationship between the PS and the factors affecting it. The model was found to have 'F_{cal}' value of 62.04 with P<0.0001. The lack-of-fit was insignificant (P>0.05). The Predicted R^2 value was 0.85 and the Adjusted R^2 value was 0.90. The distribution of residuals was random around zero with no specific pattern. The 3D plot for PS is given in Figure 4.1.

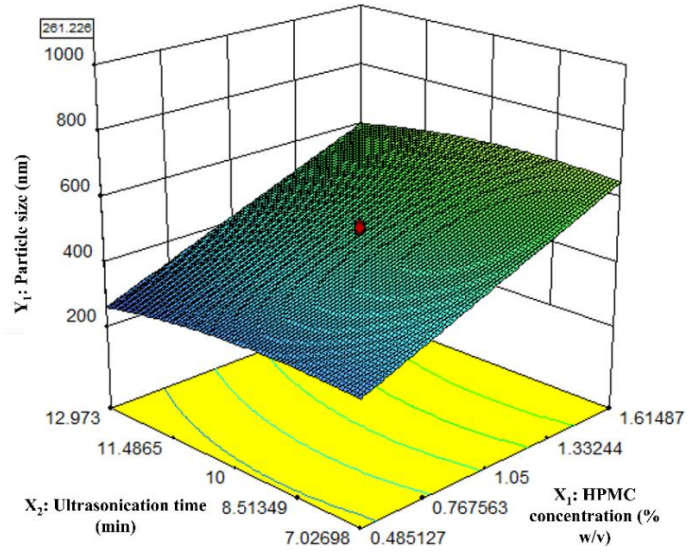

Figure 4.1 3D Response surface plot showing the effect of HPMC concentration and ultrasonication time on PS of Rufi-NCs

The experimental conditions predicted by software based on the quadratic models for PS were: HPMC concentration (% w/v) of 0.48; processing temperature of 10 °C; and total ultrasonication time of 12.9 min. The optimized formulation showed a PS of 261.2 ± 2.1 nm, PDI of 0.28 ± 0.08, and yield (%) of 89.6 ± 2.0. To check the validity of the model given by the software, six verification runs (n=6) were carried out. Formulations were prepared as per the experimental conditions given by the model. The observed values for the responses were compared with the predicted values given by the model. No significant difference (P>0.05) between the observed and predicted values.

During preliminary studies, scanning electron microscopic (SEM) imaging showed that Rufi-NCs had needle/rod shape. Measurement of PS of any dispersion using dynamic light scattering gives the hydrodynamic diameter of the particles assuming the particles in dispersion are spherical in shape. Therefore, analysing PS of Rufi-NCs using zeta-sizer which works on the principle of dynamic light scattering does not give the accurate PS as the particles are not spherical in shape. Characterization

of formulations prepared based on the experimental runs in CCD using SEM and zeta-sizer showed different PS for Rufi-NCs. However, the trend in PS obtained for the formulations from SEM analysis correlated with that of the PS determined using zeta-sizer. Hence, PS analysis using zeta-sizer was considered as a reliable measure to evaluate the effect of various factors on PS of Rufi-NCs. Therefore, the regression equation relating the effect of various factor on PS may not give the true PS of Rufi-NCs when analysed using SEM. However, the regression equation can be used to understand the direction and magnitude in which the critical factors affect the PS of Rufi-NCs.

In the screening design, it was observed that out of the three responses, ZP and yield (%) did not vary much with the experimental run conditions of the design. The ZP for all the runs ranged between -2.2 to +2.3 mV. The low ZP value can be attributed to very little ionization of Rufi in the pH range between 1-10. In addition, both the stabilizers used in the preparation of Rufi-NCs are non-ionic in nature and would not contribute to the surface charge on the NCs. The yield for all the runs varied between 85 to 92%. Hence, for the optimization design, PS was taken as the only response.

In case of optimization using CCD, the results obtained from lack-of-fit test and ANOVA for the quadratic model suggested that the model is significant. The Predicted R^2 value and the Adjusted R^2 value showed a difference less than 0.2 indicating that the results predicted by the model are significant.

From the response surface plot for PS, it is clear that as the HPMC concentration increases, the PS increases. This could be due to increased viscosity of the system with increase in concentration of HPMC. A greater difference in the viscosities of solvent and anti-solvent may result in poor mixing of the two phases. This could

result in non-uniformity in the supersaturation achieved, giving regions with high number of rapidly growing nuclei that have higher chance of aggregation, in turn resulting in higher PS.

4.3.3 Characterization of formulations using thermal analysis, powder XRD, and SEM imaging

The DSC thermograms are shown in Figure 4.2. The thermogram for pure Rufi showed a sharp endothermic peak at 240 °C. The physical mixture of Rufi with all the ingredients used in the preparation of Rufi-NCs showed an endothermic peak for Rufi at 240 °C and a small peak around 55 °C corresponding to melting endotherm of Poloxamer 407. The thermogram for freeze dried Rufi-NCs also showed a sharp endothermic peak at 160 °C which corresponds to melting point of mannitol, which was used as the cryoprotectant in the freeze-drying process of Rufi-NCs.

The pXRD graphs of pure freeze dried Rufi-NCs, physical mixture of constituents of Rufi-NCs, and pure Rufi are shown in Figure 4.3. The pXRD graphs reaffirm the observations of DSC studies that the polymorphic form of Rufi did not change with the nanocrystal formulation. The prominent crystalline peaks of pure Rufi between 2θ values of 15°–30° seen in pure Rufi graph were also present in the physical mixture and Rufi-NCs.

The SEM analysis was performed for the Rufi-NCs prepared using the experimental conditions given in standard run number 9 (with lowest PS of 234 nm as per zeta-sizer), standard run number 10 (with highest PS of 910 nm as per zeta-sizer) and standard run number 20 (with PS of 468 nm as per zeta-sizer) to compare the PS analysis obtained from zeta-sizer with SEM analysis. The SEM images are given in Figure 4.4.

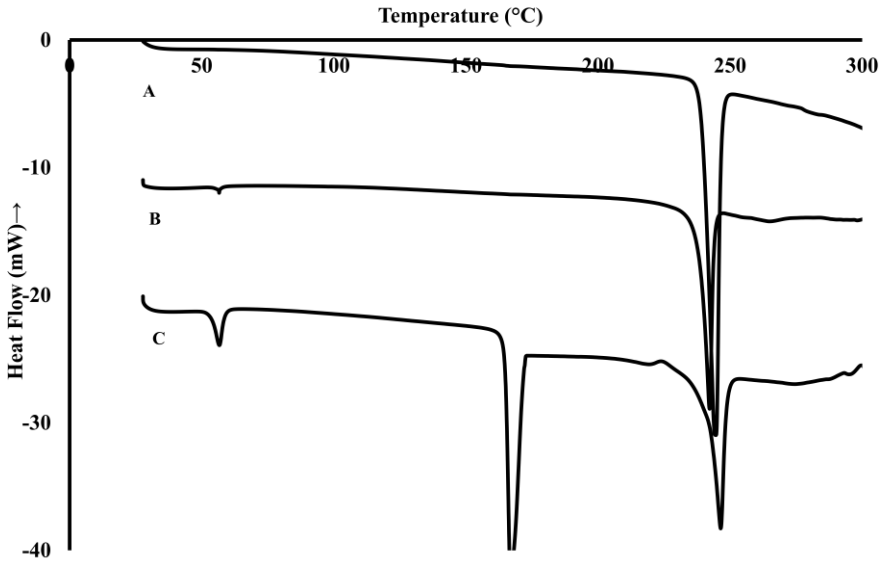

Figure 4.2 DSC thermograms of pure Rufi (A), physical mixture of Rufi with all excipients used in preparation of Rufi-NCs (B), and freeze-dried Rufi-NCs (C)

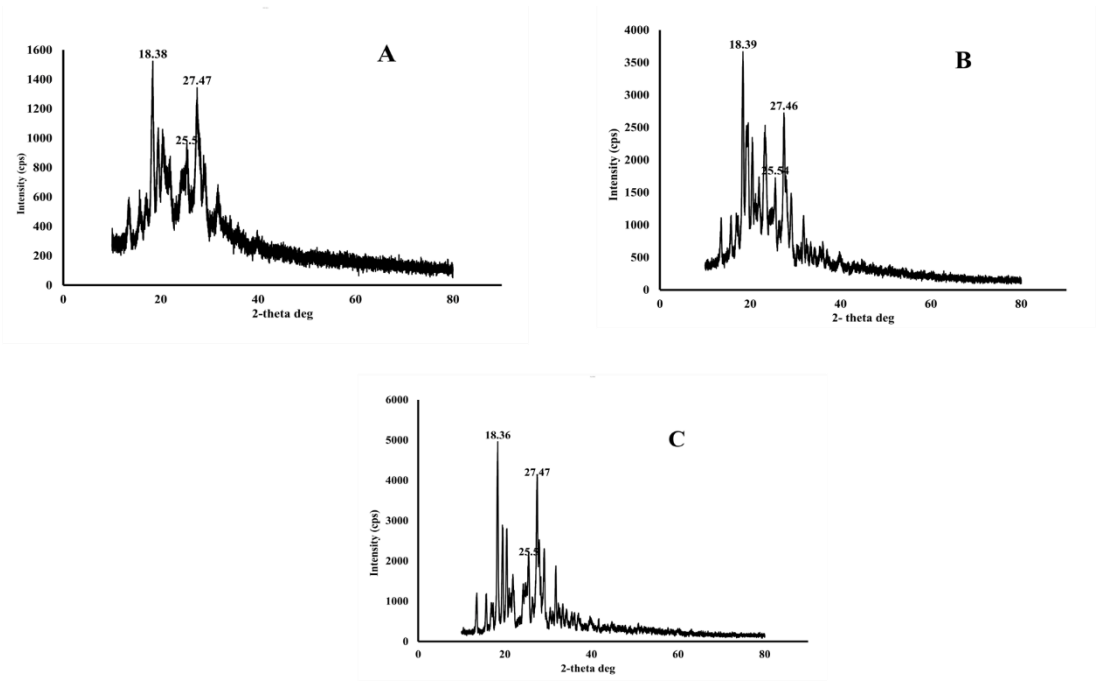

Figure 4.3 X-ray diffractograms of (A) freeze dried Rufi-NCs; (B)Physical mixture of constituents of Rufi-NCs; (C) pure Rufi

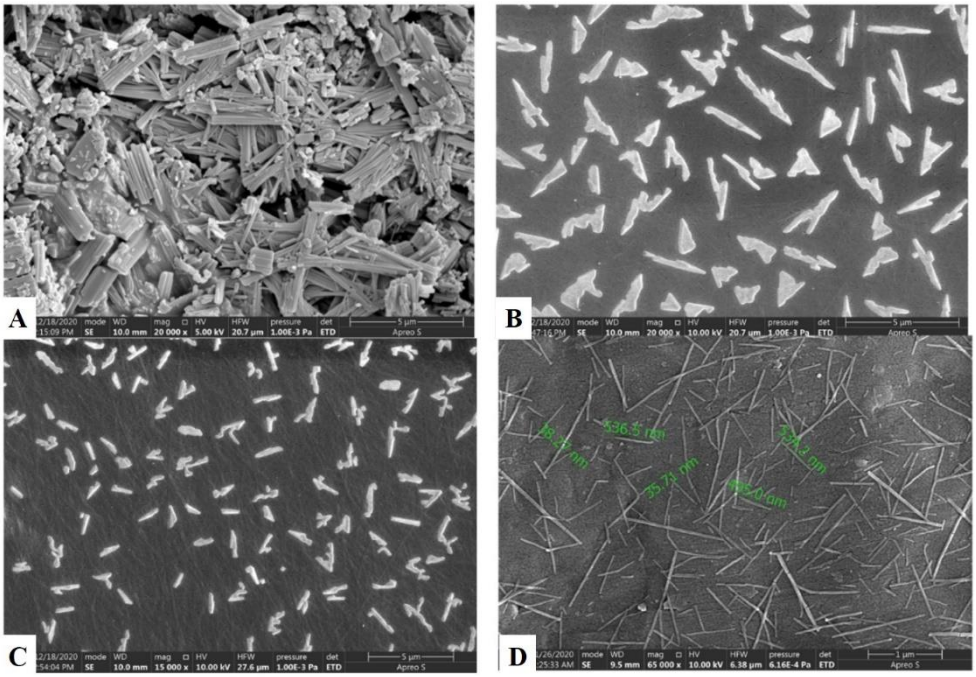

Figure 4.4 SEM images of bulk Rufi (A), Rufi-NCs prepared using Standard run number 10 (PS of 910 nm as per DLS) (B), Standard run number 20 (PS of 468 nm as per DLS) (C) and Standard run number 9 (PS of 234 nm as per DLS) (D)

4.3.4 Rheological evaluation

The $T_{sol \rightarrow gel}$ was determined in the LVER of the formulations. The $T_{sol \rightarrow gel}$ for Rufi-NC-RXG was compared with the $T_{sol \rightarrow gel}$ of Blank-RXG (data taken from section 3.3.3.1). The data of $T_{sol \rightarrow gel}$ of Blank-RXG was taken from our previous published work. The G' values for both formulations at different temperatures are given in Figure 4.4. The plots for G' values vs temperature for Rufi-NC-RXG and Blank-RXG are shown in Figure 4.5. From the rheological evaluation, it can be seen that the G' values of Rufi-NC-RXG were consistently higher than that of Blank-RXG. This may be attributed to the high suspended solid content present in Rufi-NC-RXG. Higher viscosity of Rufi-NC-RXG even below intranasal temperatures, did not affect the dosing precision of the formulation. Greater strength of Rufi-NC-RXG in the gel

state proved to be beneficial in retaining the formulation in the nasal cavity for a longer time.

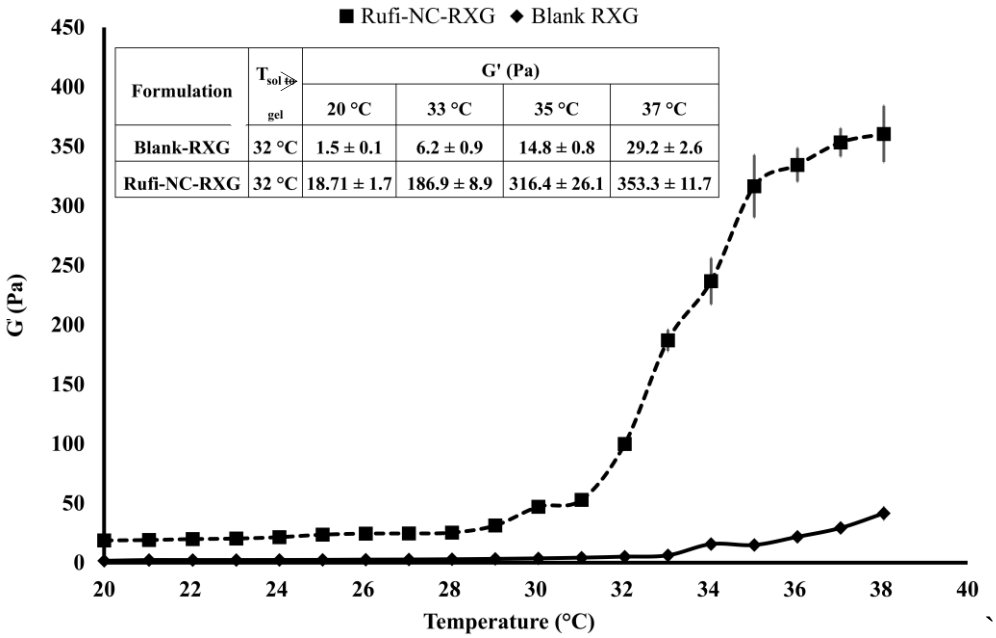

Formulation	$T_{sol \rightarrow gel}$	G' (Pa)			
		20 °C	33 °C	35 °C	37 °C
Blank-RXG	32 °C	1.5 ± 0.1	6.2 ± 0.9	14.8 ± 0.8	29.2 ± 2.6
Rufi-NC-RXG	32 °C	18.71 ± 1.7	186.9 ± 8.9	316.4 ± 26.1	353.3 ± 11.7

Figure 4.5 Rheological evaluation for Rufi-NC-RXG and Blank-RXG using temperature sweep *(Each data point is represented as mean ± SD of n=3 determinations)*

4.3.5 *In vitro* drug release study from Rufi-NC-Susp and Rufi-NC-RXG formulations

The *in vitro* release studies were performed to evaluate the kinetics and mechanism of drug release from Rufi-NCs in RXG *in-situ* gel (Rufi-NC-RXG). The release profile is shown in Figure 4.6. Rufi-NC-Susp dispersed in the medium as soon as the formulation was added, and at the first time point we found that ~100% drug was dissolved in the medium. With Rufi-NC-RXG formulations, ~50% drug release was achieved within 120 min and > 80% drug release was seen at 8.3 h. The sustained release in case of Rufi-NC-RXG is due to the presence of RXG gel network, which hinders the diffusion of the drug. The release profile of Rufi from the Rufi-NC-RXG formulation was fit to different release kinetics models and it was observed that the Higuchi kinetics model (R^2=0.9818) was the best fit when compared to zero order

kinetics model (R^2=0.9418), and first order kinetics model (R^2=0.8884). The 'n' value for Korsmeyer-Peppas model was 0.74 indicating that the mechanism of drug release was non-Fickian. According to the exponent 'n' obtained from Korsmeyer-Peppas model, the release mechanism is a special case of non-Fickian transport - 'Anomalous transport'. In Anomalous transport, the velocity of solvent diffusion and the polymeric relaxation have similar values, i.e., the solvent diffusion process and relaxation of polymeric chains are taking place simultaneously facilitating the drug release. Similarity factor (f2) value obtained for the comparison of the drug release profiles of Rufi-RXG (from Chapter 3, Section 3.3.4) and Rufi-NC-RXG (f2=45) indicated that drug release profiles were not similar.

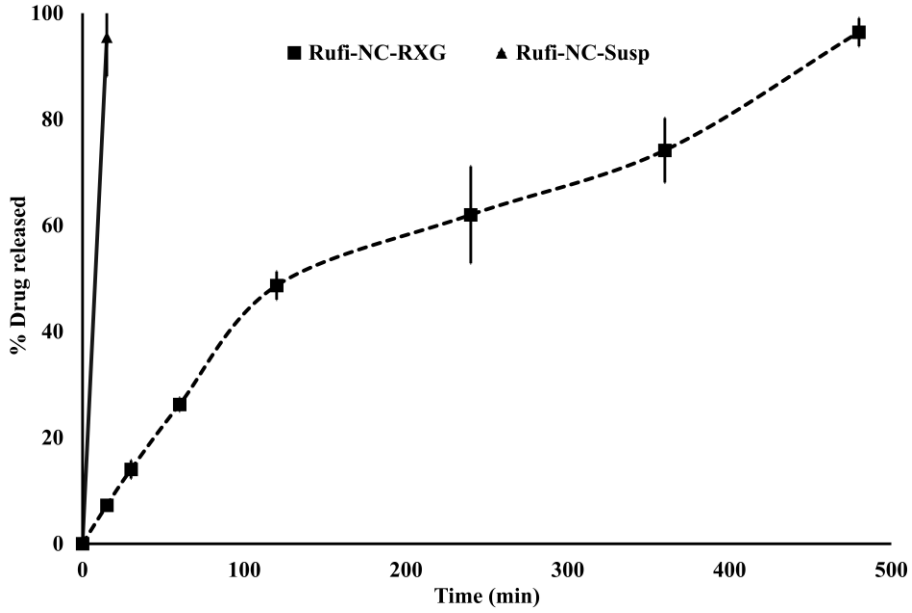

Figure 4.6 *In vitro* release profiles of Rufi-NC-RXG and Rufi-NC-Susp in Simulated nasal electrolyte solution (SNES) (*Each data point is a mean ± SD of three independent observations (n=3)*)

4.3.6 Stability of formulations

No significant difference was observed in the PS and yield (%) of Rufi-NCs (stored at 25 ± 2 °C and relative humidity of 60 ± 5%) and Rufi-NC-RXG (stored in

refrigerated condition, 2-8 °C) for a period of 60 days. The %bias calculated for PS and yield (%) at each sampling time point for both the formulations was found to be not more than 5.0%. This is indicative of physical and chemical stability of both the formulations. The stability data is given in Table 4.4.

Table 4.4 Stability studies of freeze dried Rufi-NCs and Rufi-NC-RXG

Parameter evaluated	Time (days)				
	0	15	30	45	60
Freeze dried Rufi-NCs (stored at 25 °C and 60 ± 5% RH)					
PS (nm)	244 ± 5.2	243 ± 7.3	244 ± 8.7	254 ± 14.3	255 ± 12.8
Yield (%)	87.3 ± 5.6	86.3 ± 5.5	85.6 ± 5.5	83.6 ± 4.5	83 ± 3.6
Rufi-NC-RXG (stored under refrigeration, 2-8 °C)					
PS (nm)	248 ± 6.5	243 ± 7.5	244 ± 21.5	239 ± 15.3	253 ± 6.1
Yield (%)	89.6 ± 2.0	86 ± 2.6	87.6 ±2.5	85 ± 4.5	85.3 ± 5.6

Note: Data is represented as mean ± SD of n = 3 replicates of each formulation stored at their respective stability conditions

4.3.7 *In vivo* studies in male Wistar rats

4.3.7.1 Administration of i.n. dose to rats and dosing precision studies

Formulations were administered using the microtip-cannula setup that was designed specifically for delivery of formulations near the olfactory region in rats. The maximum dose volume that can be administered to a rat weighing around 250 g is up to 30 µL (120 µL/kg) [80]. The dose volume for Rufi-NCs loaded *in-situ* gelling formulations was optimized at 40 µL/kg per nostril. The possibility of the formulation leaking out of the animal's nose was studied before performing the actual PK studies. Prior to *in vivo* studies, *n*=4 animals were dosed with Rufi-NC-Susp mixed with Amaranth dye. To check for any leakage, the nasopalatine duct of the animals was monitored continuously for appearance of the dye. The dose volume of 40 µL/kg did not cause any immediate leakage from the animal's nose.

Loading high amounts of solids in any formulation may bring in variability while administering the dose intranasally. Therefore, a dosing precision study was carried

out for Rufi-NC-RXG and Rufi-NC-Susp formulations. The %RSD values for the amount of Rufi delivered using the nasal delivery set up for both formulations were less than 10% indicating precise dosing of the formulations.

4.3.7.2 Assessment of mucociliary transport time (MTT)

The MTT values of Rufi-Susp, Rufi-NC-Susp, and Rufi-NC-RXG were 11.6 ± 2.8 min, 26.6 ± 5.7 min and 43.3 ± 5.7 min, respectively. Rufi-NC-RXG showed statistically higher (P<0.05) MTT value than compared to Rufi-NC-Susp. The MTT values for both the nanocrystal formulations (Rufi-NC-Susp and Rufi-NC-RXG) were significantly higher than Rufi-Susp (P<0.05). Higher residence time of Rufi-NC-RXG compared to Rufi-NC-Susp can be attributed to its higher gel strength which resists mucociliary clearance of formulation from the nasal cavity.

The mucociliary clearance (MCC) process is a defence mechanism of the nose to push away foreign particles entering the nose. To have higher residence time in the nasal cavity, a formulation must resist the MCC process. A significantly higher MTT was observed for Rufi-NC-RXG when compared to Rufi-NC-SUSP and Rufi-Susp. The higher gel strength of Rufi-NC-RXG resulted in a higher MTT which increased its retention in the nose.

4.3.7.3 PK analysis and quantification of N2B direct uptake

The plasma time course profiles of Rufi-NC-Susp and Rufi-NC-RXG are shown in Figure 4.7A. We compared the pharmacokinetic performance of Rufi-NC-Susp and Rufi-NC-RXG with that of Rufi-Susp (Table 4.5). (PK data for Rufi-Susp was taken from Chapter 3, Section 3.3.5.4).

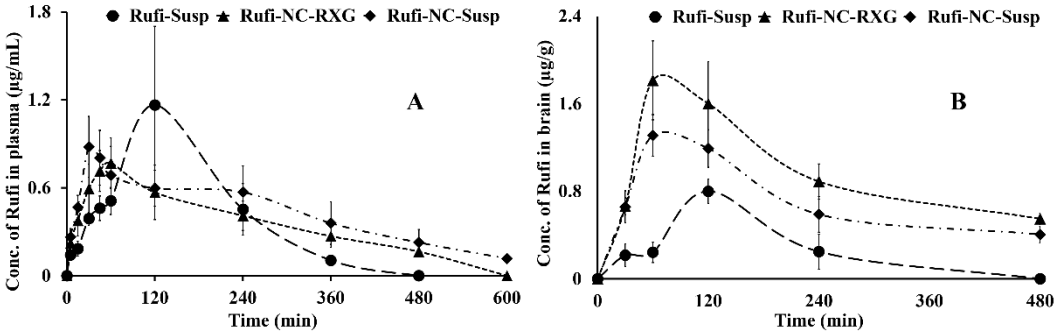

Figure 4.7 Plasma and brain PK performance of Rufi-NC formulations

A: Mean concentration-time profiles of Rufinamide obtained following intranasal administration of Rufi-NC-Susp, Rufi-NC-RXG, and Rufi-Susp in plasma;
B: Mean concentration-time profiles of Rufinamide obtained following intranasal administration of Rufi-NC-Susp, Rufi-NC-RXG, and Rufi-Susp in brain
Each data point is a representation of mean ± SD of n=4 animals for plasma PK, and for brain PK n=4 animals' brains were used at every time point

PK parameters like $AUC_{0\rightarrow tlast}$, C_{max}, T_{max}, MRT were calculated by NCA (Non-compartmental analysis) using Phoenix WinNonlin Version 8.1. A one-way ANOVA comparison for plasma $AUC_{0\rightarrow tlast}$ values for all three formulations showed that there was no statistically significant difference between any of the three formulations. The plasma MRT values of both the nanocrystal formulations were significantly higher than the MRT for Rufi-Susp. The C_{max} values of all the three formulations did not show any statistically significant difference.

Table 4.5 PK parameters of Rufi-NC-RXG, Rufi-NC-Susp, and Rufi-Susp in brain and plasma following i.n. administration at a drug dose of 1 mg/kg

Matrix	PK Parameter	Units	Formulations		
			Rufi-NC-Susp	Rufi-NC-RXG	Rufi-Susp
Plasma	$AUC_{0\rightarrow tlast}$	min×(µg/mL)	258.2 ± 68.6	192.3 ± 59.5	200.75 ± 74.4
	C_{max}	µg/mL	0.92 ± 0.17	0.76 ± 0.17	1.16 ± 0.53
	T_{max}	min	30-45	60	120
	MRT	min	223.8 ± 9.0	177.4 ± 16.4	147.4 ± 9.4
Brain	$AUC_{0\rightarrow tlast}$	min×(µg/g)	340.7	471.3	104.28
	C_{max}	µg/g	1.31 ± 0.19	1.81 ± 0.3	0.79 ± 0.11
	T_{max}	min	60	60	60
	% DTE		373.16	693.1	146.8
	% DTP		73.3	85.5	31.9

Note: All the parameter values are expressed as mean ± SD of (n=4) animals per treatment group. Tmax is expressed as a range or a single value wherever applicable.
In case of plasma data, mean $AUC_{0\text{-}tlast}$ obtained from four animals (n=4) was used while in case of brain data $AUC_{0\text{-}tlast}$ obtained from composite sampling with four animals sacrificed at each time point was used

The brain PK parameters for all three treatments are shown in Table 4.5. The brain concentrations vs time profile of Rufi-NC-Susp, Rufi-NC-RXG, and Rufi-Susp are shown in Figure 4.7B. The brain $AUC_{0\rightarrow tlast}$ values for Rufi-NC-Susp and Rufi-NC-RXG were almost 3 and 4.5 times the brain $AUC_{0\rightarrow tlast}$ values for Rufi-Susp, respectively.

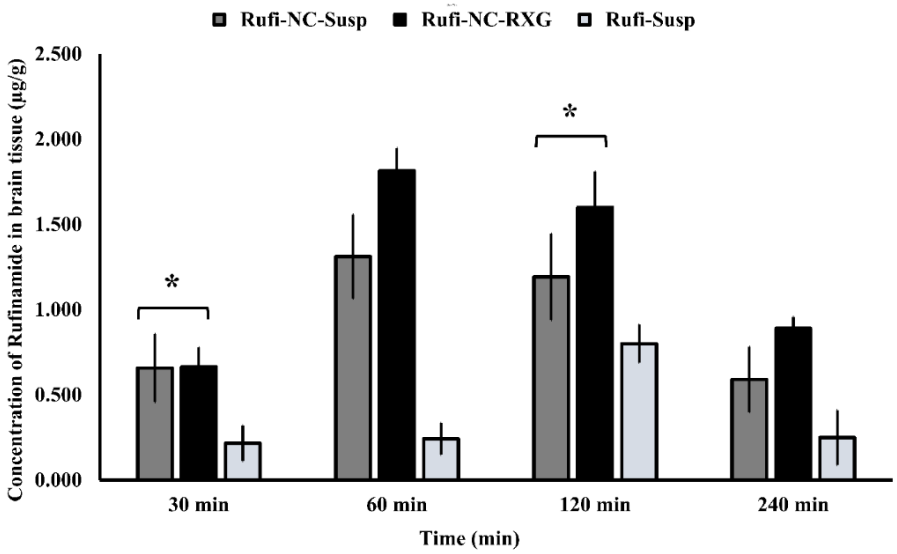

Figure 4.8 Comparison of Rufi brain concentrations following i.n. administration of Rufi-NC-Susp, Rufi-NC-RXG, and Rufi-Susp at different sampling points

**Statistically no significant difference unless mentioned otherwise; All statistical tests were performed for dose normalized concentrations using t-test at α=0.05. n=4 animals were used for brain PK at every time point; Each bar represents brain concentration of Rufi as mean ± SD of n=4 replicates*

Further, the brain concentrations were compared for all three treatments at four different time points: 30, 60, 120 and 240-min using t-test at 5% level of significance (α=0.05) (Figure 4.8). At each time point for every treatment group, *n=4* animals were sacrificed. The concentration of Rufi at each time point was an average of the pooled concentration from 4 animals, the underlying assumption being that inter-individual differences accounted for residual variability rather than the inherent differences in PK process of different treatments. The average brain concentration vs time profile could be constructed only from pooled concentration data, and hence, values of brain $AUC_{0\rightarrow tlast}$ were given as single values without standard deviation. Consequently, ANOVA and other statistical comparison tests could not be applied to brain concentrations unlike plasma concentrations. Instead, the brain concentrations

were compared at four different time points for all treatments using t-tests. The %DTE and values for Rufi-NC-Susp and Rufi-NC-RXG were 373.1 and 693.1 and the %DTP values were 73.3 and 85.5, respectively.

The ANOVA of the plasma PK data showed no significant difference between the plasma $AUC_{0\rightarrow tlast}$ values of both the nanocrystal formulations. This may be due to the enhanced solubility of Rufi-NCs and thereby greater absorption of Rufi into the systemic circulation. However, the brain $AUC_{0\rightarrow tlast}$ of Rufi-NC-RXG was approximately 1.4 and 4.5 times greater than the brain $AUC_{0\rightarrow tlast}$ of Rufi-NC-Susp and Rufi-Susp, respectively. This can be attributed to the greater residence time of Rufi-NC-RXG in the nasal cavity, thereby allowing sufficient time for Rufi to get absorbed into the brain directly. The brain concentrations of both the nanocrystal formulations were significantly higher than Rufi-Susp at all time points. Except for 30 min and 120 min time points, Rufi-NC-RXG showed significantly higher concentration than Rufi-NC-Susp at all time points. The same is reflected in the %DTP values of both nanocrystal formulations.

4.4 Conclusion

This chapter describes the design, optimization, *in vitro* and *in vivo* characterization of Rufi-NCs. Rufi-NCs were prepared using a bottom-up approach by anti-solvent precipitation technique. Rufi-NCs were characterized for their PS, PDI, and percentage yield. The optimized Rufi-NCs were further loaded in a thermoresponsive *in-situ* gelling system. The thermoresponsive *in-situ* gel was formulated using modified tamarind seed polysaccharide, Xyloglucan. *in vivo* plasma and brain pharmacokinetic studies were performed for intranasally administered Rufi-NC-Susp and Rufi-NC-RXG. The results were compared with

intranasally administered plain aqueous suspension of Rufinamide (Rufi-Susp). Comparison of the data showed that Rufi-NC-RXG showed significantly higher brain uptake when compared to Rufi-NC-Susp and Rufi-Susp. The results from this work suggest that intranasally administered nanocrystal formulations of Rufinamide would be beneficial for enhancing its delivery to the brain. This would make its therapeutic regimen less complicated; especially when Rufinamide is prescribed to manage Lennox Gastaut Syndrome in patients from ages 1 to 18.

5 DESIGN, OPTIMIZATION, PHYSICAL CHARACTERIZATION, AND *IN VIVO* EVALUATION OF CHITOSAN NANOPARTICLES OF RUFINAMIDE LOADED IN THERMORESPONSIVE NASAL *IN-SITU* GELLING SYSTEM

5.1 Introduction

Treating Central Nervous System (CNS) disorders has been an ongoing challenge faced by healthcare professionals. Recent advancements made in the field of nanotechnology have made treatment of CNS disorders better. Nanotechnology in nose to brain (N2B) delivery of drugs has also shown encouraging results so far. Nanoparticles have certain features which may be helpful for N2B delivery, such as stabilization by encapsulation, sustained or delayed release, enhanced nasal residence and possible uptake of nanoparticles by the mucosal membranes through endocytosis. Optimization of the particle size (PS), surface charge, surface modification with ligands, and certain polymers/lipids for nanoparticles production can enhance N2B delivery. Researchers have shown that nanoparticulate formulations deliver significantly higher concentrations of drugs to the brain when compared to plain suspension/solution when administered through nasal route [67,81].

In this chapter, we have developed and optimized Rufinamide (Rufi) loaded chitosan – tri polyphosphate nanoparticles (Rufi-Ch-NPs) using the ionic gelation method based on the principles of DoE. Chitosan is a cationic polymer which consists of randomly arranged groups of 2- amino-2-deoxy-D-glucose (D-glucosamine) and 2-acetamido-2-deoxy-D-glucose (N-acetyl-D glucosamine). Chitosan is available in a range of molecular weights (<50 kDa to >350 kDa) and at varying degrees of de-acetylation (35 to 85% de-acetylation). Chitosan is soluble in aqueous media with pH less than 6. At pH less than 6, the amino groups on the molecule ionize resulting in the solubilization of chitosan. Extensive ability to form intra and intermolecular hydrogen bonding and its cationic nature are responsible for its bio-adhesive properties. Chitosan based nanocarriers, hydrogels, mucoadhesive formulations have

shown great applicability in transport of drugs to the brain when administered intranasally [67,82,83]. Chitosan has been widely reported to alter epithelial membrane permeability by interacting with cell-to-cell junctional complexes. Chitosan molecules can open the junction complexes transiently thereby allowing the passage of small molecules via the paracellular pathway. This has been attributed to its ability to alter the junction protein- ZO-1 by acting on protein kinase Cα [84]. In a study reported by Wang *et. al.*, the overall uptake of oestradiol when administered as chitosan based intranasal (i.n.) formulation was much higher than intravenous (i.v.) oestradiol solution [85]. Kumar *et al* have shown the differences in risperidone uptake when formulated as nano-emulsions alone and chitosan coated nano-emulsions. Both the formulations were radiolabelled using ^{99m}Tc and administered through i.n. route. It was observed that with chitosan modified mucoadhesive nano formulation, the accumulation of risperidone was significantly higher than plain nano formulation and i.v. solution [86]. Similar studies on two more molecules, olanzapine and tacrine, were performed by the same research group. The researchers showed that mucoadhesive nano formulation could be used as a platform technology for N2B delivery of therapeutics [86,87]. An *ex vivo* study using porcine olfactory epithelium mounted on a Franz diffusion apparatus was carried out by Mistry *et.al.* The study aimed at evaluating the *in vitro* uptake of polystyrene nanoparticles (100 nm in size) coated with chitosan. The same was also evaluated in an *in vivo* murine model. Both models showed a greater retention period of chitosan coated polystyrene nanoparticles in the olfactory mucus layer as opposed to their uncoated counterparts. It was also reported that the charge on chitosan molecules had a direct relation to the extent of interaction with mucus layers. They inferred that the higher delivery to the brain in case of chitosan coated nanoparticles may be due to its passive targeting

ability via mucoadhesion, thereby increasing the residence time of the formulations in the olfactory region. The authors also stated that chitosan could modify tight junctions in between cells thereby enhancing uptake via the paracellular pathway [67].

In chapter 4, we have shown that Rufi nanocrystals loaded thermoresponsive *in-situ* nasal gelling systems enhance the delivery of Rufi to the brain compared to plain Rufi suspension. In this chapter, Rufi-Ch-NPs were designed and optimised using DoE. Nanoparticles were characterized for their PS, zeta potential (ZP), entrapment efficiency (EE) and drug loading (DL) efficiency. Further, the optimized Rufi-Ch-NPs were suspended in water to get an aqueous suspension of Rufi-Ch-NPs (Rufi-NP-Susp) and also in reacted xyloglucan based thermoresponsive *in-situ* nasal gel described in chapter 3. (Rufi-NP-RXG), separately. Rheological analysis was carried out on optimized nanoparticles loaded in the *in-situ* gelling vehicle to determine its solution to gel ($T_{sol \rightarrow gel}$) temperature [88]. *In vivo* studies were conducted to evaluate mucociliary clearance time, plasma, and brain pharmacokinetic (PK) studies, and nasal toxicity of optimized nanoparticles loaded in the *in-situ* gelling formulation (Rufi-NP-RXG) as compared to aqueous suspension of optimized nanoparticles (Rufi-NP-Susp).

5.2 Materials and Methods

5.2.1 Chemicals and reagents

Rufinamide (Rufi) was obtained from Glenmark Pharmaceuticals, India. Piribedil (Internal Standard (IS) in bio-analytical RP-HPLC method) was a gift sample from Dr. Reddy's Laboratories, Hyderabad, India. Tamarind seed Xyloglucan (TSX) was a gift sample from Encore Natural Polymers Pvt. Ltd. Ahmedabad, India. β-

Galactosidase from Aspergillus oryzae was purchased from Sigma Aldrich, Mumbai, India. Medium molecular weight chitosan (1,90,000-3,50,000 Da; 75-85% de-acetylated), sodium tri poly phosphate (STPP), mannitol, poloxamer 407, polyethylene glycol 400 (PEG 400), and N-methyl - 2 - pyrrolidone (NMP) were obtained from Sigma-Aldrich, Mumbai, India. HPLC grade methanol, acetonitrile (ACN), glacial acetic acid (GAA), and ammonium acetate, and thiomersal were procured from SRL Chemicals Pvt. Ltd., Mumbai, India. For all experimental processes and analysis, HPLC grade Milli Q water from our in-house water purification unit (Millipore®, MA, USA) was used. Male Wistar rats were procured from VAB Biosciences Pvt. Ltd., Hyderabad, India.

5.2.2 Preparation of Rufi loaded Chitosan Nanoparticles

Rufi loaded chitosan nanoparticles (Rufi-Ch-NPs) were prepared using the ionic gelation method. First, the solutions of Rufi, STPP and chitosan were prepared separately. Chitosan solution (1.0% w/v) was prepared by medium molecular weight chitosan in 1.5% v/v of GAA in water. For the preparation of Rufi solution, 5 mg of Rufi and poloxamer 407 were dissolved in 300 µL of NMP followed by the addition of PEG 400 (volume as per the design). STPP solution (30 mg/mL) was prepared by dissolving STPP in water. STPP solution (volume as per the design) was added to Rufi solution to form a mixture which was then added to chitosan solution under high-speed homogenization (Polytron PT 3100D, Kinemetica, Lucerne, Switzerland) at room temperature, using a syringe in a dropwise manner. The amount of chitosan (25 mg) taken was kept same in all the experimental runs. The volume of STPP solution added in the preparation of nanoparticles was varied based on the level of chitosan: STPP mass ratio required in the experimental run. Following the

homogenization process, the dispersion was subjected to ultrasonication (Vibra cell, Sonics, Connecticut, USA). In the optimization runs, the amplitude (20%) and pulse (3s on followed by 3s off) of ultrasonication and homogenization time were kept at fixed values while the homogenization speed was varied according to the design. The dispersion containing Rufi loaded chitosan nanoparticles obtained after processing was subsequently centrifuged and washed three times to remove the free drug. The nanoparticle pellet was re-dispersed in Milli Q water containing 3.0% w/v mannitol as a cryoprotectant (3.0% w/v of the total volume used to re-disperse the nanoparticles) and freeze-dried (Coolsafe 110-4, Scanvac, Lynge, Denmark). The freeze-dried formulation was stored in airtight glass vials at 2-8 °C until further use.

5.2.3 Experimental design for preparation of Rufi loaded chitosan nanoparticles (Rufi-Ch-NPs)

DoE was used in the design and optimization of Rufi-Ch-NPs. Particle size (PS, nm), zeta potential (ZP, mV), and entrapment efficiency (EE, %) of the nanoparticles were identified as critical quality attributes or responses. Critical factors/variables affecting the PS and EE (%) of nanoparticles were first identified using a minimum resolution (Minires) screening design. A total of 6 factors were screened at 2 levels as mentioned in Table 5.1. A few preliminary trials combined with knowledge from previously reported literature helped in selection of the polymers, solvents, processing conditions and their respective high and low levels used in the screening design. The Minires design consisted of 17 runs including 3 centre points.

Table 5.1 Levels of factors used in screening design for optimization of Rufi-Ch-NPs

Factor Code	Actual factors	Levels		
		-1	0	+1
X_1	Chitosan: STPP mass	1	5.5	10
X_2	Volume of PEG 400 (µL)	200	700	1200
X_3	Amount of Poloxamer 407 (mg)	2	6	10
X_4	Homogenization speed (rpm)	5000	10000	15000
X_5	Homogenization time (min)	5	10	15
X_6	Ultrasonication time (min)	2	5	8

From the results of Minires design, four factors *viz*. X_1, X_2, X_3, and X_4 were found to be significantly affecting the responses. Further, a high-resolution BBD was applied to understand how these critical factors and their interactions impacted the responses, and to optimize the preparation of Rufi-Ch-NPs. The BBD is a type of a response surface design, used to obtain a second order polynomial equation to optimize a formulation by performing very few experiments. The BBD consisted of 27 runs (inclusive of 5 centre runs to check reproducibility) for 4 factors. The second order polynomial equation generated from BBD is of the following form:

Equation 5.1

$$Y = \beta_0 + \beta_1 X_1 + \beta_2 X_2 + \beta_3 X_3 + \beta_4 X_4 + \beta_{12} X_1 X_2 + \beta_{23} X_2 X_3 + \beta_{34} X_3 X_4 + \beta_{14} X_1 X_4 + \beta_{13} X_1 X_3 + \beta_{24} X_2 X_4 + \beta_{11} {X_1}^2 + \beta_{22} {X_2}^2 + \beta_{33} {X_3}^2 + \beta_{44} {X_4}^2$$

Where, *Y* is the dependent variable, 'β_0' is the arithmetic mean response of the 27 runs and β_i's and β_{ii}'s (i = 1–4) are coefficients of individual linear and quadratic effects of the factors respectively and β_{ij}'s (i,j = 1–4; $i < j$) are coefficients of the effect of interaction between i^{th} and j^{th} factor.

5.2.4 Desirability function model validation

The optimum values for all factors were given by the Design-Expert version 11 software (Stat-Ease Inc., Minneapolis, MN) based on the desirability function criteria. The desirability function was calculated based on the constrains for the critical responses *viz* minimize PS ($\boldsymbol{Y_1}$) and maximize both ZP ($\boldsymbol{Y_2}$) and EE (%) ($\boldsymbol{Y_3}$). To validate the model, n=6 repetitions were performed based on the experimental conditions predicted by the optimization model. PS, ZP and EE (%) were determined for all the repetitions. Wilcoxon signed rank test was performed to check if there was any significant difference between observed values and values predicted by the model.

5.2.5 Preparation of Rufi-Ch-NPs loaded in reacted xyloglucan (RXG) based *in-situ* gel (Rufi-NP-RXG)

RXG *in-situ* gel was prepared using a method given in Section 3.2.5 in Chapter 3. The formulation development and optimization were based on several parameters which are discussed in detail in Section 3.3 in Chapter 3. The optimized, freeze dried Rufi-Ch-NPs were dispersed in 2.0% w/v solution of RXG using a magnetic stirrer to form a homogenous Rufi-NP-RXG suspension.

5.2.6 Characterization of formulations

5.2.6.1 Measurement of PS, Polydispersity index (PDI) and ZP of Rufi-Ch-NPs

PS, PDI and ZP of Rufi-Ch-NPs were measured using a zeta-sizer instrument (Nano ZS, Malvern Instruments Ltd., Worcestershire, UK). The intensity of the scattered light was measured at a backscatter angle of 173°. All measurements were performed at 25 °C and the samples were equilibrated for 2 min before the measurements were made.

5.2.6.2 Determination of entrapment efficiency and drug loading

EE (%) and DL (%) were evaluated using an indirect and direct method respectively. For the indirect method, the nanoparticle suspension was centrifuged at 12,000 rpm for 30 min at 10 °C to obtain a pellet. This was washed thrice to remove free drug adhering to the surface of NPs. The supernatant was suitably diluted, and free drug was analysed using a previously developed and validated HPLC method (Chapter 2, Section 2.3). The EE (%) was calculated using the following equation:

Equation 5.2

$$\boldsymbol{EE}(\%) = \frac{\boldsymbol{W_{total\ Rufi} - W_{free\ Rufi}}}{\boldsymbol{W_{total\ Rufi}}} \times \mathbf{100}$$

Where, '$\boldsymbol{W_{total\ Rufi}}$' is the amount of Rufi used in the preparation of nanoparticle formulation and '$\boldsymbol{W_{free\ Rufi}}$' is the amount of Rufi in the supernatant. In case of the direct method for estimation of EE (%), the nanosuspension formulation was washed with thrice its volume of water and centrifuged at 12,000 rpm for 30 min at 10 °C. The supernatant was discarded, and the pellet obtained was dried under vacuum and dissolved in a suitable solvent to extract Rufi. Rufi was quantified using a previously developed and validated HPLC method (Chapter 2, Section 2.3).

For the estimation of DL (%) direct method was followed. The nanosuspension formulation was washed with thrice its volume of water and centrifuged at 12,000 rpm for 30 min at 10 °C. The supernatant was discarded, and the pellet obtained was dried under vacuum. The dried pellet was weighed. Further, it was dissolved in a suitable solvent to extract Rufi. Rufi in the pellet was quantified using a previously developed and validated HPLC method (Chapter 2, Section 2.3). The DL (%) was calculated using the following equation:

Equation 5.3

$$\boldsymbol{DL}(\%) = \frac{\boldsymbol{W_{Rufi}}}{\boldsymbol{W_{pellet}}} \times \mathbf{100}$$

Where, '$\boldsymbol{W_{Rufi}}$' is the weight/amount of Rufi present in the pellet and '$\boldsymbol{W_{pellet}}$' is the weight of the dried nanosuspension pellet.

5.2.6.3 Morphological analysis of Rufi-Ch-NPs

A scanning electron microscope with a sputter coater (FE-SEM, FEI, Apreo LoVac, TermoFisher Scientific, MA, USA; EM UC7 Leica Ultra Microtome, Wetzlar, Germany (Sputter Coater)) was used to view the surface and size of the formed nanoparticles. 50 µL of formulation was spread evenly on an aluminium stub and left to dry under vacuum for 12 h. Sputter coating was achieved with gold under an inert environment. The sputter coated sample was kept in a vacuum chamber to capture images at an acceleration voltage of 5 kV.

5.2.6.4 Differential scanning calorimetric (DSC) analysis

DSC analysis (DSC 60; Shimadzu Corporation, Kyoto, Japan) was performed for Rufi-Ch-NPs and its components. Briefly, weighed samples (5 mg) were taken in aluminium pans and crimp sealed. The thermograms were obtained in the temperature range of 10 to 300 °C with a heating rate of 10 °C/min in an inert (Nitrogen) environment.

5.2.7 Rheological evaluation

Rheological evaluation (Anton Paar MCR 302, Graz, Austria) was carried out to determine the $T_{sol \rightarrow gel}$ (solution to gel transition temperature) for Rufi-NP-RXG and Blank-RXG (as per optimized RXG concentration discussed in Section 3.2.5.2 in Chapter 3). The LVER (linear viscoelastic region) was identified for the samples

using an amplitude sweep. Measurements were performed in the oscillatory mode using a temperature sweep within the LVER of the samples. $T_{sol \rightarrow gel}$ and the strength of gel formed were assessed using a plot depicting the storage modulus (G′) vs temperature.

5.2.8 *In vitro* drug release study from Rufi-NP-Susp and Rufi-NP-RXG formulations

In vitro drug release study was carried out by membrane-less sample and separate method for Rufi-NP-Susp and Rufi-NP-RXG formulations. Dissolution was carried out in 250 mL beakers, all of the same dimensions. At the base of the beaker, an aluminum pan was glued at the center. The beakers were pre equilibrated at 34 ± 1 °C for around 30 min. Formulation quantity equivalent to 2.5 mg of Rufi were carefully dropped into the aluminum pan which was glued to the beaker. Within 2 min of addition of the formulations, 125 mL of dissolution medium, (simulated nasal electrolyte solution (SNES)) pre-equilibrated at 34 ± 1 °C was carefully poured into the beakers. The beakers were left in the incubator orbital shaker at 34 °C, 100 rpm. Samples of 2 mL were withdrawn at predetermined time points (60, 120, 240, 360, 480, 720, and 1440 min) from each beaker at different time points. The samples were centrifuged at 12,000 rpm for 30 min at 10 °C. Samples were analysed using a validated RP-HPLC analytical method (as given in Chapter 2, Section 2.3). The results from the *in vitro* study were fitted into different mathematical models viz. zero order, first order, Higuchi and Korsmeyer-Peppas model. The mechanism of drug release was determined based on the value of ‘n’ obtained from the Korsmeyer-Peppas model. Similarity factor (f2) was used for pair-wise comparison of the dissolution profiles of Rufi-NP-Susp and Rufi-NP-RXG formulations.

5.2.9 Stability of Rufi-Ch-NPs and Rufi-NP-RXG formulations

Stability was assessed for both formulations- Rufi-Ch-NPs and Rufi-NP-RXG. Freeze-dried Rufi-Ch-NPs were stored separately in airtight vials (*n=3*) at room temperature conditions (25 ± 2 °C and relative humidity of 60 ± 5%), and Rufi-NP-RXG formulation was stored separately in refrigerated conditions (2-8 °C). Samples were collected after every 15 days and evaluated for their PS, EE (%), ZP, and drug content.

5.2.10 *In vivo* studies

In vivo studies included the assessment of nasal mucociliary transit time (MTT) and PK evaluation of Rufi-NP-RXG and aqueous suspension of Rufi-Ch-NPs (Rufi-NP-Susp). Adult male Wistar rats weighing 240–260 g were used for these studies. Animals were housed in our institute's animal housing facility which was maintained at controlled temperature, humidity, and light dark cycle (22 ± 1 °C, 55 ± 10% relative humidity and 12 h light dark cycle). After procuring animals, they were allowed to acclimatize to the new environment for at least 10 days before using them for experimentation. Food and water were provided *ad libitum*; except during experimentation, water was provided throughout the experiment and food was provided 4 h post dosing. Prior to a PK study, animals were kept for overnight fasting before carrying out PK studies. Prior approval was obtained from the institute's animal ethics committee (Approval number- BITS-Hyd/IAEC/2017/19) for all the procedures carried out during animal experimentation.

5.2.10.1 Nasal dose administration and dosage precision

The set up and the technique used for nasal administration of the dose was optimised as given in Section 3.2.7.1 in Chapter 3. 10 µL of formulation was administered in

one nostril of the animals using a pipette and a cannula-microtip set up while maintaining the animal under isoflurane anaesthesia. After administering the dose, the animal was laid down in supine position till it recovered from the anaesthesia.

5.2.10.2 Dosing precision studies

Dosing precision study was carried out for Rufi-NP-Susp and Rufi-NP-RXG. Using the nasal dosing set up shown in Figure 3.1 (in Chapter 3, Section 3.2.7.1), 10 µL of formulation was pipetted out and analysed for Rufi after suitable dilutions. This was repeated 6 times for each formulation, and the per cent relative standard deviation (%RSD) for the concentration of Rufi delivered each time was calculated.

5.2.10.3 Measurement of mucociliary transit time (MTT) of formulations

MTT for Rufi-NP-RXG and Rufi-NP-Susp was measured as per the method given in Section 3.2.7.3 in Chapter 3. After administering the formulations as per the abovementioned technique, the oropharyngeal cavity of rats was swabbed with cotton buds at pre-determined time points till 360 min. Rats were not allowed access to food and water till 2 h after administering the dose. Swab samples were analysed for Rufi using HPLC analytical method as mentioned in Section 2.3 in Chapter 2. The time point at which Rufi was detected in the swab samples was recorded for each animal for both formulation groups. The study was done in triplicates (n=3 animals for each formulation).

5.2.10.4 Pharmacokinetic (PK) studies in male Wistar rats

Plasma and brain distribution PK studies were performed for Rufi-NP-Susp and Rufi-NP-RXG. The results from these studies were compared with Rufi-Susp (plain aqueous suspension of Rufi). In the study, for both the treatments, formulation equivalent to 1 mg/kg of Rufi dose with a dose volume of 40 mL/kg was

administered to the rats. Retro orbital puncture technique was used to withdraw blood samples at pre-determined time points: pre dose, 5, 15, 30, 45, 60, 120, 240, 360, 480, and 600 min. Around 200 µL of blood was collected at each time point in centrifuge tubes containing 4.5% w/v solution of EDTA sodium salt (EDTA solution was used at 10% v/v of blood collected).

Brain tissue from animals were harvested at pre-determined time intervals post dosing of the formulations: 30, 60, 120, 240, and 480 min (*n*=4 animals were used at every time point). Plasma and brain samples were processed using the validated HPLC method mentioned in Section 2.4 in Chapter 2. PK parameters were computed using Phoenix WinNonlin software version 8.1 by employing NCA analysis of the data obtained from the study.

5.2.10.5 Quantification of N2B uptake of formulations

Two parameters viz. %DTE (Direct transport efficiency) and %DTP (N2B direct transport percentage) were computed to quantify and compare the brain uptake of Rufi-NP-RXG and Rufi-NP-Susp. The %DTE and %DTP were calculated as per Equation 3.1, Equation 3.2, and Equation 3.3 mentioned in Section 3.2.7.4 in Chapter 3.

5.2.11 Statistical evaluation of data

To determine statistically significant/critical variables affecting the response variables, Analysis of Variance (ANOVA) was performed for the data obtained from the experimental runs conducted based on Minires screening design. In case of the optimization design using (BBD) model, the regression model between each of the response variables and their corresponding critical factors were tested and validated based on various diagnostic plots (half-normal probability plot for the response

variables, residuals versus predicted response plot, residuals versus run number plot, difference in fits versus run number plot and Box-Cox Plot). In addition, the significance of the regression model for each of the response variables (PS ($\boldsymbol{Y_1}$), ZP ($\boldsymbol{Y_2}$) and EE (%) ($\boldsymbol{Y_3}$)) were evaluated based on the results obtained from ANOVA, Adjusted R^2 and Predicted R^2 values.

In case of *in vivo* PK studies and *in vitro* characterization the data were expressed as mean ± SD. One-way ANOVA was used to compare PK data obtained from different experimental groups at 5% level of significance. If the ANOVA results showed statistically significant difference, a suitable post hoc test was applied to further compare the groups.

5.3 Results and Discussion

5.3.1 Preliminary trials and screening for critical factors using MiniRes design

Prior to the identification of critical factors using a screening design, a few preliminary trials were performed to choose the right grade of chitosan (right molecular weight of chitosan) and stabilizer, and to set the limits for various factors used in the screening design. A few trials were performed with low, medium, and high molecular weight chitosan with the same degree of de-acetylation (75-85%). It was observed that at same processing conditions and same concentrations, high molecular weight chitosan consistently yielded nanoparticles with greater PS than medium and low molecular weight chitosan. This may be because of higher viscosity of high molecular weight chitosan than the other two grades, which impeded the diminution of the particles beyond a certain size [89]. It was observed that the EE (%) values with low molecular chitosan were consistently lesser than 50%. Similar observation was reported by Kouchak *et al* [90]. Out of several stabilizers tested,

poloxamer 407 was chosen because it did not increase the solubility of Rufi in the dispersion medium (used in preparation of nanoparticles). PEG 400 was used as a co-solvent to maintain Rufi in the solubilized form during the addition of STPP solution into the Rufi solution in the preparation of nanoparticles.

From the preliminary trials, a total of six independent factors/variables were identified with their upper and lower limits. A screening design was performed to select the statistically significant critical factors effecting the response variables (PS, ZP and EE (%)). A MiniRes screening design with resolution IV was selected for screening the factors. In a resolution IV design, the main effects are not confounded with other main effects or even two factor interactions. The screening design consisted of 17 runs (including 3 centre point runs) with each factor at two different levels. Centre point runs were performed to determine if the curvature (or the quadratic terms) is significant in the regression model. The information provided by the centre point runs (significance of curvature) can help in selecting the appropriate optimization design.

Out of the six factors, the main effects of four factors viz. $\boldsymbol{X_1}$- chitosan: STPP mass ratio, $\boldsymbol{X_2}$ - volume of PEG, $\boldsymbol{X_3}$- amount of poloxamer 407, and $\boldsymbol{X_4}$- homogenization speed were found to be statistically significant. Statistical analysis of the model revealed that the regression models obtained in the screening design were significant for all the three responses. The 'F_{cal}' values for regression models of the responses were 8.33 (P<0.05) for PS, 312.2 (P<0.001) for ZP, and 934.15 (P<0.001) for EE (%). In addition, the ANOVA results revealed that the curvature was significant in all the three regression models.

5.3.2 Optimization of critical factors for the preparation of Rufi-Ch-NPs

BBD, being one of the two popular quadratic response surface methods, was selected for the optimization of response variable as a function of the four critical factors. The composition of various runs generated by BBD and their corresponding responses obtained for each run are given in Table 5.2. The sum of squares, 'F_{cal}' value and *'P'* value for the factorial term are given in Table 5.3. The factors with *'P'* values less than 0.05 were considered to have statistically insignificant effect on the response. Table 3 also shows the 'F_{cal}' values for lack-of-fit, pure error and model terms for each response. Factors affecting individual response variable and their regression equation is discussed in the subsequent sections.

Table 5.2 BBD generated by Design Expert software and the observed responses

Run	Critical Factors				Responses			
	Chitosan: STPP mass ratio; $\mathbf{X_1}$	Volume of PEG 400 (µL); $\mathbf{X_2}$	Amount of Poloxamer (mg); $\mathbf{X_3}$	Homogenization speed (rpm); $\mathbf{X_4}$	PS (nm); $\boldsymbol{Y_1}$	ZP (mV); $\boldsymbol{Y_2}$	EE (%); $\boldsymbol{Y_3}$	DL (%) ; $\boldsymbol{Y_4}$
1	1	200	6	10000	2034.8	10.9	69.04	10.0
2	10	700	2	10000	234.9	40.4	74.89	12.2
3	5.5	700	6	10000	224.7	36.1	63.25	9.3
4	10	1200	6	10000	289	41.1	75.41	10.8
5	5.5	200	6	15000	250.2	31.4	69.4	10.1
6	1	700	6	5000	2029.6	7.6	72.15	10.4
7	5.5	700	10	5000	220.9	30.6	67.38	8.8
8	1	1200	6	10000	1949.6	9.3	68.59	9.9
9	1	700	2	10000	2077.1	8.9	70.73	11.6
10	5.5	1200	2	10000	246.7	31.3	65.84	10.9
11	10	700	6	15000	245.8	28.3	73.41	10.6
12	5.5	200	6	5000	226.1	29.7	63.43	9.3
13	5.5	700	6	10000	215.3	32.2	70.08	10.2
14	5.5	1200	6	5000	184.9	35.4	70.61	10.2
15	5.5	1200	10	10000	252.4	34.9	64.16	8.4
16	1	700	6	15000	2007.3	9.1	70.12	10.2
17	5.5	700	6	10000	235.9	29.4	67.92	9.9
18	1	700	10	10000	2009.5	8.3	71.43	9.3
19	5.5	1200	6	15000	270.2	33.4	68.16	9.9

20	5.5	200	10	10000	238.8	36.2	66.72	8.7
21	5.5	700	2	5000	218.2	34.1	63.31	10.5
22	10	200	6	10000	179.9	27.6	72.79	10.5
23	5.5	700	2	15000	265.2	32.4	66.45	10.9
24	5.5	200	2	10000	221.6	33.9	63.96	10.6
25	10	700	6	5000	266.4	30.3	69.13	10.0
26	5.5	700	10	15000	216.1	30	66.28	8.6
27	10	700	10	10000	255.7	28.2	73.61	9.5

Table 5.3 Statistical output (ANOVA) for the critical responses for Rufi-Ch-NPs

Source	PS (nm) ($\boldsymbol{Y_1}$)			ZP (mV) ($\boldsymbol{Y_2}$)			EE (%) ($\boldsymbol{Y_3}$)		
	SS	df	P value	SS	df	P value	SS	df	P value
Model	1.48E+07	4	< 0.0001	2697.21	4	< 0.0001	212.69	2	< 0.0001
$\boldsymbol{X_1}$	9.43E+06	1	< 0.0001	1675.6	1	< 0.0001	24.6	1	0.0365
$\boldsymbol{X_2}$	142.83	1	*0.6263	20.54	1	*0.1520			
$\boldsymbol{X_1X_2}$	9438.12	1	0.0006	57.002	1	0.0217			
$\boldsymbol{{X_1}^2}$	5.39E+06	1	< 0.0001	944.06	1	< 0.0001	188.09	1	< 0.0001
Residual	12885.57	22		205.23	22		92.97	21	
LoF	12672.85	20	0.1533[#]	182.59	20	0.6894[#]	68.59	19	0.9170[#]
Pure error	212.72	2		22.65	2		24.37	2	
Total	1.48E+07	26		2902.45	26		333.06	26	

Note: SS: Sum of Squares; [^]Only statistically significant terms, expect for those which are required to maintain model hierarchy, are presented in the table; [#]Lack-of-fit of the model is insignificant; [*]Though the P>0.05 for these terms, they are included in their respective regression model to preserve hierarchy of the model

5.3.2.1 Effect of critical factors on PS

The least square polynomial equation (in terms of coded factors) describing the effect of critical factors on PS (after ignoring insignificant factors) at 95% confidence level is:

Equation 5.4

$$\boldsymbol{PS\ (Y_1) = 232.48 - 886.35X_1 + 3.45X_2 + 48.58X_1X_2 + 899.15{X_1}^2}$$

A quadratic model was suggested by the software for PS. The model was found to have 'F_{cal}' value of 6328.59 with P<0.0001. The lack-of-fit was insignificant (P>0.05). The Predicted R^2 value was 0.9985 and the Adjusted R^2 value was 0.9990. The difference between the two values was less than 0.2 which is indicative of the

closeness of observed and predicted responses by the model equation for PS. The distribution of residuals was random around zero with no specific pattern. All these indicated that the chosen model fitted well to the response variable, PS. Highest PS was observed for the 9th run with a PS of 2077.1 nm and smallest PS was observed for the 22nd run with a PS of 179.9 nm.

The effect of Chitosan: STPP mass ratio and volume of PEG 400 on PS is shown in Figure 5.1A. With increases in Chitosan: STPP mass ratio from 1 to 7 units, PS of the nanoparticles decreased significantly. However, as the Chitosan: STPP mass ratio is increased beyond 7 units to 10 units, the PS of nanoparticles did not change significantly. This observation was found to be in line with the observations reported by F. Rázga et al. in their review article [89]. As the chitosan: STPP ratio decreases below 6, the balance between NH_3^+ ions and O^- ions shifts towards STPP. For the same amount of STPP, a greater number of NH_3^+ groups can bind to the O^- ions rapidly. Such a strong ionic interaction hinders further breakdown of particles at the same amount of energy input. No significant was observed in PS with change in volume of PEG 400 used in the formulation. Similarly, change in the amount of Poloxamer 407 did not have a significant effect of the PS of the nanoparticles (Figure 5.1 B). The effect of homogenisation speed on PS of nanoparticles was also insignificant.

The least square polynomial equation (in terms of coded factors) describing the effect of critical factors on ZP (after ignoring insignificant factors) at 95% confidence level is as follows:

Equation 5.5

$$\boldsymbol{ZP\ (Y_2) = 32.73 + 11.82X_1 + 1.31X_2 + 3.78X_1X_2 - 11.90{X_1}^2}$$

The quadratic model for ZP was found to have 'F_{cal}' value of 72.28 with P<0.0001. The *'P'* value for 'lack-of-fit' for the model was 0.6894, suggesting that lack-of-fit is insignificant (Table 5.3). Both these results indicate how well the model fits the data obtained for ZP. The distribution of residuals for different runs was randomly distributed around zero with no specific pattern. Higher values of Predicted R^2 (0.8857) and Adjusted R^2 (0.9164) with their difference less than 0.2 indicate that values predicted using the model will be in close agreement with the observed values. Overall, the model diagnostics showed that the model fitted the data well. Chitosan: STPP mass ratio, volume of PEG 400 and their interaction had significant effect on ZP. It is evident from Figure 5.1C, as the chitosan: STPP mass ratio increases, the ZP also increases. This increase in positive ZP can be attributed to NH_3^+ groups on chitosan which were left unbound from the O^- ions of STPP. The interaction term $\boldsymbol{X_1X_2}$ showed a statistically significant effect on the ZP. Hence, to maintain hierarchy of model, the factor $\boldsymbol{X_2}$ (volume of PEG 400) although not significant had to be included. Overall, the ZP was profoundly affected by Chitosan: STPP mass ratio. The optimized formulations showed a high ZP which resulted in strong repulsion, no particle aggregation and therefore good stability for the formulation.

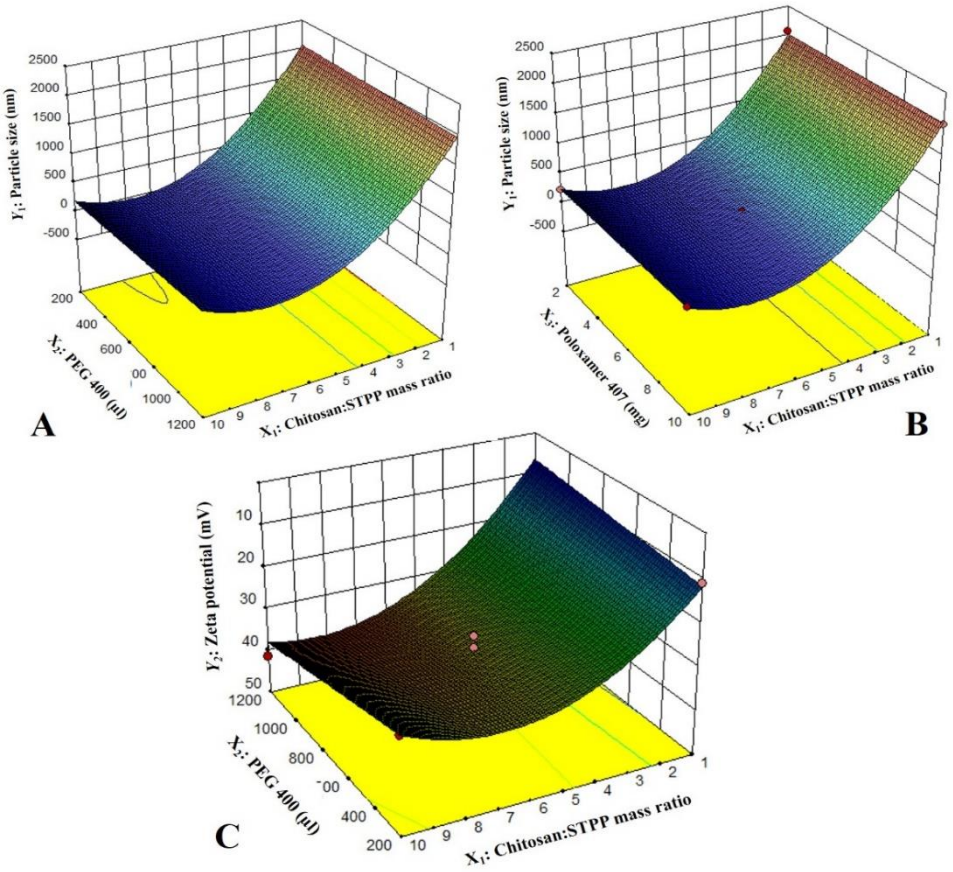

Figure 5.1 3-D response surface plots for A: Effect of factors $\boldsymbol{X_1}$ (Chitosan: STPP mass ratio) and $\boldsymbol{X_2}$ (PEG 400) on PS; B: Effect of factors $\boldsymbol{X_1}$ (Chitosan: STPP mass ratio) and $\boldsymbol{X_3}$ (Poloxamer 407) on PS; C: Effect of factors $\boldsymbol{X_1}$ (Chitosan: STPP mass ratio and $\boldsymbol{X_2}$ (PEG 400) on ZP

5.3.2.2 Effect of critical factors on entrapment efficiency

The EE (%) did not vary significantly for the runs in the design. The EE (%) varied between 64% to 75% across various experimental runs in the optimization. Based on the results obtained from ANOVA, only Chitosan: STPP mass ratio had significant impact on the EE (%). The change in EE (%) from 64% to 75% is primarily due to the increase in Chitosan: STPP mass ratio in those runs. The remaining factors did not have any significant effect on the EE (%) of the Rufi-Ch-NPs.

5.3.2.3 Desirability value and validation of the model

Desirability is a mathematical method to find the optimum values of experimental conditions in order to achieve the desired responses. A set of experimental conditions (given by the optimization model) having a desirability value close to 1 is chosen as the optimum point in the design space. The desirability value obtained Design Expert software for the simultaneous optimization of PS and EE% was 0.960. The experimental conditions predicted by software based on the quadratic models for PS and EE% were - Chitosan: STPP mass ratio = 9.3; volume of PEG 400 = 1200 µL; amount of poloxamer 407 = 3.5 mg; homogenization speed =11473 rpm. The optimized formulation showed a PS of 180 ± 1.5 nm, PDI of 0.29 ± 0.08, ZP of 38.3 ± 1.5 mV, EE% of 75 ± 2.0 % and DL of 11 ± 0.3%. To check the validity of the model given by the software, six verification runs (n=6) were carried out. Formulations were prepared as per the experimental conditions given by the model and the responses viz. PS, ZP and EE% were measured. The observed values for the responses were compared with the predicted values given by the model. The two sets of values were compared using a Wilcoxon signed rank test at 5% level of significance (α=0.05). No significant difference between the observed and predicted values; PS (P=0.069) and ZP (P=0.347).

5.3.3 Characterization studies

The DSC thermograms are shown in Figure 5.2 A. The thermogram for pure Rufi showed a sharp endothermic peak at 240 °C. Pure chitosan showed a broad endothermic peak at 80 °C which is attributed to the loss of water molecules from chitosan. There was no change in the characteristic peak of Rufi in the physical mixture, which indicates an absence of incompatibility between Rufi, and other excipients used in the preparation of the Rufi-Ch-NPs. The thermogram of freeze

dried Rufi-NP-RXG showed a sharp endothermic peak at 160 °C which corresponds to melting point of mannitol, which was used as the cryoprotectant in the freeze-drying process of Rufi-Ch-NPs. Apparently, the absence of the characteristic peak for Rufi in Rufi-Ch-NPs might be due to its presence in amorphous form in the nanoparticle matrix. The SEM image of optimized Rufi-Ch-NPs is shown inFigure 5.2B. From the image, it can be seen that the nanoparticles are spherical in nature.

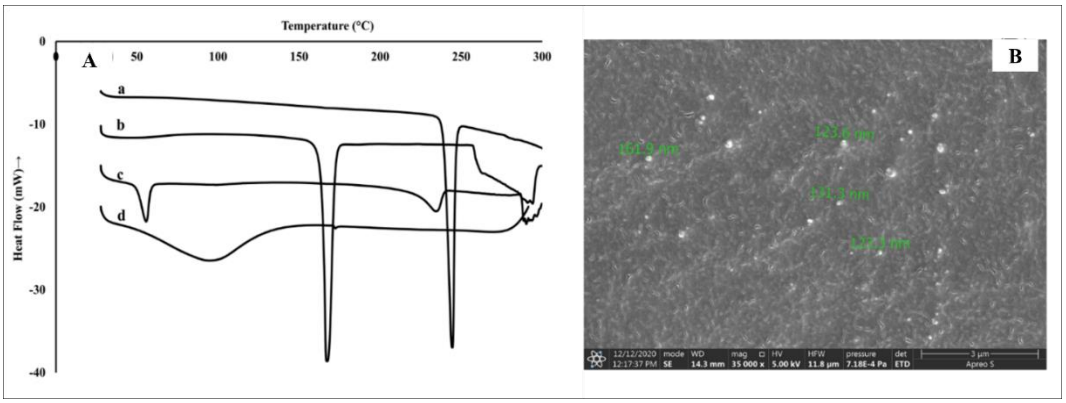

Figure 5.2 Characterization of Rufi-Ch-NPs

A: DSC thermograms of pure Rufi (a), Freeze dried Rufi-Ch-NPs (b), physical mixture of all components of Rufi-Ch-NPs (c), and pure chitosan (d).
B: Scanning electron microscope image of Rufi-Ch-NPs

5.3.4 Rheological evaluation

The $T_{sol \rightarrow gel}$ was determined in the LVER of the formulations. The $T_{sol \rightarrow gel}$ for Rufi-NP-RXG was compared with the $T_{sol \rightarrow gel}$ of Blank-RXG. The plots for G' values vs temperature for Rufi-NP-RXG and Blank-RXG are shown in Figure 5.3. The G' values for Rufi-NP-RXG were consistently higher than Blank-RXG at all temperatures. This can be attributed to hydrophobic interactions, and some ionic interactions between chitosan and xyloglucan molecules [91]. Although the strength of the Rufi-NP-RXG (indicated by G' values) was higher than Blank-RXG even at temperatures below the intranasal temperature, it did not affect the dosing precision of the formulation. Greater strength of Rufi-NP-RXG than Blank-RXG in the gelled

state was found to be beneficial in order to retain the formulation in the nasal cavity for a longer time.

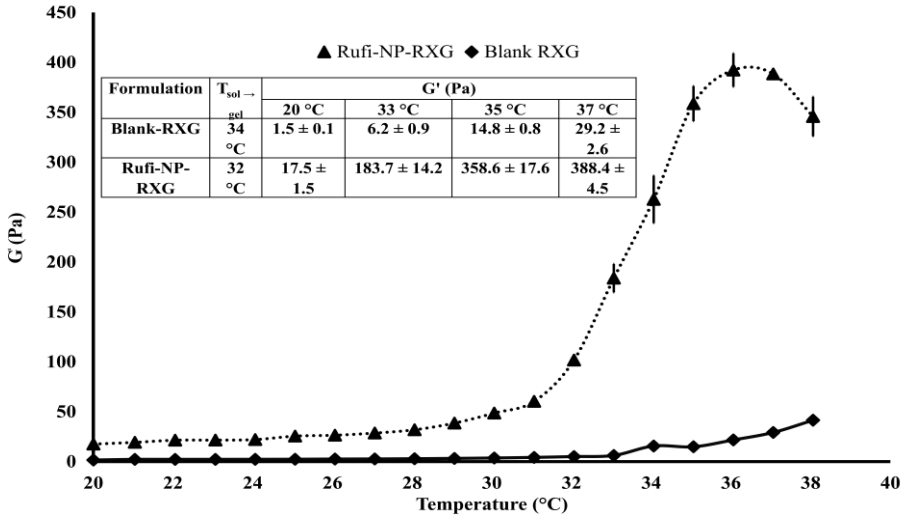

Formulation	$T_{sol \rightarrow gel}$	G' (Pa)			
		20 °C	33 °C	35 °C	37 °C
Blank-RXG	34 °C	1.5 ± 0.1	6.2 ± 0.9	14.8 ± 0.8	29.2 ± 2.6
Rufi-NP-RXG	32 °C	17.5 ± 1.5	183.7 ± 14.2	358.6 ± 17.6	388.4 ± 4.5

Figure 5.3 Rheological evaluation for Rufi-NP-RXG and Blank-RXG using temperature sweep

Analysis for each formulation was performed in triplicates. Each data point is represented as mean ± SD of n=3 determinations

5.3.5 *In vitro* drug release study from Rufi-NP-Susp and Rufi-NP-RXG formulations

The *in vitro* release studies were performed to evaluate the kinetics and mechanism of drug release from Rufi-NP-Susp and Rufi-NP-RXG formulations. The release profile is shown in Figure 5.4. We have modelled the release of Rufi only from Rufi-NP-Susp formulation, because in case of Rufi-NP-RXG formulation, the release of Rufi is affected at two different stages- release of Rufi from the Rufi-Ch-NPs and release of free Rufi from the RXG gel formulation in the dissolution medium. The release profile of Rufi from the Rufi-NP-Susp formulation was fit to different release kinetics models and it was observed that the Higuchi kinetics model (R^2 = 0.9267) was the best fit model when compared to zero order kinetics model (R^2 = 0.7313), and first order kinetics model (R^2 = 0.8691). The ‘n’ value for Korsmeyer-Peppas model was 0.64 for Rufi-NP-Susp indicating that the mechanism of drug release

followed non-Fickian diffusion (a special case of non-Fickian transport - 'Anomalous transport'). In Anomalous transport, the velocity of solvent diffusion and the polymeric relaxation have similar magnitudes. Around 50% of the drug was released at 360 min and 480 min in Rufi-NP-Susp and Rufi-NP-RXG respectively. At the time point of 1440 min, Rufi-NP-Susp and Rufi-NP-RXG showed percentage Rufi released as 78% and 70% respectively. A slightly delayed release in case of Rufi-NP-RXG formulation may be attributed to strong cohesive interaction between chitosan chains and RXG chains. Similarity factor (f2) value obtained for the comparison of the drug release profiles of Rufi-NP-RXG and Rufi-NP-Susp (f2 = 52) indicating that drug release profiles were similar.

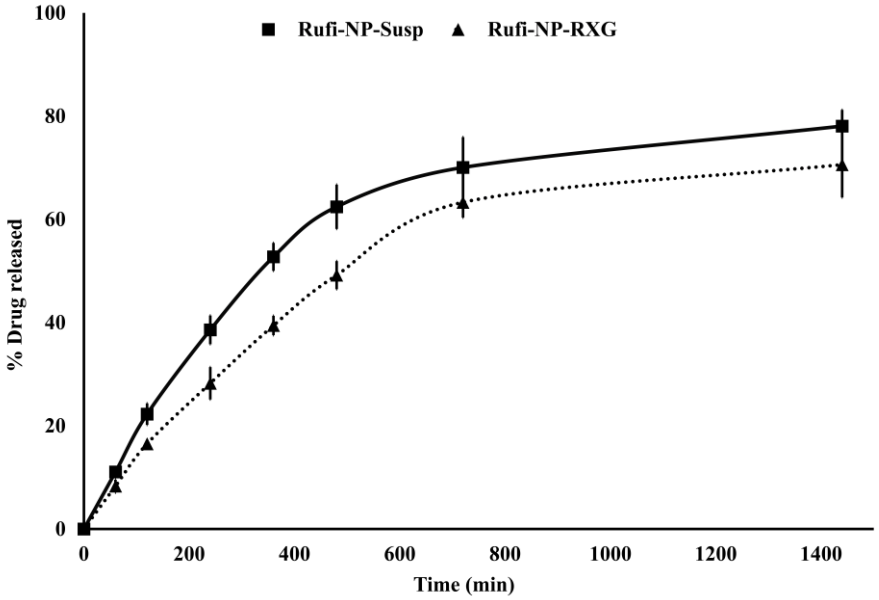

Figure 5.4 *In vitro* drug release profiles of Rufi-NP-Susp and Rufi-NP-RXG in Simulated nasal electrolyte solution (SNES)

Each data point is a mean ± SD of three independent observations (n = 3)

5.3.6 Stability of formulations

Rufi-Ch-NPs and Rufi-NP-RXG did not show a significant difference in their PS, PDI, ZP and EE (%) for a period of 60 days. The %bias calculated for all the

parameters at each interval for both the formulations was found to be not more than 5.0%. This is indicative of physical and chemical stability of both the formulations. The stability data is given in Table 5.4.

Table 5.4 Stability studies of freeze dried Rufi-Ch-NPs and Rufi-NP-RXG

Parameter evaluated	Time (days)				
	0	15	30	45	60
Freeze dried Rufi-Ch-NPs (stored at 25 °C and 60 ± 5% RH)					
PS (nm)	180 ± 1.5	185 ± 4.5	179 ± 5.3	188 ± 5.1	189 ± 2.8
ZP (mV)	38.3 ± 1.5	39.1 ± 0.94	39.3 ± 2.9	37.3 ± 1.15	39.9 ± 0.9
EE (%)	75 ± 2	76 ± 2	72 ± 1.5	71 ± 2	73 ± 2
PDI	0.29 ± 0.08	0.28 ± 0.02	0.28 ± 0.03	0.28 ± 0.02	0.31 ± 0.02
Rufi-NP-RXG (stored under refrigeration, at 2-8 °C)					
PS (nm)	181 ± 2.3	180 ± 2.9	179 ± 7.4	186 ± 3.1	186 ± 5.7
ZP (mV)	39.1 ± 1.0	40.4 ± 1.0	39.6 ± 0.73	40.8 ± 2.4	37.6 ± 1.98
EE (%)	72 ± 2.5	72 ± 2.8	73 ±3.2	74 ± 3	70 ± 2
PDI	0.29 ± 0.02	0.29 ± 0.06	0.29 ± 0.04	0.28 ± 0.05	0.30 ± 0.04

Note: Data is represented as mean ± SD of n = 3 replicates of each formulation stored at their respective storage conditions

5.3.7 *In vivo* studies in male Wistar rats

5.3.7.1 Nasal dose administration and dosing precision studies

Formulations were administered using the microtip-cannula setup that was designed specifically for delivery of formulations near the olfactory region. The details of microtip-cannula setup were reported in our previous research work on *in-situ* gelling systems for N2B delivery [88]. The PK studies for all the formulations were carried out at a drug dose of 1 mg/kg. The maximum dose volume that can be administered to a rat weighing around 250 g is up to 30 µL (120 µL/kg) [80]. The dose volume for nanoparticle loaded formulations was optimized at 40 µL/kg per nostril. The possibility of the formulation leaking out of the animal's nose was ruled out before performing any studies. Prior to *in vivo* studies, *n*=4 animals were dosed with Rufi-NP-Susp mixed with Amaranth dye. To check for any leakage, the nasopalatine duct of the animals was monitored continuously for appearance of the

dye. The dose volume of 40 µL/kg did not cause any immediate leakage from the animal's nose.

Loading high amounts of solids in any formulation may bring in variability while administering the dose intranasally. Therefore, a dosing precision study was carried out for Rufi-NP-RXG and Rufi-NP-Susp formulations. The %RSD values for the amount of Rufi delivered using the nasal delivery set up for both formulations were less than 10% indicating precise dosing.

5.3.7.2 Mucociliary transit time (MTT)

The mucociliary clearance (MCC) process pushes any foreign particles trapped in the mucus, towards the nasopharyngeal duct. For the formulation to stay in the nose for a longer time, it should resist immediate clearance. The MCC was measured by a method described in Section 3.2.7.3 in Chapter 3. The MTT of Rufi-Susp, Rufi-NP-Susp, and Rufi-NP-RXG were 11.6 ± 2.8 min, 33.5 ± 5.7 min and 53.3 ± 11.5 min, respectively. Statistical comparison of MTT values of Rufi-NP-RXG and Rufi-NP-Susp using a t-test showed significant difference (P = 0.027). A significantly higher residence time of Rufi-NP-RXG can be attributed to mucoadhesive properties of chitosan arising from an interaction between negatively charged sialic acid residues in mucin and NH_3^+ groups of chitosan [92].

5.3.7.3 PK analysis and quantification of N2B direct uptake

PK studies were performed according to the procedures given in Section 4.2.9.4. The plasma time course profiles of Rufi-NP-Susp and Rufi-NP-RXG are shown in Figure 5.5A. We compared the PK performance of Rufi-NP-Susp and Rufi-NP-RXG with that of Rufi-Susp (Table 5.5). (PK data for Rufi-Susp was taken from Section 3.3.5.4 in Chapter 3).

Table 5.5 PK parameters of Rufi-NP-RXG, Rufi-NP-Susp, and Rufi-Susp in brain and plasma following i.n. administration at a drug dose of 1 mg/kg

Matrix	PK Parameter	Units	Treatments		
			Rufi-NP-Susp	Rufi-NP-RXG	Rufi-Susp
Plasma	$AUC_{0\rightarrow tlast}$	min×(µg/mL)	145.7 ± 21.7	123.1 ± 10.3	200.75 ± 74.4
	C_{max}	µg/mL	0.49 ± 0.06	0.35 ± 0.04	1.16 ± 0.53
	T_{max}	min	60	90	120
	MRT	min	232.9 ± 3.7	218.4 ± 4.9	147.4 ± 9.4
Brain	$AUC_{0\rightarrow tlast}$	min×(µg/g)	509.3	512.17	104.28
	C_{max}	µg/g	1.68 ± 0.2	1.60 ± 0.2	0.79 ± 0.11
	T_{max}	min	60	60	60
	% DTE		988.5	1177.3	146.8
	% DTP		86.06	91.5	31.9

Note: All the parameter values are expressed as mean ± SD of (n=4) animals per treatment group. T_{max} is expressed as a range or a single value wherever applicable; In case of plasma data, mean $AUC_{0\text{-}tlast}$ obtained from four animals (n=4) was used while in case of brain data $AUC_{0\text{-}tlast}$ obtained from composite sampling with four animals sacrificed at each time point was used

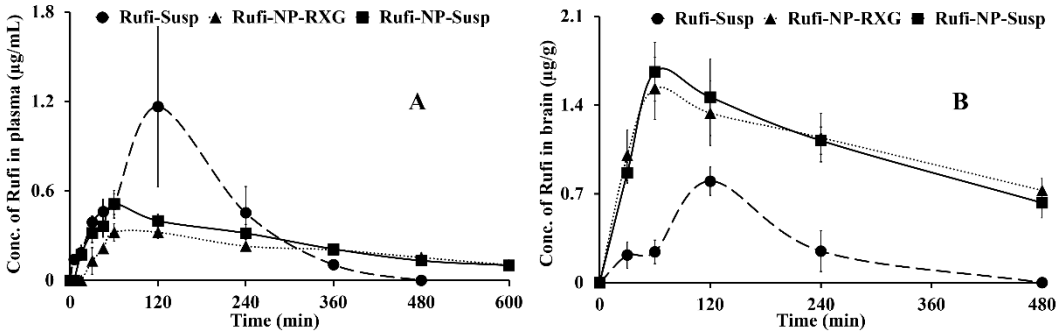

Figure 5.5 PK profiles of Rufi obtained following i.n. administration of Rufi-NP-Susp, Rufi-NP-RXG, and Rufi-Susp in A: Plasma and B: Brain

Each data point is a representation of mean ± SD of n=4 animals for plasma PK, and for brain PK n=4 animals' brains were used at every time point

PK parameters like $AUC_{0\rightarrow tlast}$, C_{max}, T_{max}, MRT were calculated by NCA (Non-compartmental analysis) using Phoenix WinNonlin Version 8.1. A one-way ANOVA comparison for plasma $AUC_{0\rightarrow tlast}$ values for all three formulations showed that there was no statistically significant difference between any of the three formulations. The MRT values of both the nanocrystal formulations were significantly higher than the MRT for Rufi-Susp.

The brain PK parameters for all three treatments are shown in Table 5.5. The brain concentrations vs time profile of Rufi-NP-Susp, Rufi-NP-RXG, and Rufi-Susp are shown in Figure 5.5. The brain $AUC_{0\rightarrow tlast}$ values for the nanoparticulate formulations were almost 5 times the brain $AUC_{0\rightarrow tlast}$ values for Rufi-Susp. Further, the brain concentrations were compared for all three treatments at four different time points: 30, 60, 120, and 240 min using t-test at 5% level of significance (Figure 5.6). At each time point for every treatment group, n=4 animals were sacrificed. The concentration of Rufi at each time point was an average of the pooled concentration from 4 animals, the underlying assumption being that inter-individual differences accounted for residual variability rather than the inherent differences in PK process of different treatments. The average brain concentration vs time profile could be constructed only from pooled concentration data, and hence, values of brain $AUC_{0\rightarrow tlast}$ were given as single values without standard deviation. Consequently, ANOVA and other statistical comparison tests could not be applied to brain data unlike plasma data. Instead, the brain concentrations were compared at four different time points for all treatments using t-tests.

At all the time points (at 30, 60, 120, and 240 min), there was no significant difference between the brain concentrations of Rufi-NP-RXG and Rufi-NP-Susp formulations. However, at all the time points, the brain concentrations of both the nanoparticulate formulations were significantly higher than Rufi-Susp.

To evaluate the performance of formulations further, %DTE and %DTP values were calculated as per Equation 3.1, Equation 3.2, and Equation 3.3 and are given in Table 5.5. %DTP for Rufi-NP-Susp, Rufi-NP-RXG, and Rufi-Susp were 86.1, 91.5 and 31.9, respectively. Although the brain concentrations of Rufi-NP-Susp and Rufi-NP-RXG were not significantly different at any time point, the %DTE and %DTP values

were slightly greater for Rufi-NP-RXG formulation. This could be attributed to slightly higher brain $AUC_{0\rightarrow tlast}$ value and lower plasma $AUC_{0\rightarrow tlast}$ value for Rufi-NP-RXG when compared to Rufi-NP-Susp.

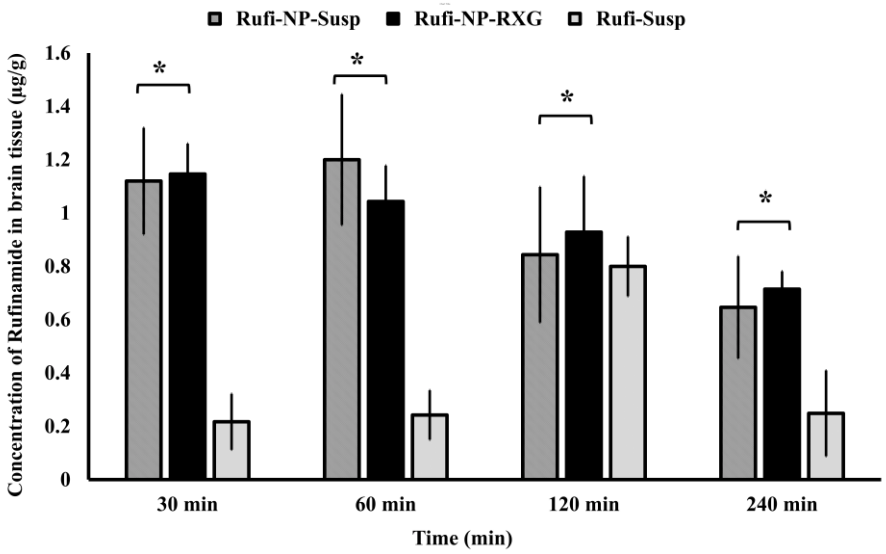

Figure 5.6 Comparison of concentration of Rufi in brain following i.n. administration of Rufi-NP-Susp, Rufi-NP-RXG, and Rufi-Susp

**Statistically no significant difference unless mentioned otherwise. All statistical tests were performed for dose normalized concentrations using t-test at 5% level of significance.; Each bar is a representation of mean ± SD of n=4 replicate analysis for brain concentrations*

5.4 Conclusion

In this work, Rufi loaded Chitosan–STPP nanoparticles were prepared using ionic gelation technique and optimized based on the principles of DoE. Nanoparticles were characterized for their PS, ZP and EE (%). The optimized nanoparticles were loaded in a thermoresponsive nasal *in-situ* gel based on modified tamarind seed polysaccharide (Xyloglucan) as the thermoresponsive polymer. *In vivo* plasma and brain PK evaluation was performed for aqueous suspension of nanoparticles and nanoparticles dispersed in the *in-situ* gel. The results were compared with the PK data of aqueous suspension of Rufi. Data comparison revealed that both the nanoparticle formulations showed better direct N2B uptake than aqueous suspension

of Rufi. This was evident from higher %DTP values obtained for both nanoparticle formulations. Chitosan nanoparticles of Rufi significantly enhanced its brain uptake via direct N2B pathway. Given the low oral bioavailability and high dose and dosing frequency of Rufi, intranasally administered nanoparticulate formulation of Rufi would provide better therapeutic outcome than compared to orally administered formulations of Rufi.

6 COMPARISON OF THE VARIOUS OPTIMIZED NANO FORMULATIONS OF RUFINAMIDE

6.1 Introduction

In this research work we have designed and optimised several intranasal (i.n.) formulations of Rufinamide (Rufi) with an intent of increasing the drug's distribution to the brain via direct nose to brain (N2B) pathways. Two different approaches *viz. in-situ* gelling systems and nanoparticulate formulations and their combination were explored to improve the N2B delivery of Rufi. In this research work, we have formulated and evaluated the physical and pharmacokinetic (PK) profiles (in brain and plasma) of the following formulations for N2B delivery of Rufi: 1. Aqueous suspension of plain Rufi (Rufi-Susp), 2. Reacted xyloglucan (RXG) based thermoresponsive *in-situ* gel of plain Rufi (Rufi-RXG), 3. Aqueous suspension of Rufi-NCs (Rufi-NC-Susp), 4. RXG based thermoresponsive *in-situ* gel of Rufi-NCs (Rufi-NC-RXG), 5. Aqueous suspension of Rufi-Chitosan nanoparticles (Rufi-NP-Susp) and 6. RXG based thermoresponsive *in-situ* gel of Rufi-Chitosan nanoparticles (Rufi-NP-RXG). Brain and plasma PK studies of intravenously (i.v.) and orally administered Rufi was also performed for comparison with the i.n. administered formulations and to determine certain PK parameters.

In this chapter, we have compared the rheological properties and mucociliary transit times of *in-situ* gelling formulations like Blank-RXG, Rufi-RXG, Rufi-NC-RXG and Rufi-NP-RXG. The physical properties of the nano formulations like Rufi-NCs and Rufi-Ch-NPs in terms of PS, zetapotential (ZP), polydispersity index (PDI) and entrapment efficiency (EE) were compared. Finally, the efficiency of N2B delivery of nano formulations loaded nasal *in-situ* gelling systems, Rufi-NC-RXG and Rufi-NP-RXG, were compared with aqueous suspension of plain Rufi (Rufi-Susp), aqueous suspension of Rufi-NCs (Rufi-NC-Susp) and aqueous suspension of Rufi-Chitosan nanoparticles (Rufi-NP-Susp).

6.2 Comparison of formulation processes of the nano formulations for Rufinamide

Rufinamide NCs (Rufi-NCs) were prepared using a bottom-up approach by antisolvent-precipitation technique. In the antisolvent-precipitation technique, the processing conditions and the choice of stabilizers played a critical role in obtaining the desired PS growth in the nanometre range. A combination of HPMC E5LV grade and Poloxamer 407 were used as the stabilizer system. Based on the results obtained from DoE, concentration of HPMC and ultrasonication time were found to be the most critical factors affecting the PS of Rufi-NCs.

Rufinamide chitosan nanoparticles (Rufi-Ch-NPs) were prepared using a top-down approach. An ionic gelation technique was used to formulate Rufi-Ch-NPs. Sodium tri poly phosphate (STPP) was used as the crosslinking agent. Optimization using DoE showed that the chitosan: STPP ratio, ultrasonication time, and homogenization speed and time were the critical factors affecting the PS, ZP and EE (%) of Rufi-Ch-NPs. Relatively, the method of manufacture of Rufi-NCs was simple, since it involved fewer steps as compared to processing of Rufi-Ch-NPs. However, both the methods are reproducible and can be easily adapted in pharmaceutical industries.

6.3 Comparison of PS, ZP, EE/% yield, *in vitro* drug release and physical stability of Rufinamide nano formulations

The PS, ZP, EE (%), and yield (%) (in case of Rufi-NCs) of the optimized Rufi-NCs and Rufi-Ch-NPs are given in Table 6.1 A slightly smaller PS was observed in case of Rufi-Ch-NPs. The ZP of Rufi-Ch-NPs was much higher than that of Rufi-NCs. The high positive ZP in case of Rufi-Ch-NPs can be attributed to positive groups on chitosan molecules. In case of Rufi-NCs, the ZP varied from +2 to -2 mV. This can be attributed to very little ionization of Rufi and also due to the fact that we have

used a non-ionic stabiliser- HPMC and Poloxamer 407 in the preparation of Rufi-NCs which would not contribute to the surface charge on the NCs. In case of Rufi-Ch-NPs, physical stability was achieved mainly by electrostatic stabilization, while in case of Rufi-NCs, the stabilization was achieved by primarily by steric stabilization.

In vitro drug release studies revealed that the drug release was extended in the case of Rufi-NP-RXG while the drug release was relatively faster in the case of Rufi-NC-RXG. In case of Rufi-NP-RXG, the drug was released from Rufi-Ch-NPs and further, the drug had to diffuse through the RXG gel network. In case of Rufi-NC-RXG, the solubility of Rufi greatly increased with the nanocrystal formulation. Also, once dissolved the drug could freely traverse the RXG gel network chains. This observation is in line with rheological evaluation of Rufi-NC-RXG and Rufi-NP-RXG formulations, where the gel strength of Rufi-NP-RXG was higher than the gel strength of Rufi-NC-RXG at all temperatures. Stronger gel caused a slightly more delay in the release of Rufi. The release profiles from Rufi-NP-Susp and Rufi-NP-RXG were similar (f2=52), while the release profiles of Rufi-NC-RXG and Rufi-RXG were not similar (f2=45).

Both nano formulations were found to be stable for a period of 60 days when stored at 25 °C and RH 60 ± 5%. The %bias calculated at the end of 60 days for all the physical characteristics of the formulations was less than 5.0%. This is indicative of physical and chemical stability of both the formulations. EE (%) for Rufi-Ch-NPs was 75.0 ± 2.0% and the DL (%) was 11.0 ± 0.3%. The yield (%) for Rufi-NCs was 87.3 ± 5.6%.

Table 6.1 Physical characteristics of the two nano formulations for Rufi

Physical characteristics	Rufi-NCs	Rufi-Ch-NPs
PS (nm)	244 ± 5.2	180 ± 1.5
PDI	0.31 ± 0.1	0.29 ± 0.08
ZP (mV)	-2 ± 1.0	38.3 ± 1.5
EE (%)	NA	75.0 ± 2.0
yield (%)	87.3 ± 5.6	NA

Note: All values for physical characteristics of formulations are represented as mean ± SD of n=3 measurements

6.4 Comparison of rheological properties and MTT of *in-situ* gelling formulations of Rufinamide

6.4.1 Rheological properties of *in-situ* gelling formulations

The rheological properties of *in-situ* gelling formulations, Blank-RXG, Rufi-RXG, Rufi-NC-RXG and Rufi-NP-RXG, were compared in terms of their sol-to-gel transition temperature ($T_{sol \rightarrow gel}$) and their gel strength. It can be seen from Table 6.2 that the $T_{sol \rightarrow gel}$ for all formulations was lower than Blank-RXG formulation. This can be attributed to faster gelation due to presence of high amounts of suspended solids. The highest gel strength was observed for Rufi-NP-RXG. The higher gel strength for Rufi-NP-RXG at all temperatures can attributed to cohesive association between chitosan and xyloglucan. In case of both nano formulations (Rufi-NC-RXG and Rufi-NP-RXG), the gel strength was found to be higher than Blank-RXG at all temperatures. This can be because of the presence of mannitol, a sugar added as a cryoprotectant during freeze drying of nano formulations.

Table 6.2 Rheological evaluation of formulations

Formulation	**$T_{sol\text{-}to\text{-}gel}$**	**G' (Pa)**			
		20 °C	33 °C	35 °C	37 °C
Blank-RXG	34 °C	1.5 ± 0.1	6.2 ± 0.9	14.8 ± 0.8	29.2 ± 2.6
Rufi-RXG	32 °C	9.6 ± 0.5	161.8 ± 4.2	242.7 ±2.1	273.1 ± 2.6
Rufi-NC-RXG	32 °C	18.7 ± 1.7	186.9 ± 8.9	316.4 ± 26.1	353.3 ± 11.7
Rufi-NP-RXG	32 °C	17.5 ± 1.5	183.7 ± 14.2	358.6 ± 17.6	388.4 ± 4.5

Note: Each data point is represented as mean ± SD of n=3 determinations

6.4.2 Comparison of mucociliary transit times (MTT) of *in-situ* gelling formulations

MTT was measured for i.n. administered Rufi-Susp, Rufi-RXG, Rufi-NC-Susp and Rufi-NC-RXG, Rufi-NP-Susp and Rufi-NP-RXG formulations. MTT values of all the formulations are given in Table 6.3. Statistical comparison shows that the MTT for Rufi-Susp was significantly lower than the rest of the formulations. No significant (P>0.05) difference observed between the MTT values of Rufi-RXG, Rufi-NP-Susp, and Rufi-NC-Susp. The difference in the MTT values for Rufi-NC-RXG and Rufi-NP-RXG was not significantly different (P>0.05). A statistically significant (P<0.05) difference was observed between the plain aqueous suspension of all formulations and their RXG *in-situ* gel counterparts (i.e., Rufi-Susp versus Rufi-RXG; Rufi-NC-Susp versus Rufi-NC-RXG and Rufi-NP-Susp versus Rufi-NP-RXG). This shows that RXG *in-situ* gel is beneficial in retaining formulations in the nasal cavity for long time by resisting the mucociliary clearance process, as intended.

Table 6.3 MTT for Rufi formulations

Formulation	Time of appearance (min) (mean ± SD)
Rufi-Susp	11.6 ± 2.8
Rufi-RXG	36.6 ± 5.7
Rufi-NC-Susp	26.6 ± 5.7
Rufi-NC-RXG	43.3 ± 5.7
Rufi-NP-Susp	33.5 ± 5.7
Rufi-NP-RXG	53.3 ± 11.5

Note: The study was performed in triplicates for each formulation. The recorded data is presented as mean ± SD of n=3 replicates

6.5 Comparison of brain and plasma pharmacokinetic studies of Rufinamide nano formulations and *in-situ* gel loaded Rufinamide nano formulations

The data obtained from the brain and plasma PK studies for Rufi nano formulations (Rufi-NC-Susp and Rufi-NP-Susp) and Rufi nano formulation loaded *in-situ* gelling systems (Rufi-NC-RXG and Rufi-NP-RXG) are given in Chapters 4 and 5. The plasma $AUC_{0\rightarrow tlast}$ of nanocrystal formulations were significantly higher than plasma

$AUC_{0\rightarrow tlast}$ of chitosan nanoparticle formulations. The plasma $AUC_{0\rightarrow tlast}$ of Rufi-NC-Susp was significantly higher than Rufi-NP-Susp and similarly, the plasma $AUC_{0\rightarrow tlast}$ of Rufi-NC-RXG was significantly higher than Rufi-NP-RXG. This can be attributed to enhanced solubility and rapid dissolution rate of drug in the nasal secretions, thereby leading to rapid and higher extent of systemic absorption of Rufi when presented as NCs as compared drug loaded polymeric nanoparticles. No significant difference was observed with plasma $AUC_{0\rightarrow tlast}$ of both the nanocrystal formulations (i.e., Rufi-NC-Susp versus Rufi-NC-RXG) and similarly no significant difference was observed in the plasma $AUC_{0\rightarrow tlast}$ of both the chitosan nanoparticle formulations (i.e., Rufi-NP-Susp versus Rufi-NP-RXG).

The brain AUCs of chitosan nanoparticle formulations were significantly higher than the nanocrystal formulations. Rufi-NP-Susp showed the higher brain $AUC_{0\rightarrow tlast}$ than Rufi-NC-Susp while Rufi-NP-RXG showed higher brain $AUC_{0\rightarrow tlast}$ than Rufi-NC-RXG. The %DTP values for all the i.n. formulations were in the order: Rufi-NP-RXG > Rufi-NP-Susp > Rufi-NC-RXG > Rufi-RXG. This could be due to a combined effect of permeation enhancing ability of chitosan, PS of nanoparticles, and mucoadhesive properties of chitosan and RXG.

Table 6.4 Plasma and brain PK parameters for different formulations of Rufi.

Matrix	PK Parameter	Units	Formulations			
			Rufi-NP-Susp	Rufi-NP-RXG	Rufi-NC-Susp	Rufi-NC-RXG
Plasma	$AUC_{0\rightarrow tlast}$	min×(µg/mL)	145.7 ± 21.7	123.1 ± 10.3	258.2 ± 68.6	192.3 ± 59.5
	C_{max}	µg/mL	0.49 ± 0.06	0.35 ± 0.04	0.92 ± 0.17	0.76 ± 0.17
	T_{max}	min	60	90	30-45	60
	MRT	min	232.9 ± 3.7	218.4 ± 4.9	223.8 ± 9.0	177.4 ± 16.4
Brain	$AUC_{0\rightarrow tlast}$	min×(µg/g)	509.3	512.17	340.7	471.3
	C_{max}	µg/g	1.68 ± 0.2	1.60 ± 0.2	1.31 ± 0.19	1.81 ± 0.3
	T_{max}	min	60	60	60	60
	% DTE		988.5	1177.3	373.16	693.1
	% DTP		86.06	91.5	73.3	85.5

Note: Rufi dose for all i.n. formulations = 1 mg/kg; n=4 animals were used for plasma PK, and for brain PK n=4 animals' brains were used at every time point; The plasma data is represented as mean ± SD. The brain data is represented as single values. The time points in the brain PK profile were an average of the pooled concentration data obtained from 4 animals. the average brain concentration profile was constructed from the pooled concentration data and hence, PK parameters like $AUC_{0\rightarrow tlast}$ and MRT were calculated as single values without standard deviation

6.6 Conclusion

Plasma and brain PK performance of all the four optimized nano formulations revealed that Rufi-NP-RXG formulation was better performing with respect to delivery of Rufi to the brain compared to other nano formulations. However, all the four optimized nano formulations showed better performance in terms of N2B delivery of Rufi compared to i.v. bolus administration of Rufi solution, oral administration of aqueous suspension of Rufi, and i.n. administration of aqueous suspension of Rufi.

7 FUTURE SCOPE OF WORK

7.1 Future scope and directions

In this work, we attempted to improve the N2B delivery of Rufi by delivering it through the i.n. route as different formulations. The N2B uptake of Rufi significantly improved when formulated as nano formulations suspended in *in-situ* gelling systems. However, N2B delivery of any molecule can be made holistic when the developed formulations are delivered using an appropriate delivery device. The pathways of absorption followed by molecules administered by i.n. route is greatly affected by the deposition of the formulation in the nose. In order to administer the formulations in humans, further research needs to be carried out with respect to the delivery device for i.n. delivery of Rufi.

8 References

[1] Stafstrom and Carmant 2015. Seizures and epilepsy: An overview. Addit Perspect Epilepsy Biol a Spectr Disorde. 2016;65–77. Available from:https://www.ncbi.nlm.nih.gov/pmc/articles/PMC4448698/pdf/cshperspectmed-BEP-a022426.pdf.

[2] Simon D. Shorvon, Emilio Perucca JEJ. The Treatment of Epilepsy. Bmj. 1996.

[3] Selvaraj K, Gowthamarajan K, Karri VVSR, et al. Rufinamide. Adv Drug Deliv Rev. Sixth Edit. 2018;4:155–162. Available from: http://dx.doi.org/10.1016/j.jpba.2017.11.003.

[4] K. F. & FERRIERO DM 2017. ASGALSNFFRSS. Swaiman's Pediatric Neurology: Principles and Practice. Elsevier.;

[5] Beghi E, Giussani G, Abd-Allah F, et al. Global, regional, and national burden of epilepsy, 1990–2016: a systematic analysis for the Global Burden of Disease Study 2016. Lancet Neurol. 2019;18:357–375. Available from: 1016/S1474-4422(18)30454-X.

[6] Rao M. Addressing the burden of epilepsy in India... Neurol India. 2017;65:S4–S5.

[7] LODHA P. All About Epilepsy – a Condition Rarely Talked About & Only Occasionally Understood in India. MINDS Found. 2017 [cited 2020 May 1]. Available from: https://www.thebetterindia.com/110561/epilepsy-a-concern-to-be-addressed-in-india/.

[8] Nandanavana Subbareddy Santhosh, Sanjib Sinha and PS. Epilepsy: Indian perspective. Ann Indian Acad Neurol. 2014;

[9] Camfield PR. Definition and natural history of Lennox-Gastaut syndrome. Epilepsia. 2011;52:3–9.

[10] Markand ON. Lennox-Gastaut Syndrome (Childhood Epileptic Encephalopathy). J Clin Neurophysiol. 2003;20:426–441.

[11] Douglass LM, Salpekar J. Surgical options for patients with Lennox-Gastaut syndrome. Epilepsia. 2014;55:21–28. Available from: https://doi.org/10.1111/epi.12742.

[12] Cedars-Sinai. Lennox-Gastaut Syndrome. [cited 2020 May 20]. Available from: https://www.cedars-sinai.org/health-library/diseases-and-conditions/l/lennox-gastaut-syndrome.html.

[13] Karceski S. Epilepsy Essentials: Rufinamide in the Treatment of Lennox-Gastaut Syndrome. 2009. Available from: https://practicalneurology.com/articles/2009-nov-dec/1109_08-php/pdf.

[14] Villanueva-Meyer JE, Mabray MC, Cha S. Current clinical brain tumor imaging. Clin Neurosurg. 2017;81:397–415.

[15] EMEA. SCIENTIFIC DISCUSSION - RUFINAMIDE. 2007. Available from: https://www.ema.europa.eu/en/documents/scientific-discussion/inovelon-epar-scientific-discussion_en.pdf.

[16] Salunke N, Thipparaboina R, Chavan RB, et al. Rufinamide: Crystal structure elucidation and solid state characterization. J Pharm Biomed Anal. 2018;149:185–192. Available from: http://dx.doi.org/10.1016/j.jpba.2017.11.003.

[17] James W. Wheless, Vazquez B. RUFINAMIDE: A NOVEL BROAD-SPECTRUM ANTIEPILEPTIC DRUG. Epilepsy Curr. 2010;10:1–6.

[18] Arroyo S. Rufinamide. Neurotherapeutics. 2007;4:155–162.

[19] Perucca E, Cloyd J, Critchley D, et al. Rufinamide: Clinical pharmacokinetics and concentration-response relationships in patients with epilepsy. Epilepsia. 2008;49:1123–1141.

[20] US FDA. INDICATIONS AND USAGE BANZEL is indicated for adjunctive treatment of seizures associated with Lennox-Gastaut Syndrome in pediatric patients 1 year of age and older and in adults . 2 DOSAGE AND ADMINISTRATION Pediatric patients (1 year to less than 17 ye. 2015;

[21] Epilepsy Foundation. Rufinamide. Available from: https://www.epilepsy.com/medications/rufinamide.

[22] Tajes M, Ramos-Fernández E, Weng-Jiang X, et al. The blood-brain barrier: Structure, function and therapeutic approaches to cross it. Mol Membr Biol. 2014;31:152–167.

[23] Orthmann A, Fichtner I, Zeisig R. Improving the transport of chemotherapeutic drugs across the blood-brain barrier. Expert Rev Clin Pharmacol. 2011;4:477–490.

[24] Mittal D, Ali A, Md S, et al. Insights into direct nose to brain delivery: Current status and future perspective. Drug Deliv. 2014;21:75–86.

[25] Pires A, Fortuna A, Alves G, et al. Intranasal drug delivery: How, why and what for? J Pharm Pharm Sci. 2009;12:288–311.

[26] Crowe TP, Greenlee MHW, Kanthasamy AG, et al. Mechanism of intranasal drug delivery directly to the brain. Life Sci. 2018;195:44–52. Available from: https://doi.org/10.1016/j.lfs.2017.12.025.

[27] Van Riel D, Leijten LM, Verdijk RM, et al. Evidence for influenza virus CNS invasion along the olfactory route in an immunocompromised infant. J Infect Dis. 2014;210:419–423.

[28] Ruda M, Coulter JD. Axonal and transneuronal transport of wheat germ agglutinin demonstrated by immunocytochemistry. Brain Res. 1982;249:237–246.

[29] Li Y, Field PM, Raisman G. Olfactory ensheathing cells and olfactory nerve fibroblasts maintain continuous open channels for regrowth of olfactory nerve fibres. Glia. 2005;52:245–251.

[30] Lochhead JJ, Thorne RG. Intranasal delivery of biologics to the central nervous system. Adv Drug Deliv Rev. 2012;64:614–628. Available from: http://dx.doi.org/10.1016/j.addr.2011.11.002.

[31] Iwasaki S, Yamamoto S, Sano N, et al. Direct Drug Delivery of Low-Permeable Compounds to the Central Nervous System Via Intranasal Administration in Rats and Monkeys. Pharm Res. 2019;36.

[32] Bourganis V, Kammona O, Alexopoulos A, et al. Recent advances in carrier mediated nose-to-brain delivery of pharmaceutics. Eur J Pharm Biopharm. 2018;128:337–362.

[33] Aderibigbe B. In Situ-Based Gels for Nose to Brain Delivery for the Treatment of Neurological Diseases. Pharmaceutics. 2018;10:40. Available from: http://www.mdpi.com/1999-4923/10/2/40.

[34] Coppola G, Besag F, Cusmai R, et al. Current role of rufinamide in the treatment of childhood epilepsy: Literature review and treatment guidelines. Eur J Paediatr Neurol. 2014;18:685–690.

[35] Contin M, Mohamed S, Candela C, et al. Simultaneous HPLC – UV analysis of rufinamide , zonisamide , lamotrigine , oxcarbazepine monohydroxy derivative and felbamate in deproteinized plasma of patients with epilepsy. 2010;878:461–465.

[36] Gáll Z, Vancea S, Dogaru MT, et al. Liquid chromatography – mass spectrometric determination of rufinamide in low volume plasma samples. J Chromatogr B. 2013;940:42–46. Available from: 10.1016/j.jpba.2010.07.015.

[37] Malvagia S, Filippi L, Innocenti M, et al. Journal of Pharmaceutical and Biomedical Analysis Rapid assay of rufinamide in dried blood spots by a new liquid chromatography – tandem mass spectrometric method. J Pharm Biomed Anal. 2011;54:192–197. Available from: 10.1080/10826076.2010.484356.

[38] Taylor P, Swartz M. Journal of Liquid Chromatography & HPLC DETECTORS : A BRIEF REVIEW. 2010;37–41.

[39] Sahu PK, Ramisetti NR, Cecchi T, et al. An overview of experimental designs in HPLC method development and validation. J. Pharm. Biomed. Anal. Elsevier B.V.; 2018. Available from: http://dx.doi.org/10.1016/j.jpba.2017.05.006.

[40] Carini JP, Kaiser S, Ortega GG, et al. Development, optimization and validation of a stability-indicating HPLC method of achyrobichalcone quantification using experimental designs. Phytochem Anal. 2013;24:193–200.

[41] Procedures A. Guidance for Industry Q2B Validation of Analytical Procedures: Methodology. 1996;20857:301–827. Available from: http://www.fda.gov/cder/guidance/index.htm%5Cnhttp://www.fda.gov/cber/guidelines.htm.

[42] US. Food and Drug Administration. Bioanalytical Method Validation Guidance for Industry. Food Drug Adm. 2018;1–41. Available from: https://www.fda.gov/files/drugs/published/Bioanalytical-Method-Validation-Guidance-for-Industry.pdf.

[43] Alshammari TM, Al-Hassan AA, Hadda TB, et al. Comparison of different serum sample extraction methods and their suitability for mass spectrometry analysis. Saudi Pharm J. 2015;23:689–697.

[44] Li, Pei and MGB. A review of sample preparation methods for quantification of small-molecule analytes in brain tissue by liquid chromatography

tandem mass spectrometry (LC-MS/MS). Anal Methods. 2015;647–655. Available from: https://doi.org/10.1039/C4AY00915K.

[45] Kozlovskaya L, Abou-kaoud M, Stepensky D. PT NU SC Department of Clinical Biochemistry and Pharmacology , The Faculty of Health Sciences , Ben-. J Control Release. 2014; Available from: http://dx.doi.org/10.1016/j.jconrel.2014.06.053.

[46] Hanson LR, Frey WH. Intranasal delivery bypasses the blood-brain barrier to target therapeutic agents to the central nervous system and treat neurodegenerative disease. BMC Neurosci. 2008;9:1–4.

[47] Illum L. Transport of drugs from the nasal cavity to the central nervous system. Eur J Pharm Sci. 2000;11:1–18.

[48] Stützle M, Flamm J, Carle S, et al. Nose-to-brain delivery of insulin for Alzheimer's disease. ADMET DMPK. 2015;3:190–202.

[49] Harkema JR, Carey SA, Wagner JG. The Nose Revisited: A Brief Review of the Comparative Structure, Function, and Toxicologic Pathology of the Nasal Epithelium. Toxicol Pathol. 2006;34:252–269.

[50] Charlton S, Jones NS, Davis SS, et al. Distribution and clearance of bioadhesive formulations from the olfactory region in man: Effect of polymer type and nasal delivery device. Eur J Pharm Sci. 2007;30:295–302.

[51] Sabale AS, Kulkarni AD, Sabale AS. Nasal In Situ Gel: Novel Approach for Nasal Drug Delivery. J Drug Deliv Ther. 2020;10:183–197.

[52] Sakakibara CN, Sierakowski MR, Chassenieux C, et al. Xyloglucan gelation induced by enzymatic degalactosylation; kinetics and the effect of the molar mass. Carbohydr Polym. 2017;174:517–523. Available from: http://dx.doi.org/10.1016/j.carbpol.2017.06.118.

[53] Nitta Y. Gelation and Gel Properties of Gellan Gum and Xyloglucan. 2005;

[54] Kochumalayil J, Sehaqui H, Zhou Q, et al. Tamarind seed xyloglucan - A thermostable high-performance biopolymer from non-food feedstock. J Mater Chem. 2010;20:4321–4327.

[55] Poommarinvarakul S, Tattiyakul J, Muangnapoh C. Isolation and rheological properties of tamarind seed polysaccharide from tamarind kernel powder using protease enzyme and high-intensity ultrasound. J Food Sci. 2010;75.

[56] Ravi PR, Aditya N, Patil S, et al. Nasal in-situ gels for delivery of rasagiline mesylate: Improvement in bioavailability and brain localization. Drug Deliv. 2015;22:903–910.

[57] Ruby JJ, Pandey VP. Formulation and evaluation of olanzapine loaded chitosan nanoparticles for nose to brain targeting an in vitro and ex vivo toxicity study. J Appl Pharm Sci. 2016;6:034–040.

[58] Ruel-Gariépy E, Leroux JC. In situ-forming hydrogels - Review of temperature-sensitive systems. Eur J Pharm Biopharm. 2004;58:409–426.

[59] Sunthar P. Rheology of complex fluids. Polym Rheol. Springer New York; 2010. p. 171–191. Available from: https://link.springer.com/chapter/10.1007/978-1-4419-6494-6_8.

[60] Baloglu E, Karavana SY, Senyigit ZA, et al. Rheological and mechanical properties of poloxamer mixtures as a mucoadhesive gel base. Pharm Dev Technol. 2011;16:627–636.

[61] Rahman MS, Al-Mahrouqi AI. Instrumental texture profile analysis of gelatin gel extracted from grouper skin and commercial (bovine and porcine) gelatin gels. Int J Food Sci Nutr. 2009;60:229–242.

[62] Mircioiu C, Voicu V, Anuta V, et al. Mathematical modeling of release kinetics from supramolecular drug delivery systems. Pharmaceutics. 2019;11.

[63] Grone BP, Baraban SC. Animal models in epilepsy research : legacies and new directions. 2015;18:339–343.

[64] Djupesland PG, Messina JC, Mahmoud RA. The nasal approach to delivering treatment for brain diseases: An anatomic, physiologic, and delivery technology overview. Ther Deliv. 2014;5:709–733.

[65] Dauner K, Lißmann J, Jeridi S, et al. Expression patterns of anoctamin 1 and anoctamin 2 chloride channels in the mammalian nose. Cell Tissue Res. 2012;347:327–341.

[66] Pardridge WM. The blood-brain barrier: Bottleneck in brain drug development. NeuroRx. 2005;2:3–14.

[67] Mistry A, Stolnik S, Illum L. Nanoparticles for direct nose-to-brain delivery of drugs. Int J Pharm. 2009;379:146–157. Available from: https://linkinghub.elsevier.com/retrieve/pii/S0378517309004128.

[68] Vyas TK, Babbar AK, Sharma RK, et al. Intranasal mucoadhesive microemulsions of zolmitriptan: Preliminary studies on brain-targeting. J Pharm Sci. 2006;95:570–580.

[69] Wu C, Li B, Zhang Y, et al. Intranasal delivery of paeoniflorin nanocrystals for brain targeting. Asian J Pharm Sci. 2020;15:326–335. Available from: https://doi.org/10.1016/j.ajps.2019.11.002.

[70] Junghanns JUAH, Müller RH. Nanocrystal technology, drug delivery and clinical applications. Int J Nanomedicine. 2008;3:295–309.

[71] Bonaccorso A, Gigliobianco MR, Pellitteri R, et al. Optimization of curcumin nanocrystals as promising strategy for nose-to-brain delivery application. Pharmaceutics. 2020;12.

[72] Chang TL, Zhan H, Liang D, et al. Nanocrystal technology for drug formulation and delivery. Front Chem Sci Eng. 2015;9:1–14.

[73] Sinha B, Müller RH, Möschwitzer JP. Bottom-up approaches for preparing drug nanocrystals: Formulations and factors affecting particle size. Int J Pharm. 2013;453:126–141.

[74] Sase SM, Merekar AN, Dokhe MD, et al. A Review On Nanocrystals In Drug Delivery. Am J PharmTech Res. 2020;10:93–121.

[75] De Waard H, Frijlink HW, Hinrichs WLJ. Bottom-up preparation techniques for nanocrystals of lipophilic drugs. Pharm Res. 2011;28:1220–1223.

[76] Khan S, Matas M De, Zhang J, et al. Crystal Growth _ Design Volume issue 2013 [doi 10.1021_cg4000473] Khan, Shahzeb; Matas, Marcel de; Zhang, Jiwen; Anwar, Jamshed -- Nanocrystal Preparation- Low-Energy Precipitation Method Revisited.pdf. 2013;

[77] Thorat AA, Dalvi S V. Liquid antisolvent precipitation and stabilization of nanoparticles of poorly water soluble drugs in aqueous suspensions: Recent developments and future perspective. Chem Eng J. 2012;181–182:1–34. Available from: http://dx.doi.org/10.1016/j.cej.2011.12.044.

[78] Sanofi's Solvent Selection Guide: A Step Toward More Sustainable Processes Available from: https://www.who.int/ipcs/publications/cicad/en/cicad35.pdf.

[79] Tuomela A, Hirvonen J, Peltonen L. Stabilizing agents for drug nanocrystals: Effect on bioavailability. Pharmaceutics. 2016;8.

[80] Turner P V., Brabb T, Pekow C, et al. Administration of substances to laboratory animals: Routes of administration and factors to consider. J Am Assoc Lab Anim Sci. 2011;50:600–613.

[81] Zhang QZ, Zha LS, Zhang Y, et al. The brain targeting efficiency following nasally applied MPEG-PLA nanoparticles in rats. J Drug Target. 2006;14:281–290.

[82] Aderibigbe BA, Naki T. Chitosan-based nanocarriers for nose to brain delivery. Appl Sci. 2019;9.

[83] Saikia C, Gogoi P. Chitosan: A Promising Biopolymer in Drug Delivery Applications. J Mol Genet Med. 2015;s4.

[84] Smith J, Wood E, Dornish M. Effect of Chitosan on Epithelial Cell Tight Junctions. Pharm Res. 2004;21:43–49.

[85] Ying W ying. Addressing the PEG Mucoadhesivity Paradox to Engineer Nanoparticles that “Slip” through the Human Mucus Barrier. Bone. 2008;23:1–7. Available from: https://www.ncbi.nlm.nih.gov/pmc/articles/PMC3624763/pdf/nihms412728.pdf.

[86] Kumar M, Misra A, Babbar AK, et al. Intranasal nanoemulsion based brain targeting drug delivery system of risperidone. Int J Pharm. 2008;358:285–291.

[87] Jogani V V., Shah PJ, Mishra P, et al. Intranasal mucoadhesive microemulsion of tacrine to improve brain targeting. Alzheimer Dis Assoc Disord. 2008;22:116–124.

[88] Dalvi A V., Ravi PR, Uppuluri CT, et al. Thermoresponsive nasal in situ gelling systems of rufinamide formulated using modified tamarind seed xyloglucan for direct nose-to-brain delivery: design, physical characterization, and in vivo evaluation. J Pharm Investig. 2021; Available from: https://doi.org/10.1007/s40005-020-00505-9.

[89] Rázga F, Vnuková D, Némethová V, et al. Preparation of chitosan-TPP sub-micron particles: Critical evaluation and derived recommendations. Carbohydr Polym.2016;151:488–499.Available from: http://dx.doi.org/10.1016/j.carbpol.2016.05.092.

[90] Kouchak M, Avadi M, Abbaspour M, et al. Effect of different molecular weights of chitosan on preparation and characterization of insulin loaded nanoparticles by ion gelation method. Int J Drug Dev Res. 2012;4:272–277.

[91] Martínez-Ibarra DM, Sánchez-Machado DI, López-Cervantes J, et al. Hydrogel wound dressings based on chitosan and xyloglucan: Development and characterization. J Appl Polym Sci. 2019;136:1–10.

[92] Ways TMM, Lau WM, Khutoryanskiy V V. Chitosan and its derivatives for application in mucoadhesive drug delivery systems. Polymers (Basel). 2018;10.

Conclusion

Rufinamide (Rufi) is an anti-epileptic drug (AED) approved for the treatment of Lennox Gastaut Syndrome (LGS). Rufi was given the status of an orphan drug for treatment of LGS is 2004. Rufi was approved for marketing in Europe in 2007 under the trade name Inovelon®. In 2008, the US FDA approved it for treatment of LGS under the trade name Banzel®. Rufi has also been indicated for use to treat partial seizures in adults. Rufi has shown a better efficacy and better safety profile than many other drugs used to treat epilepsy and LGS. However, there are some drawbacks of the currently marketed oral formulations of Rufi. Rufi suffers from moderately low oral bioavailability. This is due to its low dissolution rate and low solubility of Rufi in GI fluids. Further, studies have reported that absorption of Rufi from the GIT is slow, with Tmax of 4-6 h irrespective of the formulation used or fed or fasted condition. Once absorbed into the systemic circulation, in order to reach the brain, Rufi has to cross the BBB. This further reduces the amount of drug reaching the brain. To overcome this problem, high doses of Rufi are being prescribed. This leads to intensification of peripheral side effects.

Given the problems associated with orally administered Rufi, it is imperative to administer it as a different formulation or through a different route of administration.

The purpose of this research work was to improve the bioavailability of Rufi in the brain by administering it via the intranasal (i.n.) route.

Over the past decade, i.n. delivery to target the brain has been recognized as a non-invasive technique to deliver drugs to the brain. It has been considered as a better alternative to oral and i.v. delivery due to better reach to the brain, easy accessibility for administration, high surface area of nasal mucosa and avoidance of hepatic first pass metabolism. Also, it is a viable option especially in case of patients suffering from epilepsy, where sometimes, swallowing of dosage form might be an issue.

Over the last decade, tailoring of nanocarriers for delivery of molecules via nose to brain (N2B) pathways has gained importance. It has been observed that both polymer and lipid-based formulations could help the drug transport through the nasal mucosa by increasing the retention time at the mucosal surface resulting in increased drug concentration at the site of interest. Nanocarriers can also protect susceptible drugs against metabolism by intranasal enzymes. Further, nanocarriers can be tuned to achieve desired release properties, desired retention time in the nasal cavity, and desired percent drug loading.

In this work, we have explored different formulation strategies to improve the direct nose to brain uptake of Rufi, while also minimizing its plasma exposure. We have formulated a thermoresponsive in-situ nasal gel for the N2B delivery of Rufi. We used a tamarind seed xyloglucan (TSX), a biodegradable, biocompatible polymer as

a thermoresponsive polymer. As an attempt to further improve the N2B delivery of Rufi, we formulated nanoparticulate systems of Rufi. Chitosan based Rufi nanoparticles (Rufi-Ch-NPs) and Rufi nanocrystals (Rufi-NCs). The formulated nanoparticles were suspended in the thermoresponsive in-situ nasal gel. In order to compare the in vivo performance, plasma and brain pharmacokinetic (PK) studies of the nano formulations and nano formulations suspended in thermoresponsive in-situ nasal gel were caried out.

Development of robust, reliable analytical and bioanalytical methods for assessing the in vitro and in vivo performance of the developed formulations is critical. Therefore, RP-HPLC based analytical and bioanalytical methods were developed and validated for the quantification of Rufi. The method was found to be selective for Rufi and was effectively employed in the analysis of samples originating from different studies that were conducted. The developed methods were validated according to the guidelines given by ICH.

A thermoresponsive in-situ gel for Rufi was formulated. TSX a natural, biodegradable polymer was used as a thermoresponsive polymer. The formulation was optimized using rheometric analysis, texture analysis, in vitro, and in vivo studies. PK studies in rats were carried out to assess direct N2B uptake for the optimized in-situ gelling formulation of Rufi and compared with intravenous bolus

and aqueous nasal suspension of Rufi. Finally, brain targeting indices %DTE, and %DTP were calculated.

Further, Rufi-NCs were prepared using a bottom-up approach by anti-solvent precipitation technique. Rufi-NCs were characterized for their particle size, PDI, and percentage yield. The optimized Rufi-NCs were further loaded in a thermoresponsive in-situ gelling system (Rufi-NC-RXG). In vitro drug release studies were carried out for Rufi-NC-Susp and Rufi-NC-RXG formulations. The drug released was modelled from Rufi-NC-RXG formulation, and it followed Higuchi kinetics. The mechanism of release observed from the exponent values of Korsmeyer-Peppas model was non-Fickian or anomalous type release. In vivo plasma and brain PK studies were performed for intranasally administered Rufi-NC-Susp and Rufi-NC-RXG. The results were compared with intranasally administered plain aqueous suspension of Rufinamide (Rufi-Susp). Comparison of the data showed that Rufi-NC-RXG showed significantly higher brain uptake when compared to Rufi-NC-Susp and Rufi-Susp.

Rufinamide loaded Chitosan–STPP nanoparticles (Rufi-Ch-NPs) were prepared using ionic gelation technique and optimized based on the principles of DoE. Nanoparticles were characterized for their particle size, zeta potential and entrapment efficiency. The optimized nanoparticles were loaded in TSX based thermoresponsive nasal in-situ gel. In vitro drug release studies were performed for

Rufi-NP-Susp and Rufi-NP-RXG formulations. The data was modelled for Rufi-NP-Susp formulations. The release followed Higuchi kinetics, and the Korsmeyer-Peppas model exponent value indicated that the release followed non-Fickian type of mechanism. The release was slightly extended in case of Rufi-NP-RXG formulation when compared to Rufi-NP-Susp formulation. In vivo plasma and brain PK evaluation was performed for aqueous suspension of nanoparticles and nanoparticles dispersed in the in-situ gel. The results were compared with the previously published data for Rufi-Susp. Data comparison revealed that both the nanoparticle formulations showed better direct N2B uptake than Rufi-Susp. This was evident from higher %DTP values obtained for both nanoparticle formulations. Overall, the Chitosan nanoparticles of Rufi showed a higher brain distribution of Rufi than its plain aqueous suspension.

Summary

The objective of this work was to enhance the brain bioavailability of Rufinamide (Rufi) by formulating several intranasal formulations of Rufi for its direct nose to brain (N2B) delivery. Rufinamide suffers from poor oral bioavailability due to low solubility and low dissolution rate in the GI fluids. Due to low oral bioavailability, sufficient amounts of drug do not reach the brain, the target organ. Therefore, Rufi is recommended to be administered at high dose (up to 3200 mg/day in children) and dosing frequency through oral route to achieve the required therapeutic concentrations in brain for effective management of the disease condition. However, administering high doses of Rufi through oral route has resulted in aggravation of its peripheral side effects. Considering the shortcomings of orally administered Rufi and given that it is prescribed in pediatric patients (1-18 years), it is essential to look for an alternate delivery route and/or formulation for Rufi.

N2B delivery is an attractive route of administration especially in case of CNS active drugs which suffer from problems in oral absorption. N2B delivery has been explored over the last two decades. Several reports have shown effective uptake of small molecules, biomolecules, and peptides via the olfactory neurons or trigeminal neurons. Formulation strategies like mucoadhesive formulations, hydrogels, *in-situ* gels, particulate formulations, lipid-based formulations have been used to enable and enhance the N2B uptake of therapeutic agents.

In this research work, we have combined two formulation approaches viz. *in-situ* gels and nanoformulations for enhancing the delivery of Rufi to the brain. Three formulations viz. thermoresponsive *in-situ* gel, nanocrystals of Rufi loaded in thermoresponsive *in-situ* gel, and Chitosan nanoparticles of Rufi loaded in thermoresponsive *in-situ* gel were formulated. All formulations were characterized for their rheological properties, stability, *in vitro* drug release, and *in vivo* plasma and brain pharmacokinetic performance.

The thesis presented for this research work entails the following chapters:

Chapter 1. Introduction

In this chapter, a review of epilepsy, and Lennox Gastaut Syndrome (LGS) is presented. Further, importance of Rufi in the management of LGS is explained. The aim of this chapter is to focus on

the currently available formulations of Rufi, their drawbacks, and formulations to overcome the shortcomings. Further, intranasal delivery, N2B delivery, and its suitability in delivering Rufi to the brain have been discussed. As a part of intranasal delivery, the anatomy of the nose and N2B uptake pathways have been discussed in detail. Different formulation strategies to deliver molecules via N2B pathways have been elaborated upon. Finally, the phases in which this research work was carried out are explained.

Chapter 2. Development of Analytical Methods, their Validation, and their Application for Quantification of Rufinamide in Different Matrices

This research work aims at developing delivery systems to enhance the uptake of Rufi in the brain. The performance of such delivery systems can be evaluated by performing certain *in vitro* and *in vivo* characterization. For this purpose, a robust analytical is required which can quantify Rufi in bulk formulations and from biological samples. Precise and accurate validated assay methods play important role in quantification of drug in biological samples to assess the pharmacokinetic data.

In this chapter, RP-HPLC based analytical and bioanalytical methods developed for quantification of Rufi in bulk formulations, *in vitro* release studies samples and biological samples are presented. The bioanalytical method was developed using the principle of Design of Experiment (DoE). The developed methods have been validated as per ICH guidelines. The applicability of the bioanalytical method for conducting i.v. and oral pharmacokinetic studies is also shown in this chapter. The developed and validated aqueous HPLC method and bioanalytical HPLC method were found to be simple, rapid, specific, precise, cost-effective and reproducible for quantification of Rufi.

Chapter 3. Rufinamide Loaded Thermosensitive Nasal *In-situ* Gelling Systems: Design, Optimization, *In vitro* and *In vivo* Evaluation

This chapter describes the formulation, *in vitro, in vivo* characterization of a thermoresponsive *in-situ* gel for N2B delivery of Rufi. The thermoresponsive gel was based on reacted Xyloglucan (RXG) as a thermoresponsive polymer. The formulation was optimized using rheometric analysis, texture analysis, *in vitro,* and *in vivo* studies. Pharmacokinetic studies in rats were carried out to assess direct N2B uptake for the optimized *in-situ* gelling formulation of Rufi (Rufi-RXG) and

compared with intravenous bolus, and a plain aqueous nasal suspension of Rufi (Rufi-Susp). Finally, brain targeting index %DTP was calculated.

All the formulations showed gelation below 35 °C. The optimized formulation comprised 2.0% w/v RXG, 0.01% v/v thiomersal (preservative), and Rufi in suspended form. The %DTP values were 79.9 and 31.91, respectively. This indicates that with Rufi-RXG almost 80% of the administered dose of Rufi reached the brain via direct N2B pathways, whereas in case of Rufi-Susp, only 31% of Rufi could reach the brain directly. This work demonstrated that the intranasal *in-situ* gel formulation Rufi is enhancing the overall brain exposure of Rufi compared to oral formulations.

Chapter 4. Design, Optimization, Physical Characterization, and *In vivo* Evaluation of Rufinamide Nanocrystals Loaded in Xyloglucan Based Thermoresponsive Nasal *In-situ* Gelling Systems.

In this chapter, the formulation and characterization of a nanocrystal formulation for Rufi has been described. Rufi nanocrystals (Rufi-NCs) were formulated by anti-solvent precipitation using the principle of DoE. Rufi-NCs were characterized for size, yield (%) and morphology. Rufi-NCs were loaded in a 2.0% w/v RXG to form a nasal *in-situ* gel for direct N2B delivery of Rufi. The *in-situ* gel formulations were characterized for rheological properties, stability, *in vitro* drug release, and *in vivo* plasma and brain pharmacokinetics. Pharmacokinetic parameters were computed for aqueous suspension of nanocrystals (Rufi-NC-Susp) and *in-situ* gelling formulation for nanocrystals (Rufi-NC-RXG) and compared with the pharmacokinetic parameters of aqueous suspension of plain Rufi (Rufi-Susp).

Rufi-NCs showed PS of 261.2 ± 2.1 nm, PDI of 0.28 ± 0.08, and yield (%) of 89.6 ± 2.0. The Rufi-NC-RXG formulation showed a gel transition temperature of 32 °C. Rufi-NC-RXG formulations showed almost 100% release around 8 h, while Rufi-NC-Susp dissolved within a few minutes after commencement of the study. Both formulations – Rufi-NCs and Rufi-NC-RXG were found to be stable for a time of 60 days at storage conditions of at 25 °C and 60 ± 5% RH for Rufi-NCs and storage condition of refrigeration, 2-8 °C for Rufi-NC-RXG. The %DTP values for Rufi-Susp and Rufi-NC-RXG were 31.9 and 85.5, respectively. This indicates that the nanocrystal formulation further improved the drug delivery of Rufi to the brain.

Chapter 5. Design, Optimization, Physical Characterization and *In vivo* Evaluation of Chitosan Nanoparticles of Rufinamide Loaded in Thermoresponsive Nasal *In-situ* Gelling System

In this chapter, the formulation and characterization of a nanoparticulate formulation for Rufi has been described. In this work, using the principle of DoE, Rufi loaded chitosan nanoparticles (Rufi-Ch-NPs) were formulated. The Rufi-Ch-NPs were suspended in a solution of 2.0% w/v RXG to form a nasal *in-situ* gel for direct N2B delivery of Rufi. The Rufi-Ch-NPs were characterized for size, entrapment efficiency, zeta potential, morphology, and physical stability. The *in-situ* gel formulations were characterized for rheological properties, *in vitro* drug release, stability, and *in vivo* plasma and brain pharmacokinetics. Pharmacokinetic parameters were computed for aqueous suspension of nanoparticles (Rufi-NP-Susp) and *in-situ* gelling formulation for nanoparticles (Rufi-NP-RXG) and compared with the pharmacokinetic parameters of aqueous suspension of plain Rufi (Rufi-Susp). The %DTE and %DTP values were calculated for all the formulations. The optimized nanoparticle formulation showed a size of 180 ± 1.5 nm, PDI of 0.29 ± 0.08, zeta potential of 38.3 ± 1.5 mV, entrapment efficiency of 75 ± 2.0 % and drug loading of 11 ± 0.3 %. The *in-situ* gelling formulation of nanoparticles showed a solution to gel transition temperature of 32 °C. Rufi-NP-RXG and Rufi-NP-Susp showed similar *in vitro* drug release profiles. For both formulations around 80% drug release was seen at the end of 24 h. Both formulations – Rufi-NPs and Rufi-NP-RXG were found to be stable for a time period of 60 days at storage conditions of at 25 °C and 60 ± 5% RH for Rufi-Ch-NPs and storage condition of refrigeration, 2-8 °C for Rufi-NP-RXG. The %DTP for Rufi-NP-Susp, Rufi-NP-RXG, and Rufi-Susp were 86.1, 91.5 and 31.9, respectively. This indicates that with Chitosan nanoparticles, the N2B uptake of Rufi increased further.

Chapter 6. Comparison of the Various Optimized Nanoformulations of Rufinamide

This chapter is a comparison chapter for both nanoformulations of Rufi. Comparisons of Rufi-NCs and Rufi-Ch-NPs are made in terms of their preparation methods, critical factors affecting the responses, their physical characteristics viz. particle size, zeta potential, PDI, EE %, DL %, % yield, *in vitro* drug release properties, and stability. Further, we have compared *in vivo* performance of plain aqueous suspension of Rufi-NCs (Rufi-NC-Susp), RXG *in-situ* gel of Rufi-NCs (Rufi-NC-RXG), plain aqueous suspension of Rufi-Ch-NPs (Rufi-NP-Susp), and RXG *in-situ* gel of

Rufi-Ch-NPs (Rufi-NP-RXG). Plasma and brain AUC0→tlast of Rufi with these formulations was compared. It was found that with Rufi-NP-RXG Rufi AUC0→tlast in the brain tissue was the highest and plasma AUC0→tlast was the lowest compared to other formulations of Rufi. Chapter

7. Conclusions

In this chapter, consolidated conclusions of the work have been presented. Pharmacokinetic and pharmacodynamic studies revealed that all the four optimized nanoformulations (Rufi-NC-Susp, Rufi-NC-RXG, Rufi-NP-Susp, and Rufi-NP-RXG) have shown better *in vivo* performance compared to conventional formulations of the drug (Rufi-Susp and Rufi-RXG). It was evident from the pharmacokinetic data, that the approaches used for increasing direct N2B uptake- viz. *in-situ* gel and nanoformulation approach helped in delivering significantly high amounts of Rufi to the brain when compared to plain aqueous suspension of Rufi. This work has also shown the benefits of intranasal delivery over other routes of administration, especially in case of drugs acting on the CNS.

APPENDICES

List of Publications and Presentations

List of Publications (From Thesis Work)

1. **Dalvi, A.V**., Uppuluri, C.T., Bommireddy, E.P. and Ravi, P.R., 2018. Design of experiments-based RP–HPLC bioanalytical method development for estimation of Rufinamide in rat plasma and brain and its application in pharmacokinetic study. Journal of Chromatography B, 1102, pp.74-82. (doi: 10.1016/j.jchromb.2018.10.014.)

2. **Dalvi AV**, Ravi PR, Uppuluri CT, Mahajan RR, Katke SV, Deshpande VS, 2021. Thermosensitive nasal in situ gelling systems of rufinamide formulated using modified tamarind seed xyloglucan for direct nose-to-brain delivery: design, physical characterization, and in vivo evaluation. Journal of Pharmaceutical Investigation.:1-13. (doi:10.1007/s40005-020-00505-9)

3. **Dalvi, A.V.,** Ravi, P.R. and Uppuluri, C.T., 2021. Rufinamide Loaded Chitosan Nanoparticles in Xyloglucan Based Thermoresponsive In Situ Gel for Direct Nose to Brain Delivery. Frontiers in Pharmacology, 12, p.1274. (doi: 10.3389/fphar.2021.691936)

Works Under Communication (From Thesis Work)

1. **Dalvi AV**, Ravi PR, Uppuluri CT, Rufinamide Nanocrystal Loaded Thermoresponsive Nasal In Situ Gelling System for Improved Drug Distribution to Brain: Optimization Using DoE, Physical Characterization and Pharmacokinetic Evaluation. (Communicated to Pharmaceutical Research)

Other Publications

1. Uppuluri, C.T., Ravi, P.R., Dalvi, A.V., Shaikh, S.S. and Kale, S.R., 2020. Piribedil loaded thermo-responsive nasal in situ gelling system for enhanced delivery to the brain: formulation optimization, physical characterization, and in vitro and in vivo evaluation. Drug Delivery and Translational Research. (doi: 10.1007/s13346-020-00800-w)
2. Shailender, J., Ravi, P.R., Reddy Sirukuri, M., Dalvi, A. and Keerthi Priya, O., 2018. Chitosan nanoparticles for the oral delivery of tenofovir disoproxil fumarate: formulation optimization, characterization and ex vivo and in vivo evaluation for uptake mechanism in rats. Drug development and industrial pharmacy, 44(7), pp.1109-1119. (doi: 10.1080/03639045.2018.1438459)

3. Shailender, J., Ravi, P.R., Saha, P., Dalvi, A. and Myneni, S., 2017. Tenofovir disoproxil fumarate loaded PLGA nanoparticles for enhanced oral absorption: Effect of experimental variables and in vitro, ex vivo and in vivo evaluation. Colloids and Surfaces B: Biointerfaces, 158, pp.610-619. (doi: 10.1016/j.colsurfb.2017.07.037)
4. Uppuluri, C.T., Dalvi, A.V., Bommireddy, E.P. and Ravi, P.R., 2018. Development and validation of rapid and sensitive LC methods with PDA and fluorescence detection for determination of piribedil in rat plasma and brain tissues and their pharmacokinetic application. Biomedical Chromatography, 32(10), p.e4303. (doi: 10.1002/bmc.4303)

List of Conference Presentations (From Thesis Work)

1. **Avantika Dalvi**, Chandra Teja Uppuluri, Punna Rao Ravi, 'Development of Xyloglucan Based Thermoresponsive Gel for Nose to Brain Delivery of Rufinamide, an Anti-Epileptic Drug: Rheological and Pharmacokinetic Evaluation' at CRS-2020 Virtual Annual Meeting, USA.
2. Shailender Joseph, Paramita Saha, **Avantika Dalvi**, Srividya Myneni, Punna Rao Ravi. 'Tenofovir disoproxil fumarate Loaded PLGA Nanoparticles for Enhanced Oral Absorption: Effect of Experimental Variables and In vitro, In vivo and Ex vivo Evaluation' at PEAR-2017, JNTU, Hyderabad.
3. **Avantika D**, Joseph S, Vanaparthi A, Ravi P R. 'Formulation Development, In vitro Evaluation, and In vivo Pharmacokinetic Studies of a Self-Emulsifying Drug Delivery System for Amlodipine Besylate' at ICCD3, BITS-Pilani
4. **Dalvi Avantika V**, Joseph Shailender, Rajith K R Rajoli, Ravi P R, 'Chitosan Nanoparticles for Oral Delivery of Tenofovir Disoproxil Fumarate: Design and Optimization, In Vivo Evaluation, and PBPK Modelling in Humans' at Sixteenth Annual Symposium of Controlled Release Society-Indian Chapter on Advances in Technology and Business Potential of New Drug Delivery System.

Workshops

1. "LCMS training" conducted by Spinco Biotech Pvt Ltd at Birla Institute of Technology and Science – Pilani, Hyderabad Campus, Hyderabad on 3rd – 4th November 2018.

Brief Biography of the Candidate

Ms. DALVI AVANTIKA VIJAY completed her B.Pharmacy from University of Pune, Maharashtra in 2014 and M.Pharmacy (with specialization in pharmaceutics) from Birla Institute of Technology and Science – Pilani, Hyderabad Campus, Hyderabad. in 2016. Immediately after her M.Pharmacy, in 2016, she joined Birla Institute of Technology and Science – Pilani, Hyderabad Campus to pursue her doctoral studies under the supervision of Prof. Punna Rao Ravi. During her masters and doctoral studies, she has authored several research papers in renowned international peer-reviewed journals.

Brief Biography of the Supervisor

Prof. Punna Rao Ravi is working as Associate Professor in Department of Pharmacy, BITS-Pilani, Hyderabad Campus. He obtained his B.Pharm, M.Pharm and PhD degrees in Pharmaceutical Sciences from BITS-Pilani University, Rajasthan. He has been working as a faculty member in BITS-Pilani since year 2000. He has many publications in reputed international and national peer-reviewed journals and has presented papers in scientific conferences both in India and abroad. He has successfully completed government sponsored research projects and is expecting more grants from scientific funding agencies.